Deformation on Impaction of a Large Diameter Carbon Fibre Reinforced Poly-Ether-Ether-Ketone Acetabular Cup and its Effects on the Tribology of the Bearing

Holly Everitt, MEng (Hons)

PhD Thesis

August 2011

Institute of Medical Engineering and Medical Physics

Cardiff University

Abstract

Limitations associated with current total hip arthroplasty implants, such as aseptic loosening and dislocation, have led to the investigation into alternative bearing materials such as Carbon Fibre Reinforced PolyEtherEtherKetone (CFR-PEEK). There are reports of press-fit acetabular cups experiencing excessive deformation on impaction into the acetabulum which could lead to unfavourable conditions for bone in-growth and could adversely affect the lubrication regime of the bearing. This may have implications for the use of a reduced modulus material such as CFR-PEEK. The aim of this project was therefore to investigate the level of deformation the prototype Biomet UK Ltd CFR-PEEK cup experiences on impaction into the acetabulum and to assess the effect this deformation would have on the tribological behaviour of the system. In order to achieve this aim three different test regimes were considered; rim loading, impaction into polyurethane foam and impaction into cadaveric bone. In each case, corresponding finite element models were created. To assess the impact cup deformation would have on the lubrication regime of the ceramic-on-CFR-PEEK bearing, friction testing was conducted on cups with various clearances.

This study has shown that that the polyurethane foam model is the most suitable method for assessing the level of cup deformation which occurs due to the impaction of a press fit acetabular cup. Testing using cadaveric specimens revealed a high level of variation in both the size of cavity produced by reaming and the level of deformation experienced by the cup. As a result cadaveric testing is unlikely to give a reliable worse case result. It was also found that rim loading is not a valid method for investigating the deformation on impaction of acetabular shells. In order to use rim loading, the load equivalent to that experienced on impaction would have to be found empirically for each individual cup design and size via imperial measurement.

The Biomet CFR-PEEK cup experienced a large diametric deformation on impaction of up to 1.084 mm. However, the large clearance between the head and the acetabular cup meant that the deformation of the PEEK cup did not result in jamming of the modular femoral head. The friction testing demonstrated that the bearing was insensitive to changes in clearance; therefore, provided the initial clearance is sufficient the deformation caused by press-fitting should not have an adverse effect on the friction and lubrication of the system.

Acknowledgments

I would like to firstly thank Dr Len Nokes, Dr Duc Pham, Dr Eric Maylia and Dr Nicky Priaulx for the complicated way I came to be on the “PhD in full time employment” scheme at Cardiff University; In addition my employer Biomet UK Ltd for sponsorship and support in my research. I would like to thank my supervisors Prof. Sam Evans, Dr Cathy Holt, Dr Robert Bisgby and Dr Imran Khan for their help and guidance over the past 3 years.

Thanks also go to Dr Mansour Youseffi at University of Bradford for conducting friction testing and allowing me to conduct testing under his supervision.
Dr QianQian Wang and Dr Junjie Wu at University of Durham who also conduced friction testing.

Thank you to Ross Cotton at Simpleware for help and advice on how to make my pelvis model using their software, Dr Hua and the radiotherapy department at Stanmore for CT scanning the pelvis, and in particular the medical student who stripped the soft tissue from the cadaver! Dr Kluess for his advice on tissue phantoms and CT resolution. Dr Mark Eaton for his patience with me and DIC equipment!

I would also like to thank everyone in my office at university in particular Rachel Groves for being the only person who understands the pain of FE. And finally my Mum for listening to me even though she has no idea what I am talking about and for proof reading much of my work.

Table of Contents

Abstract i

Acknowledgments ii

Table of Contents iii

List of Figures vii

List of Tables xi

Abbreviations xii

Notation xiii

Chapter 1: Introduction 1

1.1 Aims and Objectives 2

1.2 Chapter Summary 3

1.3 Background 5

Chapter 2 – Literature Review 1

2.1 Introduction 1

2.2 PEEK Material 4

2.2.1 Material Properties 6

2.2.2 Biological Response to PEEK 7

2.2.3 History of PEEK use in Implants 9

2.2.4 PEEK as a Material for Acetabular Components 10

2.2.5 Early Clinical Results 12

2.3 Cup Deformation 13

2.4 Modelling the Pelvis 15

2.5 Conclusion 18

Chapter 3: Acetabular Cup Deformation under Rim Loading using Digital Image Correlation and Finite Element Methods 20

3.1 Introduction 20

3.2 Method 22
3.2.1 DIC 22
3.2.2 Samples 24
3.2.3 Digital Image Correlation 25
3.2.4 Finite Element Model of Rim Loading 27
3.3 Results 29
3.4 Discussion 32
Chapter 4: Deformation on Impaction using Polyurethane Foam Model and Finite Element Model 36
4.1 Introduction 36
4.2 Materials and Methods 37
4.2.1 Materials 37
4.2.2 Experimental Method 39
4.2.3 Finite Element Model 42
4.3 Results 44
4.3.1 Validation of Dental Putty 45
4.3.2 Experimental Results 45
4.3.3 Finite Element Results 47
4.4 Discussion 51
Chapter 5: Deformation on Impaction using Cadaveric Specimens and Subject Specific Finite Element Model 58
5.1 Introduction 58
5.2 Materials and Methods: Experimental 58
5.2.1 Implants 58
5.2.2 Method 59
5.3 Method: Finite Element Model 60
5.3.1 Location Dependent Material Properties 60

5.3.2 Hemi Pelvis Model 61
5.3.3 Acetabular Model for Impaction Modelling 63
5.4 Results: Experimental 67
5.4.1 Accuracy of Reaming 67
5.4.2 Deformation 68
5.5 Results: FE Model of the Pelvis 70
5.5.1 Material Properties 70
5.5.2 Deformation 73
5.6 Discussion 78
Chapter 6 – Tribological Testing of Zirconia Toughened Alumina Femoral Head on CFR-PEEK Acetabular Cup 87
6.1 Introduction 87
6.2 Method 88
6.2.1 Clearances 88
6.3 Samples 89
6.3.1 Clearance Testing; Phase 1 89
6.3.2 Clearance Testing: Phase 2 and 3 89
6.3.3 Stribeck Analysis 90
6.3.4 Prediction of Lubrication Regime 91
6.3.5 Durham Friction Test Set Up 92
6.3.6 Bradford Friction Test Set Up 93
6.4 Results 95
6.4.1 Phase 1 Testing 95
6.4.2 Phase 2 Testing 99
6.4.3 Phase 3 Testing 104
6.4.4 Prediction of Lubrication Regime 106
6.5 Discussion 107

Chapter 7: Summary and Discussions 114

7.1 Limitations 120

Chapter 8: Conclusions 121

Chapter 9: Further Work 122

Chapter 10: References 124

List of Figures

Figure 1 Lateral view of left pelvis (image from model generated during this project) 5
Figure 2 Components of Total Hip Arthroplasty (left), reaming the acetabulum (right) (images from Biomet UK Ltd operative technique brochure) 6
Figure 3 Structure of PEEK 4
Figure 4 Areas of predominant load transfer in the pelvis (left), schematic of rim loading (right) 20
Figure 5 Digital image correlation; correlation between “before” and “after” image .. 23
Figure 6 DIC bench test set-up showing cameras and multiaxis microscope (left), x and y directions of multiaxis microscope (right) 26
Figure 7 Schematic diagram of DIC set-up showing test piece, two cameras, PC and servohydralic machine (top), close up photo of speckle cup in test machine (bottom left), photo of camera and speckle cup (bottom right) 27
Figure 8 Example of a typical mesh and assembly with rigid bodies 28
Figure 9 Internal diameter offset 28
Figure 10 Example of 2D overlay from Vic3D (Limess Messtechnik & Software GmbH, Berlin, Germany) showing displacement in y direction relative to initial image. 29
Figure 11 Load displacement plot for injection moulded PEEK cup 30
Figure 12 Load deflection plot for a 38 mm UHMWPE cup showing DIC and FE results with various mesh sizes (left), load deflection plot for 58 mm cups of various materials (right) 31
Figure 13 Graphs showing the effect of WT (top left), ID offset (top right), and outside diameter (bottom left) on cup stiffness for PEEK cups 32
Figure 14 Machined cup with porous plasma sprayed titanium coating 37
Figure 15 Material properties of Sawbones polyurethane foam blocks [196] 38
Figure 16 Diagram of Sawbones block used for impaction testing 40
Figure 17 PEEK cups being impacted into prepared Sawbones cavity using ball impactor 41
Figure 18 Abaqus model of Sawbones block and prototype cup 43
Figure 19 Initial polar gap 44

Figure 20 Example putty mould from Sawbones impaction testing, deformation in mm 45
Figure 21 Deformation versus cup size; 20 pcf foam with 1 mm under-ream (top left), 30 pcf foam with 1 mm under-ream (top right), 20 pcf foam with 2 mm under-ream (bottom left), 30 pcf foam with 2 mm under-ream (bottom right). 46
Figure 22 Cross section of FE results for 56 mm cup with 1.5 mm under-ream 47
Figure 23 Polar gap remaining after each FE displacement step (54 mm cup, 30 pcf foam) 48
Figure 24 FE output for 56 mm cup with 1.5 mm under-ream in 30 pcf foam; deformation in x direction (u1) (left) and deformation in y direction (u2) compression (right) in mm 48
Figure 25 Example deformation plot for 54 mm cup with 1 mm under-ream, deformation scaled by a factor of 10 49
Figure 26 Deformation versus cup size for 2 mm under-ream in 30 pcf foam (left) 20 pcf foam (right), experimental and FE results (note FE model had diametric interference of 1.5 mm based on the results of the accuracy of the reaming) 49
Figure 27 Deformation versus cup size for 1 mm under-ream in 30 pcf foam (right) 20 pcf foam (left), experimental and FE results (note FE model had diametric interference of 0.5 mm based on the results of the accuracy of the reaming) 50
Figure 28 Deformation versus Young's Modulus of Sawbones block (56 mm cup with 1.5 mm under-ream)..... 50
Figure 29 von Mises stresses (MPa) in 56 mm cup with 1.5 mm under-ream in 30 pcf foam, cup (left), Sawbones block (right) 51
Figure 30 Example dental putty mould of an impacted PEEK cup 59
Figure 31 Tissue characterisation phantom 60
Figure 32 Cube cropped from centre of CT phantom rod (left), example histogram for CT rod (right) 61
Figure 33 CT image through acetabulum (left) and graph of distance vs. greyscale for the profile line shown (right) 61
Figure 34 Segmentation of pelvis using Simpleware, pink = cortical mask, orange = cancellous mask..... 62
Figure 35 Acetabular model (pink areas were removed from hemi pelvis model) 63

Figure 36 Positioning of sphere for reaming in ScanCAD (left) and example of perforating the acetabular wall (right) 64
Figure 37 Acetabular model post reaming (left), acetabular model post reaming with incorrect position of sphere causing perforation of the acetabular wall (right) 64
Figure 38 Incorrect position of cup with contact between cup and bone masks (left), correct position of cup with gap between cup and bone masks (right) 64
Figure 39 Acetabular model with cup in Abaqus showing fixed boundary conditions and direction of displacement 65
Figure 40 Diagram of the location of paired nodes for assessment of diametric deformation in FE model 66
Figure 41 Example output from laser scanner for mould 1 (left) and mould 7 (right) 68
Figure 42 PEEK cup and metal head showing dome contact 69
Figure 43 Example of laser scan and 3D CAD overlay 70
Figure 44 Graph of maximum diametric closure (left) and expansion (right) versus cup size 70
Figure 45 Graph of greyscale value vs. physical density of the CT phantom 71
Figure 46 Distribution of material density (g/cm^3), section through acetabular region, with (left) and without (right) FE mesh 72
Figure 47 Distribution of bone density in cancellous bone, lateral (left) and medial (right) view 72
Figure 48 Direction of maximum cup compression and expansion in the FE model (left) exaggerated deformed cup (deformation scale factor = 4) (right) 74
Figure 49 Lateral view of pelvis showing acetabular notch, iliac column and ischial column 74
Figure 50 Plot of maximum von Mises stress for model 3 76
Figure 51 Plot of maximum von Mises stress in model 5 76
Figure 52 Plot of maximum von Mises stress model 6 (left), model 9 (right) 77
Figure 53 Example cross sections; point contact occurring part way though simulation (left) seated cup at end of simulation (right) 77
Figure 54 Idealised Stribeck plot 90
Figure 55 Durham cup holders for phase 1 testing (left) and phase 2 testing (right) 93
Figure 56 ProSim Hip Joint Friction Simulator 94
Figure 57 Stribeck plot for ZTA-on-CFR-PEEK in CMC fluid (phase 1 testing) 95

Figure 58 Stribeck plot for ZTA-on-CFR-PEEK in CMC fluid +25% bovine serum (phase 1 testing) 95
Figure 59 Stribeck plot for ZTA-on-CFR-PEEK in CMC fluid and CMC+25% bovine serum (top left 257 μm clearance, top right 661 μm clearance, bottom left 706 μm) 96
Figure 60 Friction factor versus radial clearance for different CMC lubricant viscosities a)1 Pas, b) 0.3 Pas, c) 0.1 Pas, d) 0.03 Pas, e) 0.01 Pas..... 97
Figure 61 Friction factor versus radial clearance for different CMC+BS lubricant viscosities a)1 Pas, b) 0.3 Pas, c) 0.1 Pas, d) 0.03 Pas, e) 0.01 Pas..... 98
Figure 62 Stribeck plot for ZTA-on-CFR-PEEK in CMC fluid tested at Durham University 99
Figure 63 Stribeck plot for ZTA-on-CFR-PEEK in CMC fluid +25% bovine serum tested at Durham University 100
Figure 64 Stribeck plot for ZTA-on-CFR-PEEK in CMC fluid and CMC+25% bovine serum (top left 30 μm clearance, top right 330 μm clearance, bottom left 630 μm, bottom right 930 μm) 101
Figure 65 Friction factor versus radial clearance for different CMC lubricant viscosities a)1 Pas, b) 0.3 Pas, c) 0.1 Pas, d) 0.03 Pas, e) 0.01 Pas..... 102
Figure 66 Friction factor versus radial clearance for different CMC+BS lubricant viscosities a)1 Pas, b) 0.3 Pas, c) 0.1 Pas, d) 0.03 Pas, e) 0.01 Pas..... 103
Figure 67 Stribeck plot for ZTA-on-CFR-PEEK tested at University of Bradford 104
Figure 68 Radial clearance vs. friction factor for various viscosities a) 0.155 Pas (25%BS + CMC), b) 0.0442 Pas (25%BS + CMC), c) 0.0127 Pas (25%BS + CMC), d) 0.00612 Pas (25%BS + CMC), e) 0.00143 Pas (25% BS), f) 0,00157 Pas (pure BS). 105

List of Tables

Table 1 typical Young's modulus for materials used in THA 7
Table 2 Dimensions and materials of cup samples tested 25
Table 3 Details of OD and wall thicknesses (WT) of CoCr cups, maximum diametric deformation predicted by FE (3 mm mesh density) and DIC results taken at 3000 N. 30
Table 4 Details of OD and wall thicknesses of polymer cups, maximum diametric deformation predicted by FE (3 mm mesh density) and DIC results taken at 300 N. 30
Table 5 Cup sizes used in Sawbones testing 37
Table 6 Material properties used in FE model 42
Table 7 Cup sizes modelled in FE 43
Table 8 Diameter of Sawbones cavities prepared using pillar drill measured using CMM 44
Table 9 Deformation (in mm) on impaction into Sawbones (comp=compression, exp=expansion) 46
Table 10 Compression and expansion of simulated cobalt chromium and titanium cups 50
Table 11 Cups modelled (LDT=Location Dependent Thickness, GS = Greyscale based) 67
Table 12 Results from putty moulds of reamed acetabular cavities 67
Table 13 Results for impacted cups 69
Table 14 Results from FE model of pelvis created from CT data 73
Table 15 Maximum von Mises stress in cortical bone 78
Table 16 Lambda ratio for phase 1 testing (conducted in Durham) 106
Table 17 Lambda ratio for phase 2 testing at Durham 106
Table 18 Lambda ratio for the phase 3 testing (Bradford) 106
Table 1 Examples of standard (i.e. not resurfacing) press-fit acetabular cups currently available 140
Table 2 Examples of resurfacing acetabular cups 140

Abbreviations

BS	Bovine Serum
CAD	Computer Aided Design
CFR-PEEK	Carbone Fibre Reinforced PEEK (used interchangeably with PEEK)
CMC	CarboxyMethyl Cellulose
CMM	Coordinate Measuring Machine
CoCr	Cobalt Chromium Molybdenum alloy
CoC	Ceramic-on-Ceramic
CoM	Ceramic-on-Metal
CoP	Ceramic-on-Polyethylene
CT	Computer Tomography
DIC	Digital Image Correlation
FE	Finite Element
FF	Friction Factor
GS	Grey Scale
HA	Hydroxy Apatite
ID	Inside Diameter
IDE	Investigational Device Exemption
LDT	Location Dependent Thickness
MoM	Metal-on-Metal
MoP	Metal-on-Polyethylene
OD	Outside Diameter
PEEK	Poly Ether Ether Ketone (used interchangeably with CFR-PEEK)
SD	Standard Deviation
THA	Total Hip Arthroplasty
TKA	Total Knee Arthroplasty
Ti / Ti6Al4V	Titanium Aluminium Vanadium alloy
UHMWPE	Ultra High Molecular Weight PolyEthylene
WT	Wall Thickness
ZTA	Zirconia Toughened Alumina

Notation

μ	coefficient of friction
E	Young's Modulus
E'	equivalent modulus
E_1	Modulus of head material
E_2	Modulus of cup material
H_{min}	minimum film thickness
L	load applied
η	Viscosity
r	femoral head radius
R_1	radius of femoral head
R_2	radius of cup
R_{eff}	effective radius
R_{q1}	roughness of head
R_{q2}	roughness of cup
R_x	effective radius
T	frictional torque between the bearing surfaces
u	entraining velocity
v	Poisson's radio
v_1	Poisson's ratio of head material
λ	lambda ratio
η	viscosity of lubricant
ρ	density
ρ_{app}	apparent density

Chapter 1: Introduction

Total Hip Arthroplasty (THA) is a highly successful procedure with over 1 million surgeries being performed worldwide each year [1]. Damaged and diseased parts of the hip joint are replaced with manmade materials to reduce pain and restore function. Current deigns of THA are broadly successful [1], however osteolysis as a result of wear particles generated in conventional THA bearings is a serious problem [2-4]. Polyethylene debris stimulates the greatest bone resorbing response due to the large number of particles produced, which persist within the periprosthetic tissue causing bone resorption and implant loosening [3, 4]. Although hard-on-hard bearings can reduce the volume of wear particles generated [5-10] they are susceptible to problems such as ion hypersensitivity [11, 12], toxicity, carcinogenesis [3, 13] and aseptic lymphocytic vascular and associated lesions (ALVAL) [12, 14]. Dislocation is also a serious issue for THA patients [4, 15, 16]; it has been shown that increasing the diameter of the bearing can reduce the risk of dislocation [15, 17-19], however this is not suitable for all bearing materials [20-22].

Carbon Fibre Reinforced Poly Ether Ether Ketone (CFR-PEEK) is an attractive alternative to currently available bearing materials (UHWMPE, cobalt chrome and alumina based ceramics); bulk material and wear particle studies have shown it to be biocompatible [23-29]. PEEK based materials have a history of use in long term implantable medical devices such as spinal implants [26, 30, 31] and composite hip stems [32-35] demonstrating its biocompatibility *in vivo*. A number of *in vitro* investigations also suggest its clinical viability; it is possible to coat PEEK with HA (hydroxyapatite) and porous titanium using plasma spray techniques, to enable cementless fixation via bone ongrowth, without adversely affecting the material properties [27, 36, 37]. Hip simulator testing has shown ceramic-on-CFR-PEEK to be a suitable material combination for ball and socket bearings with wear rates much lower than ceramic-on-polyethylene [27, 38-41]. The wear properties are not adversely affected by excessive gamma irradiation or accelerated oxidation [41]. Early clinical results with PEEK THA components are promising [42-44], although patient numbers are small.

An important factor to be considered in the design of a press-fit PEEK cup is the deformation the cup undergoes during impaction into the acetabulum. There are concerns that acetabular cups currently on the market deform on impaction [45-49]. Such deformation could adversely affect fluid film lubrication of metal-on-metal bearings [50], and could lead to equatorial and edge contact possibly causing the implants to jam [45, 49, 51]. Cup deformation could also influence implant stability and fixation, producing unfavourable conditions for osseointegration and possibly affecting periprosthetic bone remodelling [45, 51].

1.1 Aims and Objectives

The aim of this project was to investigate the deformation characteristics of the Biomet UK Ltd prototype CFR-PEEK cup as a result of impaction and to examine the influence of this deformation on the lubrication of the bearing.

In order meet this aim the following objectives were set;

1. Explore the validity of rim loading as a model to investigate deformation on impaction of acetabular cups.
2. Investigate the use of polyurethane foam blocks as a method to model the acetabulum.
3. Create a three dimensional finite element (FE) model of the pelvis which can be used to simulate acetabular component impaction.
4. Measure the deformation of the prototype cups on impaction into cadaveric specimens.
5. Establish the accuracy of modern reaming techniques.
6. Conduct friction testing with Ceramic-on-PEEK bearings with a range of clearances to assess the effect of clearance on the lubrication regime.
7. Make a recommendation based on the findings of objectives 1-6 for the most suitable methodology for impaction deformation testing.

1.2 Chapter Summary

Chapter 2: Literature Review

A literature survey was conducted on CFR-PEEK as a potential material for joint replacement, data on the biocompatibility of the material, the first clinical use of CFR-PEEK and PEEK, as well as wear testing and early clinical results as an acetabular component, are presented. As the focus of this project was to investigate the deformation a press-fit acetabular cup experiences on impaction into the acetabulum, this area was focussed upon. Information from *in vivo*, *in vitro* and *in silico* studies was collated. In order to find the most suitable method to create an FE model of the pelvis to investigate cup deformation, published data on creating finite element models from medical imaging techniques was examined.

Chapter 3: Acetabular Cup Deformation under Rim Loading using Digital Image Correlation and Finite Element Methods

Rim loading had been reported in the literature and proposed in a draft ISO standard as a possible method for assessing the deformation of press-fit acetabular cups. Therefore this technique was deemed a suitable starting place for this project as it represented a straightforward method. The main aim of this chapter was to investigate the suitability of rim loading as a method for assessing deformation on impaction. Digital Image Correlation (DIC) was used to record the deformation without the need to contact the samples. Cobalt chrome and UHMWPE cups were also studied for comparison. Finite Element (FE) models were created and used to investigate the effect of design parameters on cup stiffness. The results of the rim loading tests showed that this was not suitable for obtaining absolute values of deformation an acetabular cup would undergo on impaction, therefore a more representative test was required.

Chapter 4: Deformation on Impaction using a Polyurethane Foam Model and a Finite Element Model

Polyurethane foam blocks (Sawbones) have been widely used in the literature to simulate the reamed acetabulum; therefore it was decided to use this method to test the prototype PEEK cups. In this chapter, cups were impacted into prepared Sawbones cavities and the deformation was measured by taking dental putty moulds of the impacted cups. FE models we also created and validated using the experimental results.

Chapter 5: Deformation on Impaction using Cadaveric Specimens and a Patient Specific Finite Element Model

Although Sawbones have been widely used in the literature, the properties of the foam are homogeneous (whereas cancellous bone is heterogeneous) and the shape of the cavity is not identical to an acetabulum. Therefore, impaction testing was conducted in cadaveric specimens as it was felt that this was more representative of the *in vivo* conditions. A three dimensional heterogeneous FE model was also created from high resolution CT data of a cadaveric pelvis; this was used to simulate impaction of cups with different wall thicknesses and material properties (CFR-PEEK was compared to titanium and CoCr).

Chapter 6: Tribological Testing of Zirconia Toughened Alumina Femoral Head on CFR-PEEK Acetabular Cup

The impaction testing showed that the PEEK cups experienced a significant amount of deformation on impaction, this deformation could have an adverse effect on the tribology of the bearing. In order to investigate the effect that this deformation would have on the lubrication of the ceramic-on-CFF-PEEK bearing, friction testing was conducted at the University of Bradford and Durham University on cups with different radial clearances, representative of varying degrees of deformation.

1.3 Background

The acetabulum (Figure 1) is the concave surface of the pelvis; the ilium, ischium and pubis bones of the pelvis come together in the acetabulum. On the inferior side of the acetabulum is a deep indentation, the acetabular notch, which forms a foramen through which blood vessels and nerves pass. The remainder of the acetabulum is formed by a curved, crescent shaped surface in which the proximal end of the femur (femoral head) sits; this forms the acetabulofemoral or joint hip joint [52].

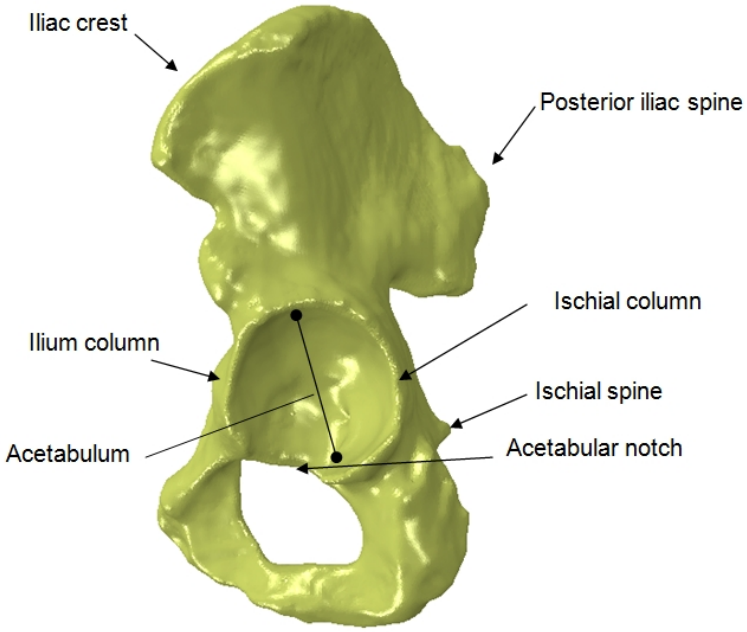

Figure 1 Lateral view of left pelvis (image from model generated during this project)

The primary function of the hip joint is to support the body weight in static and dynamic postures. The femoral head and acetabulum are covered with a thin layer of hyaline cartilage which covers the articulating surfaces, reducing friction in the joint and absorbing shock. Osteoarthritis (OA) is a progressive degenerative joint disease mainly affecting weight bearing synovial joints such as the hip and knee; articular cartilage is gradually lost as a result of ageing, obesity, irritation of the joints, muscle weakness and wear and tear. Spurs of new bone form around the subchondral areas and at the margins of the joint as the cartilage degenerates, this reduces the joint space which restricts motion. The loss of articular cartilage also results in painful bone-on-bone contact in the joint [52]. To reduce pain and restore function Total Hip

Arthroplasty (THA) may be performed. Around 95% of THA procedures are performed for OA [53], however it me may also be performed in cases of rheumatoid arthritis, tumour resection, trauma and birth defects such a dysplasia. THA involves surgical removal of diseased and damaged articular cartilage and bone, which are replaced with implants [54]. Generally a THA consists of a femoral component and modular femoral head (although mono bloc femoral components are available), and an acetabular component, which may be mono block in construction or consist of a metal shell with an inner liner (often UHMWPE or ceramic) (Figure 2 left).

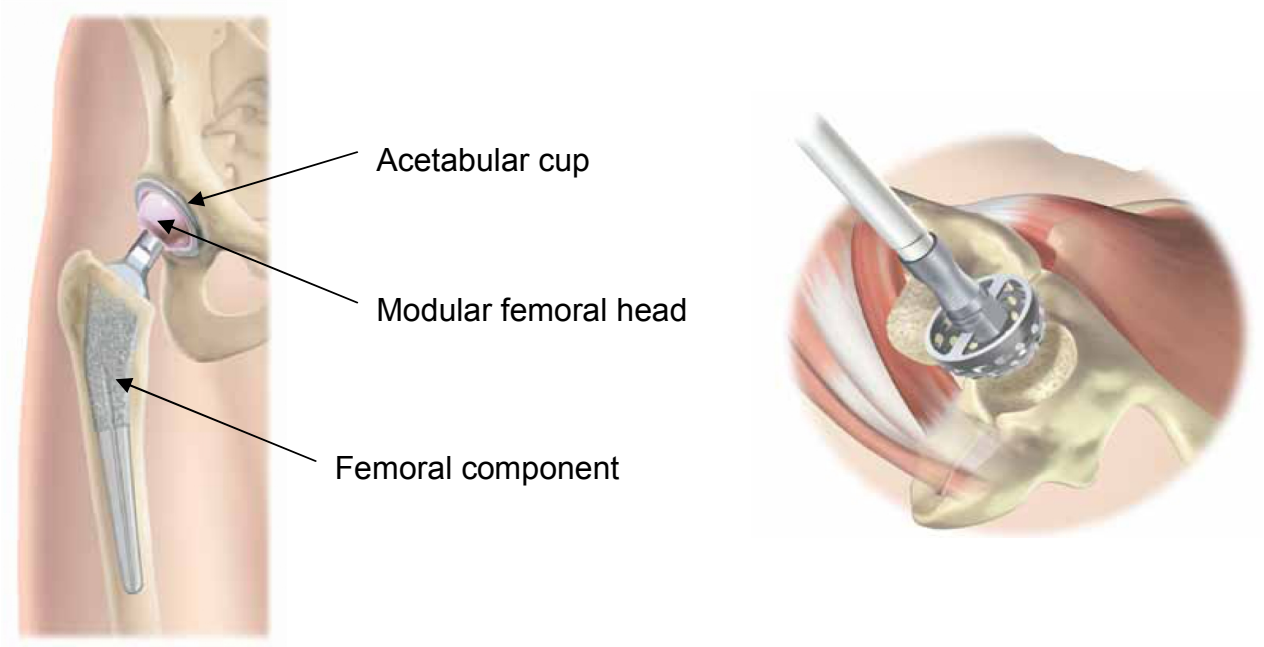

Figure 2 Components of Total Hip Arthroplasty (left), reaming the acetabulum (right) (images from Biomet UK Ltd operative technique brochure)

This project will focus on the acetabular component of THA. The components can either be fixed in place with bone cement or used without cement. In a cementless procedure the acetabulum is reamed to a slightly smaller diameter than that of the cup which is to be inserted. The cup is impacted into the bone and the pressure of the bone against the cup provides initial stability [55]. Over time, bone grows into a porous coating on the implant to provide long term fixation [56, 57]. The “under-ream” is defined as the level of interference fit between the acetabular cup and reamed acetabulum; impacting a cup with an outside diameter of 50 mm into a 49 mm diameter cavity would be a 1 mm under-ream, a 50 mm cup into a 48 mm cavity

would be a 2 mm under-ream and so on. In this project cup size has been defined as the nominal outside diameter of the implant. There are a number of cementless acetabular shells on the market, some examples, which are subsequently referred to, are summarised in appendix 1.

Chapter 2 – Literature Review

2.1 Introduction

Total joint arthroplasty is a highly successful procedure with over 1 million surgeries being performed worldwide each year [1]. However there are limitations with current designs of Total Hip Arthroplasty (THA); osteolysis is the dominant problem which results in aseptic loosening [2, 3]. In the UK aseptic loosening and lysis are the two most common reasons for revision of THA [4], with aseptic loosening accounting for 45% of revisions cases and lysis 14% [53].

Wear debris, generated primarily from the articulating surfaces, plays a central role in the initiation and development of periprosthetic osteolysis. It triggers foreign-body granuloma formation at the bone-implant interface, leading to aseptic loosening of the implant [2, 3]. The extent of the foreign body response is dependent on the size, type, number and surface area of the particulate debris [2, 3]. Polyethylene debris stimulates the greatest bone resorbing response due to the large number of particles produced, which persist within the periprosthetic tissue [2, 3].

To reduce the risk of osteolysis caused by UHMWPE, hard-on-hard bearings have been introduced. *In vitro* studies of metal-on-metal (MOM) and ceramic-on-ceramic (COC) articulations have shown considerable reductions in wear compared to hard-on-poly bearings [5, 7].

In vitro, metal-on-metal bearing couples have been shown to have wear rates of 100 time less than metal-on-polyethylene [7]. Although the wear of MOM articulations is low, local accumulation and systemic distribution of cobalt chromium particles and ions have been reported [6, 58]. The potential adverse effects of this are the subject of continuing debate [3, 13]. Adverse effects could include ion hypersensitivity [11, 12], toxicity, carcinogenesis [3, 13] and aseptic lymphocytic vascular and associated lesions (ALVAL) [12, 14]. Ceramic-on-ceramic bearings offer an alternative to MOM. It has been shown that metal ion levels in patients with COC THA were not

significantly different to a control population without THA [6]. The macrophage reaction to ceramic particles has been shown to be reduced in comparison to polyethylene particles, suggesting a biological advantage [59]. Concerns over intraoperative [60] and post operative [61-63] ceramic liner chipping have been raised, however the incidence of ceramic fracture is low [63]. There is little information in the literature concerning osteolysis associated with ceramic articulations, and generally osteolysis is limited to cases of massive wear [3]. Another rare complication with COC THA is squeaking [64], it has been suggested that this is related to acetabular component orientation, edge loading and stripe wear [64, 65]. Squeaking of metal-on-metal resurfacing arthroplasty has also been reported [66, 67].

A possible compromise between MOM and COC is ceramic-on-metal (ceramic head against metal counter face). This bearing combination has been shown to have wear rates up to 100 times lower than MOM in simulator testing, both under standard [8, 9, 68] and microseparation conditions [10, 68]. It has also been reported that COM bearings release fewer metal ions than MOM *in vitro* [9, 10] and *in vivo* [68]. Early clinical results appear to be promising [68], however patient numbers are small and follow up is short term.

Dislocation is another major problem with THA and is reported to be the 4th most common cause of revision in the UK [4]. The risk of early dislocation (within 1 year) has been reported to be 1.7% for primary and 5.1% for revision THA [15]. Higher rates of dislocation have been reported when also taking late dislocation into account; 2.6% [16]. Increasing the diameter of the femoral head has been shown to be associated with a reduction in the risk of dislocation [15, 17-19]. However with an UHMWPE bearing increasing the size of the femoral head has been shown to result in higher wear [20-22]. For a given outer diameter acetabular component, increasing femoral head size will result in a thinner UHMWPE liner, which has also been reported to increase UHMWPE wear [21]. Thus UHMWPE is not considered to be suitable material for articulation with large diameter femoral heads.

The use of large diameter articulations is not a new concept in hip arthroplasty and has been used in metal-on-metal hip resurfacing for many years. Implants such as the McKee-Farrar have reports of excellent clinical results at up to 28 years (84% survival at 20 years, 74 at 28 years) [69]. As a result of improvements in materials and manufacturing techniques resurfacing procedures gained popularity, with approximately 6500 resurfacing procedures performed in 2006 in the UK, however the numbers declined to 2500 in 2011 [53]. The Birmingham Hip Resurfacing (BHR) (Smith and Nephew) is the most commonly used resurfacing component in the UK [4]. Results reported by surgeons from the designing centre give very high survival rates [70, 71]; Daniel *et al.* reported a survival rate of 99.8% at 5 years for young active patients [71]. Slightly reduced survival has been reported by surgeons from non designing centres [66, 72] however the results are good and the authors consider them to support the use of resurfacing. Patients receiving a BHR implant have been shown to have low dislocation rates [66, 71, 73, 74] compared with patients with small diameter THA [15]. However there is some concern over osteonecrosis of the femoral head after resurfacing [73, 75] as well as femoral neck fracture [12, 75-77], and in addition the concerns previously mentioned for metal-on-metal articulations in general. Recently one resurfacing hip has been voluntarily recalled from the market by the manufacturer; the ASR (DePuy) was recalled in August 2010 based on information from the National Joint Registry showing that the 5 year revision rate was around 13% [78]. There are also reports in the literature of high revision rates with this particular resurfacing device [79, 80], and reports of adverse reactions due to metal ion release such as pseudotumors [81]. However other designs of resurfacing implant have not experienced such high revision rates [12, 82].

A potential alternative to currently available bearing combinations, which is being investigated by Biomet UK Ltd, is a large diameter ceramic head articulating on a thin polyetheretherketone (PEEK) cup. In the following sections of this review, PEEK material properties are described along with the biological reaction to PEEK, the history of PEEK as an implant material and published data on PEEK for use as an acetabular component. This review also considers cup deformation, which is a potential issue with a thin walled acetabular cup. Finite element modelling offers a

method to investigate the effect of design parameters on cup deformation without the need for large numbers of samples, therefore the available literature on creating FE models of the pelvis will also be reviewed as a potential method for design validation.

2.2 PEEK Material

Poly Ether Ether Ketone (PEEK) is part of a relatively new family of high temperature thermoplastic polymers (Poly Aryl Ether Ketones - PAEK). It consists of an aromatic backbone molecular chain, interconnected by ketone and ether functional groups [26] (Figure 3).

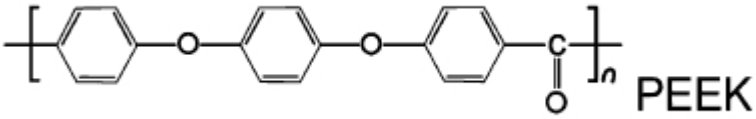

Figure 3 Structure of PEEK

This chemical structure makes PEEK stable at high temperatures (exceeding 300ºC) [83], resistant to chemical [84] and radiation damage [85] and compatible with many reinforcing agents [26, 86]. The biocompatibility of PEEK and CFR-PEEK (Carbon Fibre Reinforced PEEK) was demonstrated 20 years ago by Williams *et al.* [87]; since then their use as implant materials has been the subject of ongoing research and successful clinical use [31, 34, 88].

As PEEK is chemically inert and insoluble in conventional solvents it is challenging to synthesise. High temperatures (300 ˚C) and dangerous solvents such as bensophenone and diphenylsuphone are required for the polymerisation of PEEK; as a result dedicated plant facilities with rigorous safety procedures are required. Unlike other thermoplastics, polymerisation is usually carried out in batches, which contributes to the higher cost (PEEK being at least two orders of magnitude more expensive then low-temperature thermoplastics such a polyethylene) [89].

To produce CFR-PEEK; carbon fibres are blended with PEEK in its powder form above the melt transition temperature to give a homogeneous distribution of fibres while the polymer is in a flowing, molten state. To achieve the high degree of

consistency required for implantable CFR-PEEK, specialist equipment such as a twin screw compounder is used to blend the PEEK with the fibres, to give reproducible rheological behaviour [89].

PEEK and CFR-PEEK can be processed using traditional plastic processing methods such as; injection moulding, extrusion and compression moulding. Injection moulding is an attractive manufacturing process for mass production of PEEK implant components. PEEK pellets are introduced into to a heated screw assembly that melts and pressurises the molten polymer so that it flows into a heated mould. Injection moulding requires a significant financial investment due to the cost of designing and manufacturing the mould tool; as a result the process is not suitable for prototyping or low volume production [89].

Extrusion can be used to produce long stock shapes such as rods and sheets. PEEK pellets or granules are fed into a heated screw assembly that melts and pressurises the molten polymer, which is then forced through a heated die and allowed to cool slowly. Compression moulding produces stock shapes such as plates or thick sheets. Two heated platens are pressed together and heated to consolidate resin powder or granules. In general compression moulding is used for low volume production, prototyping and evaluation work as it is relatively inexpensive compared to injection moulding, however cycle times are longer and as a result it is not suitable for high volume production. Compression moulding is not often used to produce CFR-PEEK as it is difficult to ensure uniform fibre distribution [89].

PEEK and CFR-PEEK can be machined and finished using standard techniques used for other engineering thermoplastics, although carbide or diamond tipped tools and bits are required [90]. Moulding can result in residual stresses in CFR-PEEK and PEEK, therefore it is recommended to anneal components. In addition machining and finishing can also result in stress build up within the material due to localised heating at the cutting point. If a large amount of machining is carried out a second annealing procedure may be required [90].

2.2.1 Material Properties

The mechanical properties of PEEK are influenced by strain rate [91-94], temperature [91, 92, 95], molecular weight and the size and orientation of the crystal regions [93]. The mechanical properties of PEEK generally decrease with increasing temperature up to 250º, with a pronounced drop off above 150º (glass transition temperature) [92, 93, 96]. For biomaterials applications the operating temperature would be around 37º; in this case PEEK is relatively insensitive to temperature [91, 93]. However in some implant applications there is the potential to generate heat, such as impact loading during implantation or friction from articulating parts, although it has been shown that the temperature increase as a result of friction in a THA is only around 8 ºC [97].

Within the elastic limit temperature and strain rate should not be primary concerns for PEEK in biomaterials applications [91, 93]. The elastic properties of PEEK are relatively unaffected by rate effects at body temperature [91, 93]. However yielding and flow are slightly affected by strain rate at physiological temperatures [91, 93]. In uniaxial compression varying the strain rate from 10^{-4}-s^{-1} (nearly quasistatic loading) to 10^{3}-s^{-1} (impact loading) increased the yield strength by around 30% [93]

Crystallinity has a strong effect on the mechanical properties [93] and is dependent on the thermal processing history of the material [98]. Injection moulded parts are susceptible to heterogeneous material properties because cooling rate depends on thickness [98]. Injection moulded PEEK surfaces also typically present a thin amorphous polymer skin formed from contact with the mould. Machining removes this skin and increases the likelihood of exposing regional variations in the bulk polymer, including encapsulated carbon fibres [99].

The fatigue behaviour of CFR-PEEK has been reported to be much better than glass reinforced or neat PEEK [98, 100]. While neat PEEK is highly notch sensitive, CFR-PEEK is more insensitive to notches [100]. The fatigue behaviour of CFR-PEEK is complex, involving interactions between polymer and fibre [100]. Other mechanical

properties are also improved by reinforcing PEEK with carbon fibres, for example Nisitani *et al.* found that the tensile strength and elastic modulus of CFR-PEEK was approximately 1.3 and 2.4 times those of neat PEEK [100]. Table 1 shows the Young's modul of CFR-PEEK, traditional biomaterials and cortical bone.

Table 1 typical Young's modulus for materials used in THA

Material	Young's Modulus GPa
CFR-PEEK	15 [90]
CoCr	210 [54]
Titanium (Ti6Al4V)	100 [54]
UHMWPE	0.9 [101]
ZTA ceramic	380 [102]
Cortical bone	17 [103]

2.2.2 Biological Response to PEEK

PEEK-OPTIMA, CFR-PEEK-OPTIMA and Motis (CFR-PEEK) compounds and composites have undergone extensive biocompatibility testing to meet the criteria for FDA approval [26]. Katzer *et al.* carried out *in vitro* cytotoxicity and mutagenicity tests on PEEK according to WHO, ISO and ASTM recommendations. The tests produced no evidence of mutagenic or cytotoxic activity of PEEK [25]. The tests were carried out at body temperature (37ºC), testing at high temperature was not considered as PEEK is largely inert up to 260ºC [25, 83]. Other *in vitro* tests have also shown PEEK not to be cytotoxic [24, 28].

Biocompatibility studies have also been carried out on PEEK wear particles; Howling *et al.* investigated the response to CFR-PEEK wear particles generated from pin-on-disc tests, it was shown that that CFR-PEEK wear particles displayed significantly less cytotoxicity than metal (CoCr) wear debris [23]. Rat and mouse models have shown that CFR-PEEK wear particles elicited a similar response to UHMWPE particles when challenged with the same dose [27, 29]. It should be noted that although the response was similar PEEK has been shown to have lower wear rates than UHMWPE [104].

There have also been a number of studies on the response of osteoblasts to PEEK; it has been shown that implantable grade PEEK elicits a similar osteoblast response and bone forming capacity to rough titanium [99]. The cellular response was affected by the industrial processing, surface roughness and topography, however all PEEK variants permitted a degree of mineralization [99]. The growth behaviour of cell lines of the skeletomotor system on untreated PEEK has been compared to other biomaterials such as CoCr and UHMWPE. No toxic effects were seen for the untreated PEEK, however there was no stimulating effect on cell proliferation in comparison to the other materials tested [24].

The application of surface coatings such as porous titanium and HA to PEEK has been the subject of research [36-38, 105-107]. Vacuum plasma spraying titanium and HA on to CFR-PEEK has been shown to produce a titanium layer which completely covers the substrate [36, 37, 106, 107] without observable deterioration of the substrate's physical properties [37, 107]; a titanium coating of 10 to 150μm is achievable [107]. Cross section analysis has shown good interlocking between the HA and titanium coating and the titanium layer and the PEEK substrate [107]. *In vivo* studies have shown that titanium coated PEEK [105] and CFR-PEEK [38] specimens achieve significantly higher percentage of bone on-growth than uncoated specimens [38, 105]. There is some discrepancy in the coating adhesion values reported; Beauvais *et al* reported that that the adhesion between the HA and PEEK was significantly lower (7 MPa) than that for titanium-HA (18 MPa). However the authors suggest that this may be due to the test method used, which involves polymerisation of the adhesive at 180º for 2 hours [36]. Vedova reported adhesion values of around 17 MPa for HA coating on CFR-PEEK [37], which is within the ISO limit (ISO 13779-4) of 15 MPa. Latif *et al.* found that the Ti/HA adherence was on average 13.8 MPa and the titanium adherence was on average 33.7 MPa on the CFR PEEK Mitch cup [27]. The discrepancy between the various reported values may be due to the different test methods employed, as well as the processing parameters used to create the coatings, such as surface roughness of substrate material, particle size of powder, carrier gas rate, plasma power, spraying time etc.

2.2.3 History of PEEK use in Implants

In the mid to late 1980s researches began exploring the use of high performance thermoplastics such as PEEK and PAEK in composite trauma and hip stems [84]. The first widespread commercial application of PAEK was in spinal implants [26], PEEK was an attractive material due to its radiolucency, which facilitates radiographic assessment of fusion *in vivo*, and lower stiffness than titanium which helps load sharing and reduces stress shielding. PEEK biomaterials have over 15 years of successful clinical history in load sharing fusion applications in the spine [26]. The first implantation of carbon fibre reinforced PEEK and PEKEKK (Poly-Aaryl-Ether-Ketone-Ether-Ketone-Ketone) spinal cages was the subject of a pilot clinical study; 26 patients took part in the 2 year study [31]. Due to the encouraging results of this and other studies a prospective multi-centre IDE (investigational device exemption) study started in November 1991; the cage was clinically successful in 89% of patients at 10 years [30]. There have also been a number of studies investigating the use of neat PEEK for cervical and lumbar spinal cages [26, 88].

PEEK and other high performance thermoplastics have also been investigated as candidate materials for fracture fixation devices [26, 84, 108, 109], and carbon fibre epoxy plates have successfully used clinically [110, 111]. CFR-PEEK has been identified as a suitable material for fracture fixation devices, however this has not been investigated clinically [26]. This may be due to the fact that CFR polymer plates are more costly to manufacture than metallic devices.

CFR-PEEK has also been employed in composite femoral stems [32-35]. For example the Bradley stem (Orthodynamics, Dorset UK) which was developed in 1986 and implanted in 65 patients between 1992 and 1998 [34]. The stem consists of a tapered metallic core with a CFR-PEEK outer layer, it is proximally coated with HA [34]. The clinical results have not yet appeared in peer reviewed literature [26]. The Epoch stem (Zimmer) is a three part composite femoral stem consisting of a forged CoCr core, an intermediate layer of PEKEKK resin and an outer bone in-growth layer of commercially pure Ti fibre mesh. Human clinical trials showed the stem to have excellent intermediate term results with radiographic and histological evidence of osseous fixation, with less loss of bone mineral density compared to a

stiffer stem [32, 33]. The latest version of the stem has PEEK rather than PEKEKK as the intermediate layer [35].

2.2.4 PEEK as a Material for Acetabular Components

There have been a number of studies published on pin-on-disc (or plate) testing carried out on PEEK and PEEK composites against various counter faces [23, 112, 113]. Pin-on-disc testing with UHMWPE, PEEK and CFR-PEEK (30wt%) against steel with water as the lubricating medium has given specific wear rates of 6.5×10^{-8} mm^3/Nm for CFR-PEEK compared to 1.5×10^{-6} mm^3/Nm for UHMWPE and 2.2×10^{-5} mm^3/Nm for neat PEEK [114]. CFR-PEEK with pitch and PAN based fibres have been shown to have very low wear rates against Biolox Forte and Delta ceramics in pin-on-plate testing [23, 113]; CFR-PEEK pitch pins against Biolox Forte plates gave the lowest wear rate [113]. This study is more clinically relevant than the study by Davim *et al.* [112] as it was carried out in bovine serum and control soak samples were used. Pin-on-plate testing has also been carried out with both pitch and PAN based CFR PEEK against high and low carbon cobalt chromium, the results showed similar wear rates to pin-on-disc testing of CFR-PEEK on ceramic materials [115].

Pin-on-plate machines do not attempt to accurately recreate *in vivo* conditions, they are used for materials screening to assess the wear that will occur when two materials come in contact [113]. Therefore simulator testing is required to more accurately represent the clinical situation. Early wear testing on representations of hip joints found that CoCr heads were not suitable for articulation against CFR-PEEK [104]. The combination that gave the lowest wear rate was a zirconia head against a pitch based composite (0.39 $mm^3/10^6$cycles) displaying only 1% of the wear of the UHMWPE liner tested (35 $mm^3/10^6$cycles) [104]. Further testing of representations of a tibial component of a TKA (Total Knee Arthroplasty) and THA representations (simple cup and sockets rather than actual implants) tested with various fibre loadings (0 to 50 wt%) found that the PEEK TKA representations all exhibited significantly higher wear rates than the UHMWPE control [40]. The 20 wt% and 30 wt% CFR-PEEK THA sockets showed $1/10^{th}$ and $1/20^{th}$ of the wear rate of the UHWMPE control sample respectively when articulated with an alumina head [40].

The best wear couple was the 30% pitch-CF composite socket with a zirconia head; this gave 1/30th the wear rate of the UHMWPE control [40].

It should be noted that the UHMWPE cups used by Wang *et al.* were gamma sterilised in air [40, 104], this is no longer state of the art and has been shown to result in oxidative degradation of the material [101]. Wear of UHMWPE gamma sterilised in air has been shown to be significantly higher than that sterilised in an inert atmosphere [101]. Sterilisation of UHWMPE by gamma radiation in air results in oxidation of free radicals in the material, which persist for years and results in an increase in density and crystallinity, leading to progressive loss of mechanical properties and embrittlement [101]. It has been shown that the wear properties of PEEK are not affected by excessive gamma irradiation and accelerated oxidative aging [47].

Although studies have shown that zirconia femoral heads provided the best wear rates with CFR-PEEK [40, 104] in more recent studies zirconia has not been considered as a candidate bearing surface. Zirconia femoral heads from certain manufacturing batches experienced unacceptable fracture rates and were withdrawn from the market [116], zirconia heads may also undergo roughening *in vivo* due to hydrothermal degradation; frictional heating may result in surface phase transformation from tetragonal to a monoclinic phase, with the monoclinic phase occupying more volume and therefore resulting in roughening of the surface [117]. Thus alumina and alumina based ceramics have become the femoral head materials of choice [26].

Early simulator studies were conducted on representations of acetabular cups or tibial components, more recently actual implants have been tested. The average wear rate of 28 mm CFR-PEEK (30%) injection moulded acetabular liners with resin rich or machined surfaces against alumina and zirconia heads was reported as 0.43 mm^3/million cycles (a factor of 10 lower than a UHMWPE control sample) [39]; machining of the internal surface had no significant effect on wear rate [39]. Simulator testing of the MITCH (Stryker, New Jersey, USA) horse-shoe shaped acetabular cup showed overall weight gain during the first 1.6 million cycles due to

lubricant absorption and protein deposition [27]. The mean wear rate after 25 million cycles was 23.3 mm^3 or 0.936 mm^3/million cycles [27], Scholes *et al.* report a similar wear rate of 1.16 $mm^3/10^6$ cycles. Stribeck analysis of the friction testing before and after the wear testing showed that the joint worked under a mixed boundary lubrication regime [118] .

Joint simulator testing has also been carried out on unicondylar knee replacements (Oxford Partial Knee, Biomet UK Ltd) with pitch based CFR-PEEK meniscal bearings and CoCr tibial and femoral components. Both medial and lateral components were tested; the medial component showed higher wear rates than the lateral (1.70 mm^3 $/10^6$ cycles compared to 1.02 mm^3 $/10^6$ cycles), the difference between the medial and lateral components is due to the 5 mm axial load offset which was applied, resulting in a higher load on the medial side (as seen *in vivo)*. This was approximately three times lower than the wear rate found for metal-on-UHMWPE uni condylar knees. Friction tests showed that the bearings operated in boundary-mixed lubrication at physiological viscosities [119].

A limitation of these simulator wear results is that they are testing under idealised conditions. Microseparation has been shown to occur *in vivo* in THA [120, 121]. For hard-on-hard bearings when microseparation is replicated *in vitro* it has significant effects on the wear results [122] and tribology of bearings [123], however this is not the case for hard-on-polyethylene bearings [124]. Cup angle has also been shown to have a significant effect on wear *in vitro* [125]; wear of cups at an inclination angle of greater than 45º has been shown to be significantly higher than one at 45º (in metal-on-metal joints) [122, 125], this may be due to the break down in the fluid film as a result of edge loading.

2.2.5 Early Clinical Results

There is very little published data on CFR-PEEK acetabular components in clinical use. Pace *et al.* reported on a retrieved CFR-PEEK insert which was revised due to infection secondary to trauma 28 months after implantation [44]. The insert was part of the ABG II hip system (Stryker) and articulated with a 28 mm alumina head. At revision the insert was well secured in position in the cup. The wear depth of the

retrieved insert was 0.130 mm, and was localised in the area of maximum wear, offset from the cup pole. Due to the small volume of wear particles found in the surrounding tissue the authors suggest that a significant proportion of the measured deviation from the original surface was associated with creep deformation rather than wear [44]. However a manufacturer of medical grade PEEK (Invibio) state that CRF-PEEK has excellent creep resistance [90].

Pace *et al.* report on a 38 patient clinical review at 36 months involving a CFR-PEEK insert (ABG II). Harris hip score improved from 52 points preoperatively to 90 points, one patient was revised due to septic loosening at 28 months [43]. No material intolerance complications were reported [42]. The findings show the short term efficacy of the implant [43].

2.3 Cup Deformation

In the UK there has been a trend towards more cementless total hip replacement and fewer cemented procedures [4]. In 2010 of the 68,907 primary THAs undertaken 36% were cemented, 43% were cementless and 16% were hybrids (cemented stem, cementless cup) [53]. In the 7th annual NJR report (2009 data) it was noted that there was an increasing trend away from cemented procedures, with 2009 being the first year that cementless fixation overtook cemented fixations as the preferred method [82]. For a non-cemented acetabular cup, initial stability can be achieved by a press-fit between the cup and bone [126]. The acetabulum is reamed to a slightly smaller size than the implant, typically between 1 and 3 mm, the pressure of the bone against the cup provides initial stability [56]. Long term cementless fixation relies on bone growth into the porous surface of the implant [126]. Many currently available cementless acetabular components consist of a titanium or cobalt chromium alloy shell (often hemispherical) with a porous coating on the bone contacting side [126]. A bearing surface is then fitted into this shell, usually UHMWPE, CoCr or Ceramic, either by a taper fit in the case of hard bearing or a locking mechanism for polyethylene. In order to preserve bone stock, thinner resurfacing cups have been introduced [45, 51] which also allow larger diameter heads to be used which can also reduce the risk of dislocation [45]. The Biomet PEEK cup is intended to be monobloc

in design (i.e. the bearing surface is integral in the shell rather than fitted post impaction), inserted without cement with a plasma sprayed porous titanium coating.

The use of thinner more flexible resurfacing cups has raised concerns about the potential for deformation during press-fit impaction [45, 49, 51]; this concern has also been raised for standard acetabular cups [46-48, 127]. Such deformation could adversely affect the fluid film lubrication of metal-on-metal bearings [49, 50], it could also lead to equatorial and edge contact possibly causing the implants to jam [45, 51]. Cup deformation could also influence implant stability and fixation, producing unfavourable conditions for osseointegration and possibly affect periprosthetic bone remodelling [45, 51]. Other potential problems include chip fractures of ceramic liners during insertion into deformed cups or damage to locking mechanisms [46].

There have been a number of reports in the literature of deformation of standard acetabular shells on impaction *in vivo* [46, 48]. For example Langsdown *et al.* reported that 16% of initial post operative radiographs of patients with the titanium Trident Shell (Styker, Warsaw, USA) showed evidence of incomplete seating of the ceramic liner, which was attributed to shell deformation [47]. Squire *et al.* [46] reported that 90.5% of Pinnacle shells (DePuy) had measurable diametric compression deformity which ranged from 0 to 0.57 mm (mean 0.16 mm) when inserted with a 1 mm press-fit technique [46].

In vitro studies have measured the deformation of both resurfacing and standard cups using polyurethane foam [48, 49, 51, 128, 129], cadaveric specimens [48, 51, 127] and rim loading [46]. The current study will focus on bringing all these methods together and comparing their ability to assess the likely deformation which occurs on impaction of a press fit acetabular cup.

Using polyurethane foam Fritsch *et al.* [48] found that a standard titanium acetabular cup exhibited a change in diameter of around 22 μm on impaction [48]. Jin *et al.* found that a typical MOM resurfacing component deformed by up to 103 μm when impacted into polyurethane foam and cadaveric specimens [51]. Schmidig *et al.* found a maximum shell deformation of 0.78 mm for the Trident shell (Styker,

Warsaw, USA) when impacted into polyurethane foam using 1 and 2 mm under-reaming [128]; in a similar test Ong *et al.* found that the Trident cup deformed by 0.45 mm [129]. Squire *et al.* [46] investigated deformation of the Pinnacle (DePuy, Warsaw, USA) shell on impaction *in vivo* and *in vitro*. In the *in vitro* testing, rim loading of up to 2000 N was used to simulate tight peripheral rim fit; deformation ranged from 0 to 0.9 mm (mean 0.34 mm) [46].

In silico studies have also looked at acetabular cup deformation. Yew *et al.* [130] created a 3D FE model of the polyurethane foam construct used by Jin *et al.* [51]. The FE model slightly over estimated the cup deformation compared to the *in vitro* testing [130]. Udofia *et al.* used a homogeneous FE model of the pelvis to investigate deformation of a resurfacing cup, the deformation was greatest in the superior-inferior direction and varied as a result of press-fit technique (48.7 μm for 1 mm press-fit, 94.6 μm for the 2 mm press-fit, 7.5 μm for the line-to-line) [131].

2.4 Modelling the Pelvis

As discussed in the previous section, cup deformation is a potential issue for acetabular cups. Given that PEEK has a lower modulus than the metals used in current designs there is the potential for a greater amount of deformation on impaction. Finite element modelling of the pelvis may provide a method for validation of the design and investigation into the effect of design parameters such as wall thickness on the behaviour of the cup without the need for extensive experimental testing.

The first Finite Element (FE) models of the pelvis were 2D and axisymmetric [132, 133] due to the low computing power required to solve them. As a result of the advancement of computers and the ability to solve FE models with millions of elements on desk top computers, 3D models are now common and can model the pelvis more accurately than the early 2D models [103, 134-137] .

Three dimensional FE models of the pelvis can be divided into two main categories; homogeneous and heterogeneous. Homogeneous models assume that the material properties of cortical and cancellous bone are constant throughout the pelvis and the

values are from published literature. The thickness of the cortical bone is also assumed to be constant (generally approximately 1 mm thick). In heterogeneous models the material properties are location dependent and are assigned using a relationship between apparent Calcium density from CT scan data [103, 138], the cortical thickness is also location dependent and is determined from CT data.

It has been suggested that for comparison purposes a less elaborate homogenous model may be used, however if absolute mechanical quantities are required, use of a more detailed model is required [135]. It has also been found that the most accurate predictions of bone stresses are obtained when position dependent cortical thickness and elastic modulus are used [139]. When constant cortical bone thickness and elastic modulus are used the models are significantly stiffer [139, 140]. It has been found that the inclusion of muscle forces in 3D FE models of the pelvis tends to reduce stress concentrations compared to using fixed boundary conditions [134, 141] and that models which include muscle forces behave in a way which better represents the *in vivo* situation [137, 141].

In order to use FE models for design validation it is important that the models are capable of accurately predicting bone stresses and strains. There have been a number of studies where 3D FE models of the pelvis have been validated using cadaveric models [135, 139, 140, 142-144]. These use simplified loading conditions and do not attempt to simulate muscle forces due to the complexity of modelling these muscle forces experimentally. Good correlation has been reported between strains predicted by FE models of the pelvis and experimental results when heterogeneous material properties are used and the simple experimental boundary conditions are replicated in the FE model [135, 139, 140, 142-144].

Finite element models of the pelvis have been used to investigate the behaviour of various implants, including hip replacements [57, 131, 136, 137, 140, 145-152], tumour reconstruction [153] and fracture fixation devices [154]. These models have varying degrees of complexity, with some being heterogeneous [140, 146, 153] and some homogeneous [131, 137, 141, 145, 154], some including muscle force [137, 140, 141, 146] while others do not [136, 145, 153]. Models with varying degrees of

complexity have been used to investigate the effects of various parameters (such as level of interference fit, screw fixation, friction coefficient at the bone-implant interface, bone density and acetabular cup material) on micromotion, fixation of acetabular cups, and stresses and strains within the bone.

Janssen *et al.* found that fixation (lever out strength) was improved by increasing the interference fit between bone and cup from 1 mm to 2 mm [150], however Spears *et al.* reported that 1 mm under-reaming provided better resistance to micro motion than 2 mm [149]. Udofia *et al.* found that the maximum contact pressure at the implant-bone interface was far greater in the 2 mm press-fit model than the line-to-line or 1 mm press-fit models [131] which is in agreement with the results of Janssen *et al.* [150]. The discrepancy between the results may be due to the fact the Spears *et al.* included polar gaps in their model (based on a previous two dimensional axisymmetric model in which Spears *et al.* found that a smaller inference resulted in a smaller polar gap after simulated impaction [147]), the 2 mm under-ream having a larger polar gap than the 1 mm and thus less contact area [149]. The level of press-fit has also been found to affect the amount of acetabular cup deformation [131]. Screw fixation has been found to have only a minimal effect on the level of micromotion of an acetabular cup [149] with the reduction only in the area local to the screws [145]. However a small amount of bone on-growth (simulated by tying pairs of nodes at the bone-implant interface) resulted in reduced micromotion which in turn allowed more bone on-growth [148]. Reduced bone quality (simulated by uniformly reducing the modulus of the bone) has been found to result in increased micromotion [145, 150].

The coefficient of friction between the bone and cup has been shown to have an effect on cup micromotion in FE models, with higher friction resulting in less micromotion [145, 150] however one study suggests that the effect is minimal [145] whereas others argue that it is more important [146, 150]. Thompson *et al.* found that the friction coefficient between the bone and cup had a large effect on stress distribution and magnitude with the higher (0.5) coefficient having higher stresses than the lower (0.1) coefficient in their heterogeneous model [146]. Friction coefficient has also been shown to be important when simulating impaction; if a very

low coefficient of friction is used the cup penetrated deep into the acetabular cavity but then on removal of the load the cup rebounded back to its initial position [147].

The influence of implant material choice has also been investigated; Thompson *et al.* suggest that material (they compared CoCr, UHMWPE and polyacetal) has little effect on micromotion and loosening, and that friction between the cup and bone has more of an influence on strain in the bone than material [146]. However Manley *et al.* investigated the effect of implant material on stress shielding (i.e. maximum compressive stresses) and found that for a hemispherical cup a significant reduction in stress shielding could be achieved by reducing the modulus of the cup by two orders of magnitude but that wall thickness had only minimal effect [151, 152].

2.5 Conclusion

The deformation a press-fit acetabular cup undergoes on impaction into the acetabulum is an issue that is widely reported on in the literature [45-49, 51, 127, 130, 155-157]. The possible effects of excessive deformation include; chipping of ceramic liners [46], damage to locking mechanisms for UHMWPE liners [46], equatorial or edge loading leading the bearing becoming jammed [45, 51], unfavourable conditions for bone in-growth resulting in poor fixation of the implant [45, 51], deformation of the acetabular implant could also affect the lubrication regime of the bearing [49, 50, 155]. The focus of this study will therefore be to find a suitable test regime to investigate the level of deformation the Biomet CFR-PEEK cup experiences on impaction, and how this deformation affects the lubrication of the bearing. In order to investigate deformation on impaction, previous studies have used polyurethane foam [48, 49, 51, 155, 158] cadavers [48, 51, 127] and FE models [130, 131]. Another possible method for exploring deformation is the creation of a finite element model of the pelvis to simulate impaction; the use of FE would enable investigation into the influence of design parameters on deformation without the need for a large number of test samples. Published data has shown that FE models created from medical imaging techniques, such as MRI and CT, are capable of predicting bone stresses [135, 139, 140, 142-144], and models have been validated using cadavers. The literature suggests that in order to obtain absolute

values of deformation a heterogeneous model is necessary, rather than a simpler homogeneous model [135, 139, 140].

Chapter 3: Acetabular Cup Deformation under Rim Loading using Digital Image Correlation and Finite Element Methods

3.1 Introduction

It has been shown that in a cadaveric model of a natural hip the load transfer area between the femoral head and the acetabulum is sickle shaped in the peripheral cranial articular surface with peripheral load transfer in the posterior-inferior and anterior-inferior portions of the articular surface [159, 160]. At the iliac and ischial bones the contact area was found to reach the rim of the acetabulum [160]. On press-fitting of a hemispherical acetabular cup load transfer occurs predominantly near the rim of the cup and is maximum in the diagonal axis between the iliac and ischial bone [160] (Figure 4 left). Cadaveric testing has also shown that the predominant areas of load transfer are between the ischial and iliac columns, the authors suggest that this is a worst case scenario [51]. FE models have also shown that contact between the bone and press-fit acetabular shell occurs mainly at the periphery of the superior acetabular rim [131, 137, 139, 141].

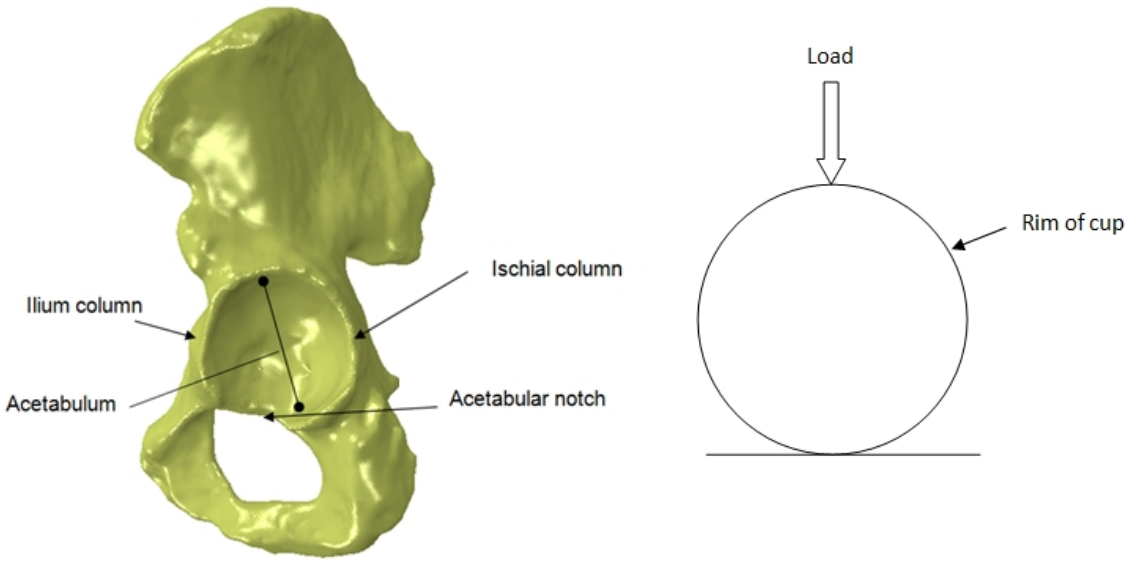

Figure 4 Areas of predominant load transfer in the pelvis (left), schematic of rim loading (right)

Rim loading (a point load applied to the rim of the acetabular cup (Figure 4 right)) has been previously used to investigate the deformation of acetabular shells; Squire *et al.* [46] investigated deformation of the Pinnacle shell (DePuy, Warsaw, USA) on impaction *in vivo* and *in vitro*. In the *in vitro* testing, rim loading of up to 2000 N was used to simulate tight peripheral rim fit; deformation ranged from 0 to 0.9 mm (mean 0.34 mm) [46]. A limitation of this study is that the deformation was measured using digital callipers which meant that the load had to be applied stepwise. Although Ong *et al.* reported using rim loading to validate their FE model of the Trident shell [129], there are no other reports in the literature where rim loading has been used to simulate tight peripheral fit.

In silico models have increased in popularity as a tool for preclinical testing [146, 151, 153, 161-163]; with this increase comes an increasing need for experimental model validation. This validation cannot always be satisfied with traditional measurement technology such as strain or clip gauges, or extensometers, which do not give full field measurements and require contact with the sample [164]. Digital Image Correlation (DIC) has been suggested as a method for validating numerical analysis without contact [165]. Few studies have reported the use of DIC to validate FE models; these include validation of a model of a tyre [166], model of a Sawbones femur [167] and modelling large plastic deformations of steel [168]. In all studies good agreement was found between the FE and DIC results.

The aims of the current study were;

1. To investigate the use of DIC as a method for validation of an FE model of rim loading.
2. To compare the deformation of two clinically successful acetabular shells to a prototype PEEK shell.
3. To assess the validity of rim loading as a pre clinical test.

3.2 Method

3.2.1 DIC

There are several methods for measuring the deformation of materials. It can be measured indirectly by assuming that the strain field is homogenious and that the displacement of the sample corresponds to the displacement of the cross bar, however this method includes the stiffness of the machine and is not necessarily a true measurement of the deformation of the sample. Contact methods such as gauges or extensiometers are accurate but limited in terms of contact points. Non contacting methods include grid methods [169], speckle laser [170] and Digital Image Correlation (DIC) [171, 172]. A non contacting method was chosen for the rim loading study. Previous studies on rim loading reported in the literature used Vernier to measure the deformation of the cups under test [46]. This requires the load to be applied and then physically measuring the deformation of the cup while the load is applied, which would not be safe in some situations; such as testing of ceramic components. DIC was chosen as the measurement method for the rim loading experiment because of the availability of the equipment at Cardiff University, the testing also provided the opportunity to investigate the suitability of DIC for future testing where gauges may not be appropriate (e.g. biological tissues such as bone).

DIC was first introduced in the early 1980's by researchers from the University of Carolina [171, 172]. It is an optical technique that uses image recognition to analyse and compare digital images acquired from the surface of a sample under test. The object is uniformly lit using an incoherent light source and digital cameras are used to record images of the sample as it is subjected to loading. A random dot pattern is applied to the surface of the test sample; this is known as a "speckle" pattern. Two images are acquired, one taken "before" and one "after" the deformation that results from the applied load. The images are digitised and stored on a computer for further processing. The surface displacements are determined from the positions of the greyscale distributions of the deformed image ("after") with respect to that of the reference image ("before") (Figure 5). The light intensity distribution at each point on the surface is unique, the distribution of light intensity of a particular point (x,y) can be described by the greyscale matrix F(x,y) over a selected subset of the image. After the object is deformed each position of the surface (x,y) is assumed to exist at

a new location (x*, y*). The displacement is determined by finding the position of the light intensity distribution F*(x*,y*) that most closely resembles the original distribution F(x,y). A search is performed on the “after” image to find the location with the greyscale distribution that is most consistent with distribution of the “before” image. The location of F*(x*,y*) is then obtained using the maximum correlation coefficient.

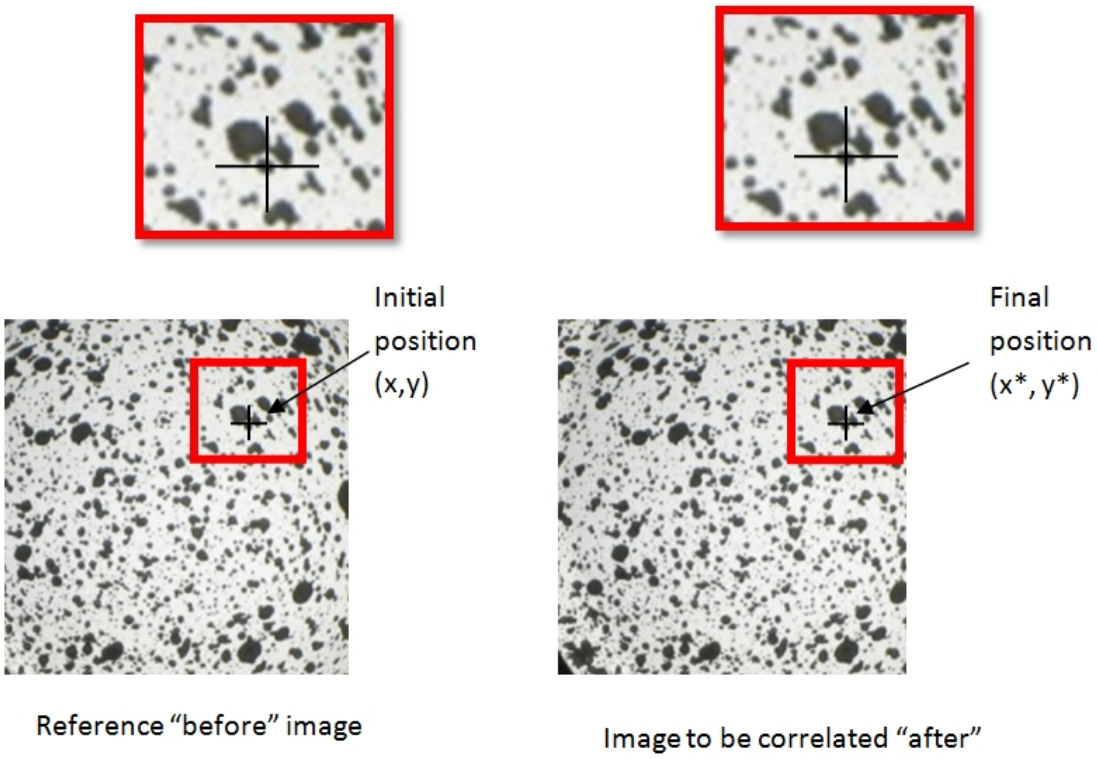

Figure 5 Digital image correlation; correlation between “before” and “after” image

The use of multiple cameras has extended application of DIC into 3D surface deformation measurement [173]. In three dimensional DIC two cameras record the deformation of a sample as it is subjected to mechanical forces [173]. A series of consecutive stereo images are taken throughout the test, which show the deformed speckle patterns relative to the initial pattern.

DIC has been used in a wide range of applications, including investigation into crack propagation and necking in steel [174], the mechanical behaviour of arterial tissue [175], fatigue and fracture behaviour of bone and hard tissues such as tooth enamel[176], loosening of cemented THA [177], damage to high performance

concrete [178], validation of an FE model of the femur [167] and deformation of pressure vessels [179]. DIC has also been used to find the mechanical properties of biological tissues by using it in conjunction with finite element methods, reducing the error between the model and the DIC results by altering the material properties used in the FE model. This method has been used to find the mechanical properties of bovine hoof [176], heart valve tissue [180], and skin [181, 182]. The majority of these studies have used a single camera resulting in 2D measurements. The use of two cameras to enable 3D non contact measurement is relatively new and not widely reported in the literature.

Factors affecting the accuracy of the calculated displacement include the size of the speckles in a given pattern and the size of the subset [183]. If the speckle size is less than two pixels, its actual location and light intensity will have higher uncertainty than that of a larger sized speckle [184]; if the centre of a speckle falls in the centre of a pixel, it will be sensed by nine pixels, however is the centre falls on the corner of a pixel, it will only be sensed by four pixels. Therefore if the speckle is only two pixels in diameter there will be greater errors in determining the speckle location and light intensity [184]. However if a speckle is too large the ability to accurately measure smaller strains will be reduced [184]. As well as the size of the speckles, random spray rather than a uniform pattern increases the accuracy of the technique [185]. In addition the speckled pattern must have sufficient contrast [186], for this reason samples without a natural textured pattern with sufficient contrast must first be painted white, and then a black speckled pattern applied. Other sources of errors include lighting, the optical lens, the CCD sensor and the arrangement of the equipment [185].

3.2.2 Samples

Table 2 gives the materials and dimensions of the cups tested, all samples were provided by Biomet UK Ltd (Bridgend, UK). Two methods of applying a speckle pattern were used; in both cases the concave surface and cup rims were first sprayed white, in the first case black spray paint was used to apply a speckle pattern, in the second black face paint was applied using a coarse sponge.

Table 2 Dimensions and materials of cup samples tested

Material	Thickness (mm)	OD (mm)	Number of samples
UHMWPE	11	58	2
UHMWPE	5	42	2
UHMWPE	5	38	2
CFR-PEEK (injection moulded)	2	45	3
CFR-PEEK (machined)	3	58	3
CoCr	3	48	2
CoCr	3	50	2
CoCr	3	56	2
CoCr	3	58	2
CoCr	3	60	2
CoCr	3	62	2

3.2.3 Digital Image Correlation

Initially a bench mark test was conducted to determine the accuracy of the DIC equipment in this test set-up. The DIC equipment (Limess Messtechnik & Software GmbH, Berlin, Germany) was set up as per the routine described below. A 20x60 mm speckle metal plate was attached to the carriage of a multi axis microscope (Pye Scientific, Cambridge, UK) in which the carriage can be moved by hand winding a Vernier scale (Figure 6 left). The carriage was moved 20 mm in steps of 0.5 mm and VicSnap (Limess Messtechnik & Software GmbH, Berlin, Germany) was used to capture the stereo images at each step. Camera calibration was performed using a calibration square provided by the DIC manufacturer (Limess Messtechnik & Software GmbH, Berlin, Germany). The “track point” function within the software was used to find the displacement of the plate. The test was repeated 4 times in both x and y directions (Figure 6 right).

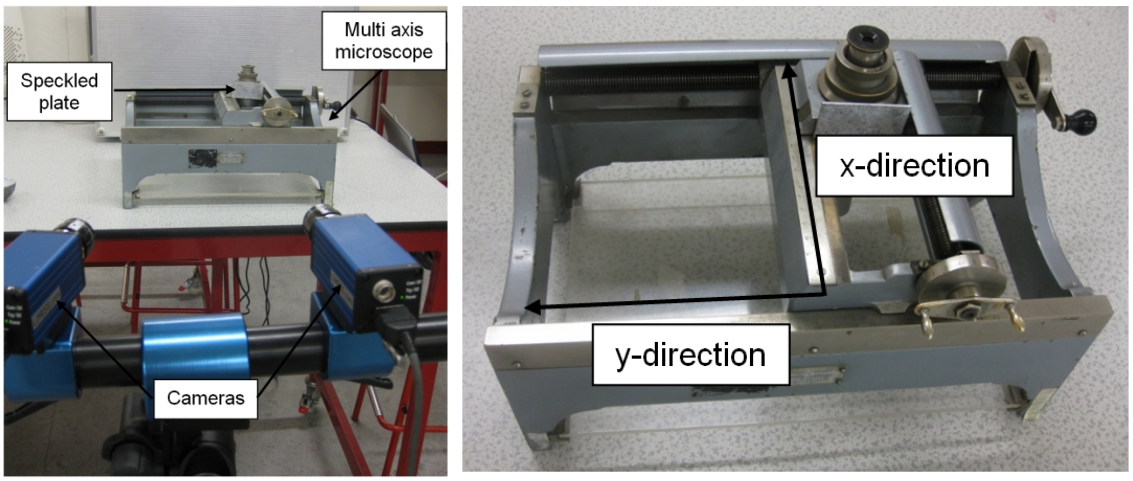

Figure 6 DIC bench test set-up showing cameras and multiaxis microscope (left), x and y directions of multiaxis microscope (right)

The cups were positioned in the (Losenhausen) servohydraulic test machine as shown in Figure 7. The platen was lowered until it just contacted the upper edge of the cup, the displacement was controlled by the PC connected to the servohydraulic test machine, at a rate of 5 mm/min. Vic Snap (Limess Messtechnik & Software GmbH, Berlin, Germany) software was used to simultaneously record the camera images and the voltage output from the servohydraulic test machine which was calibrated to the applied load. Vic 3D software (Limess Messtechnik & Software GmbH, Berlin, Germany) was used to process the images. The “track point” function allowed the deformation at the rim of the cups to be calculated by reporting the position of a specified point in each consecutive image.

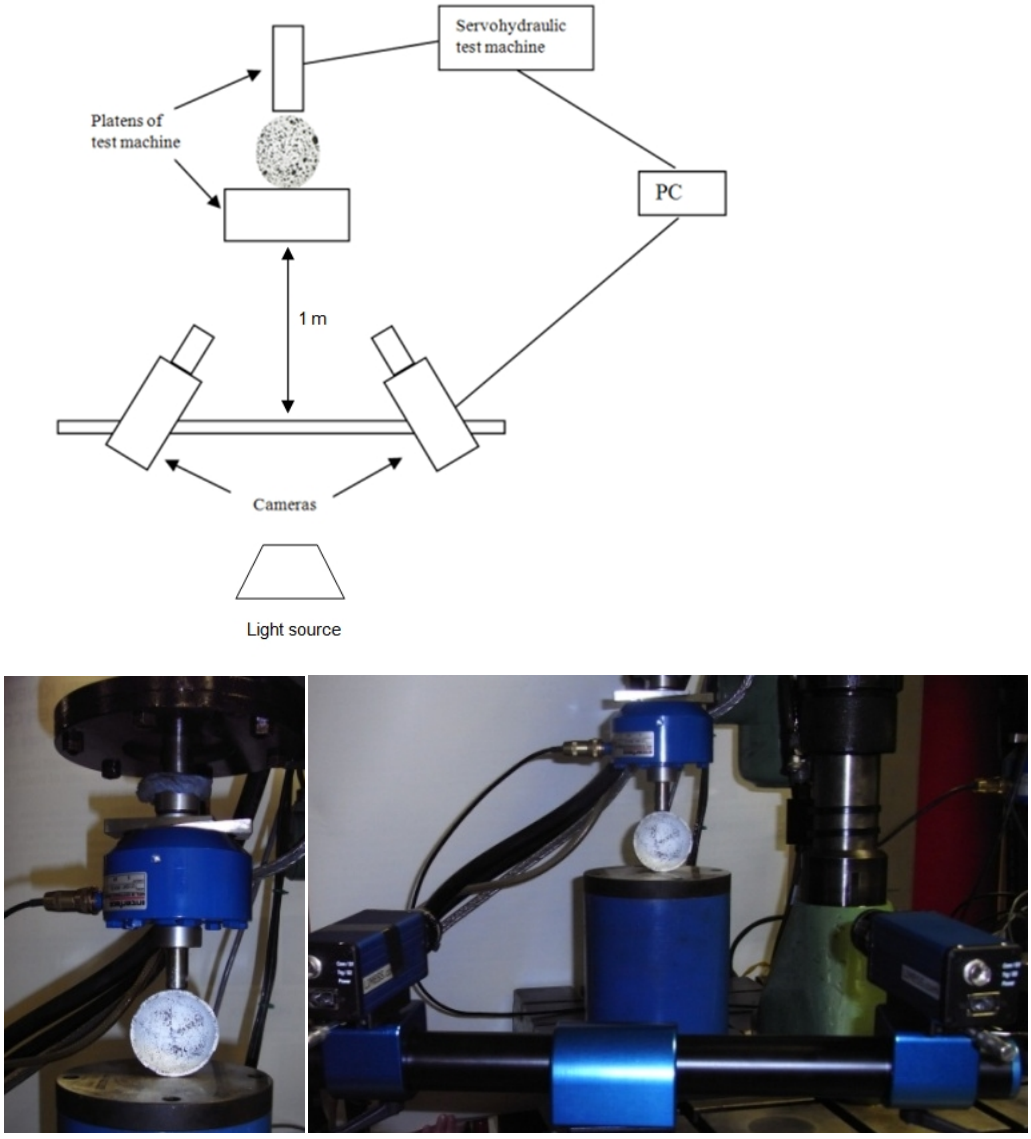

Figure 7 Schematic diagram of DIC set-up showing test piece, two cameras, PC and servohydralic machine (top), close up photo of speckle cup in test machine (bottom left), photo of camera and speckle cup (bottom right)

3.2.4 Finite Element Model of Rim Loading

Abaqus CAE version 6.8-1 was used to create models of the experimental setup for all cups tested; the cups were meshed using a free meshing technique with a modified tetrahedron mesh as this was the most suitable for the curved surfaces. Material properties were applied as per the manufactures information. The platens of the servohydraulic machine were represented as rigid bodies (Figure 8). A concentrated force was applied to the upper rigid body in the negative y direction. A frictionless surface contact was assumed between the rigid bodies and the cup.

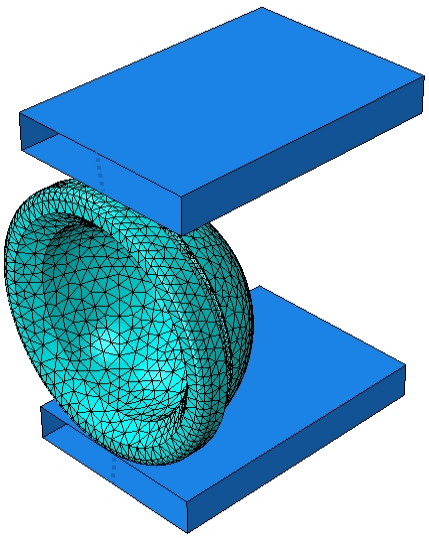

Figure 8 Example of a typical mesh and assembly with rigid bodies

FE models were also created to investigate the effect of design parameters on cup stiffness under rim loading. Cup wall thickness (WT), outside diameter (OD) and inside diameter (ID) offset were examined. In a true hemispherical cup the centres of the OD and ID have the same position; however the WT can be increased by offsetting the ID centre relative to the OD centre while maintaining the same dimensions for both diameters (see Figure 9).

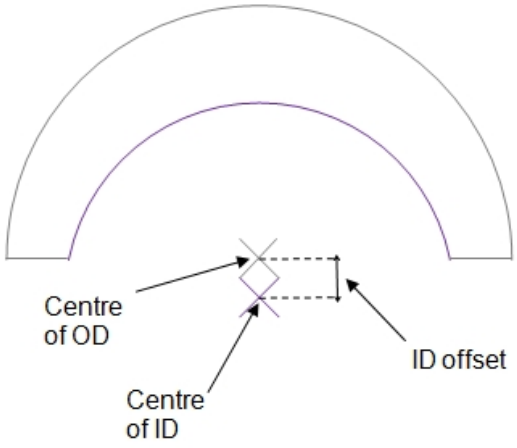

Figure 9 Internal diameter offset

3.3 Results

After an initial trial run it was found that creating a speckle pattern with black face paint allowed a more effective and quicker analysis using the Vic3D software, using the specked pattern created with spray paint the software was unable to repeatedly follow each point though the series of images. Therefore all the tests were carried out on face paint speckle samples.

The bench mark testing, described in section 3.2.3, demonstrated that over 20 mm of the microscope stage travel, in increments of 0.5 mm, with this experimental set up, the DIC was able to measure displacement with an accuracy of maximum error of ±0.08 mm and a mean error ±0.05 mm.

The Vic 3D (Limess Messtechnik & Software GmbH, Berlin, Germany) software processes the position of the speckle pattern, Figure 10 shows an example of the 2D overlay produced by the software.

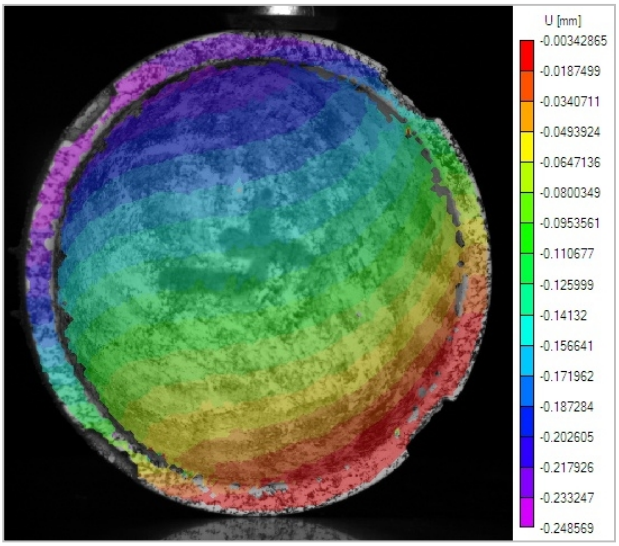

Figure 10 Example of 2D overlay from Vic3D (Limess Messtechnik & Software GmbH, Berlin, Germany) showing displacement in y direction relative to initial image.

In Figure 11 the load versus deflection curve for the injection moulded PEEK cup measured using DIC is compared to that predicted by the FE model. The FE was able to predict the stiffness of the cup with an error of less than 10%.

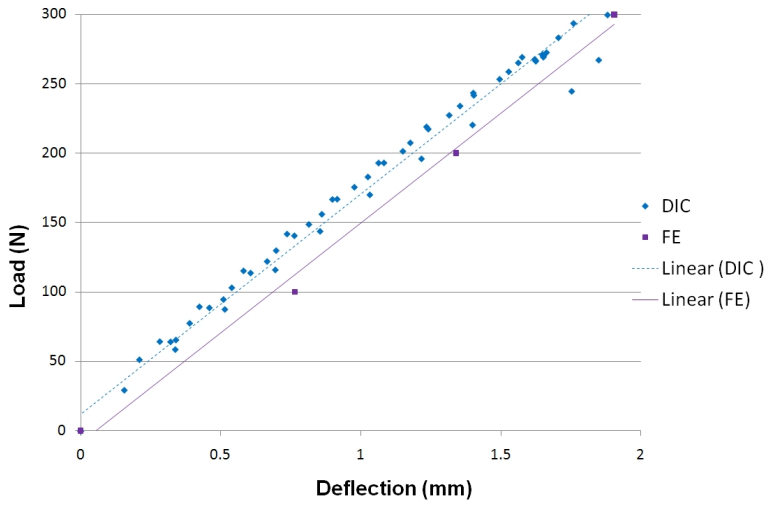

Figure 11 Load displacement plot for injection moulded PEEK cup

The experimental results (Table 3) showed that increasing the cup size of the cobalt chromium cup (with constant wall thickness) resulted in a reduction in stiffness (N/mm) of around 6% per 2 mm size increment, confirming that the largest cup size produces the worst case scenario in terms of deflection.

Table 3 Details of OD and wall thicknesses (WT) of CoCr cups, maximum diametric deformation predicted by FE (3 mm mesh density) and DIC results taken at 3000 N.

Material	WT (mm)	OD (mm)	FE prediction (deformation at 3000 N) (mm)	DIC result (deformation at 3000 N) (mm)
CoCr	3	48	0.33	0.36
CoCr	3	50	0.35	0.31
CoCr	3	56	0.42	0.47
CoCr	3	58	0.45	0.47
CoCr	3	60	0.47	0.50
CoCr	3	62	0.49	0.53

Table 4 Details of OD and wall thicknesses of polymer cups, maximum diametric deformation predicted by FE (3 mm mesh density) and DIC results taken at 300 N.

Material	WT (mm)	OD (mm)	FE prediction (deformation at 300 N) (mm)	DIC result (deformation at 300N) (mm)
UHMWPE	11	58	0.49	0.50
UHMWPE	5	42	2.80	2.98
UHMWPE	5	38	2.23	2.31
PEEK	2	45	1.78	1.79
PEEK	3	58	0.58	0.68

Table 4 shows the FE prediction and DIC results for the polymer and PEEK cups, the FE was able to predict the experimental deformation with a 10% error. A mesh convergence study was performed; it was found that reducing the mesh size improved the agreement between the FE and experimental results with no further improvement after a 2mm mesh (Figure 12 left). As expected the CoCr cup was found to be significantly stiffer than the polymer and PEEK cups of identical outside diameter (Figure 12 right).

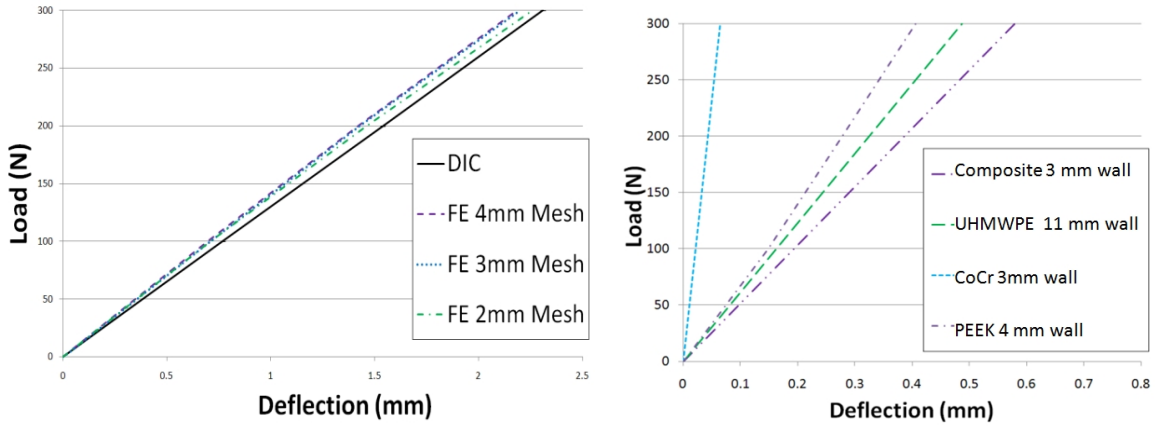

Figure 12 Load deflection plot for a 38 mm UHMWPE cup showing DIC and FE results with various mesh sizes (left), load deflection plot for 58 mm cups of various materials (right)

The FE models created to investigate the effect of design parameters on cup stiffness under rim loading (Figure 13) showed that increasing WT (with constant OD) increased the cup stiffness; for example, increasing the WT of the PEEK cup from 3 to 4 mm resulted in a 50% increase in cup stiffness. Increasing ID offset (with constant OD) also increased the stiffness of the cup for example; increasing the ID offset from 0 to 1 mm gave an increase in stiffness of approximately 20%, and increasing the ID offset from 0 to 3 mm resulted in an 85% increase in cup stiffness. Increasing the OD (with constant thickness) gave a decrease in cup stiffness of around 7% per 2 mm size increment for the smaller sizes (44-52 mm OD) with a smaller percentage decrease for larger sizes.

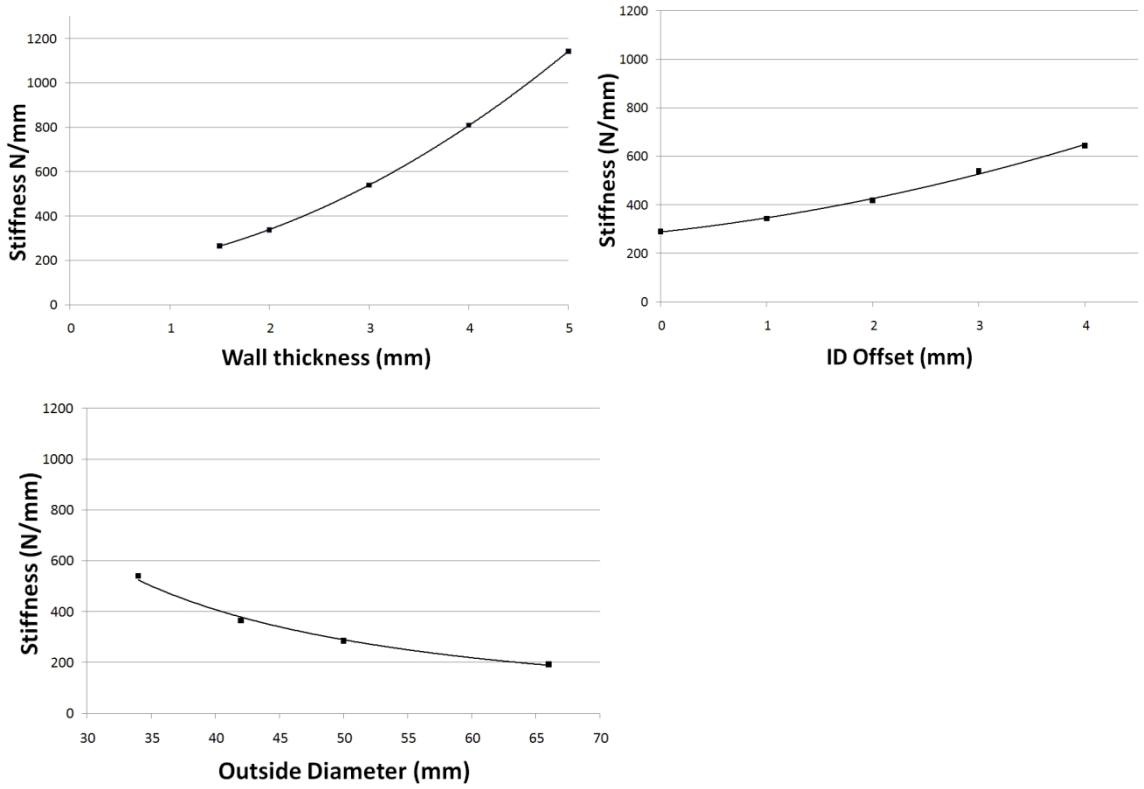

Figure 13 Graphs showing the effect of WT (top left), ID offset (top right), and outside diameter (bottom left) on cup stiffness for PEEK cups

3.4 Discussion

Physical testing has been used previously to validate FE models of implants [129, 161, 162, 187]. However to the authors' knowledge this is the first time digital image correlation has been used in this application, although DIC has been used recently to validate an FE model of a femur created using CT data of a Sawbones model [167]. Ong *et al.* [129] validated their FE model of acetabular cups using rim loading, cups were deformed under a load of 2 kN and the deformation measured using callipers, the model was able to predict the deformations with a 7.1% difference [129]. The FE model in the current study was able to predict the deformation of an acetabular cup under rim loading to within 10%, there was a trend for the FE to overestimate the stiffness of the cups. The CoCr cups were not dimensionally checked prior to testing; therefore it is possible they could have been out of tolerance; meaning that the FE models are not true representations of the actual cups tested. This could explain the variation between FE predictions and DIC results for some of the cups tested.

The load cell used is accurate to ±0.5%, the manufacturer of the DIC equipment reports an accuracy of 0.01 pixels, given the 1 mega pixel cameras used this should give an accuracy of 1 μm for the 100 mm measurement field used. However it has been shown that the properties of the speckle pattern, lighting conditions and measurement system affect the accuracy of the DIC measurement [183]. The validation work described earlier in the chapter (using microscope carriage) showed that the DIC equipment was able to measure displacement with an accuracy of ±1%. In the current study the same lighting conditions and measurement equipment was used in all cases, an initial trial run compared two methods of applying the speckle pattern and one was selected based on ease of analysis by the software. When spray paint was used to apply the speckled pattern the software failed to identify the position of selected points in every consecutive image, whereas with the pattern created with face paint applied with a course sponge the selected point was recognised in each image taken.

DIC enables continuous measurement of full field displacement throughout testing; without the requirement to contact the sample. Previous studies have used callipers to measure cup deformation [46, 129]. In these cases the load had to be applied in a stepwise fashion and human error may be introduced to the measurement. The software also has the advantage of automatically calculating strain values and the option to track the displacement of a defined point. A limitation of the system may lie in the required access to the field of view, which may be a problem for physiological loading conditions where a femoral head could be used to apply load.

Squire *et al.* [46] found the compressive force experienced by a cup on impaction to range from 0-1539 N with a mean of 414 N [46]. The largest cobalt chromium shell tested (64 mm OD) was found to have a diametric deformation of approximately 320 μm at 1539 N and 70μm at 414 N. It has been suggested that the maximum deformation for an effective metal-on-metal bearing system must be around 25μm less than the nominal diametric clearance [6]. The CoCr resurfacing system used in this study has clearances of 75 – 150 μm, thus, according to Jin *et al.* [51] a deformation of less than 87.5 μm would be acceptable. However the resurfacing system is clinically successful [4] with no reports of bearing jamming either in

published data or internal complaint files. The viscoelastic properties of bone [188] and elastic recoil of the cup may explain why the cup is successful despite the large deformation found in this study; stress relaxation would be expected in the bone after implantation, thus the cup may return to its original shape. It is also important to note that rim loading as performed in the current experimental setup and thus modelled, is a simplified and worst case test set up compared to the *in vivo* situation.

A metal-on-metal cup may not be a suitable comparison for the PEEK due to the different lubrication regimes the cups are expected to operate under. Large diameter MOM bearings can experience fluid film lubrication [189], whereas similar PEEK cups have been shown to operate under mixed lubrication conditions [118] (see chapter 6 for further details). A polyethylene cup may be a more suitable comparison as they too operate under mixed lubrication [190, 191] and the acceptable level of deflection may therefore be larger. The largest polyethylene cup tested is predicted to deform by 2.5 mm at 1539 N and 0.7 mm at 414 N, the large PEEK cup had similar deformations predicted; 2.85 mm at 1539 N and 0.76 mm at 414 N.

The parametric analysis showed that increasing the wall thickness increased the cup stiffness under rim loading. For a given outside diameter (which is set by patient physiology) increasing the wall thickness of the acetabular cup reduces the size of femoral head which may be used. As larger diameter heads can reduce the risk of dislocation [18, 45], and give a larger range of motion [18] it is preferable to use as large a head diameter as possible. However as previously mentioned in the literature review, only certain material combinations are suitable for use in large diameter bearings, for example UHMWPE is not suitable dues to high wear rates [20-22]. An alternative to increasing wall thickness is to offset the ID centre from the OD centre, which in effect increases the wall thickness without reducing the size of femoral head which can be used. The potential drawback of this is reduced coverage of the femoral head which may decrease the stability of the joint.

Rim loading of an acetabular shell provides a simple method for comparing cups made of different materials under simulated loading, and enables investigation into the effect design parameters have on cup stiffness. However it does not accurately

simulate the *in vivo* conditions and therefore may not be a valid method for investigating the deformation on impaction of acetabular cups. The draft ISO standard on cup deformation had proposed rim loading as a test method, however without knowing the load to apply, rim loading cannot provide absolute values of deformation an acetabular cup is likely to undergo on impaction in to the pelvis. Therefore a more representative test regime is required; in chapters 4 and 5 two test substrates, polyurethane foam and cadaveric specimens will be investigated.

Chapter 4: Deformation on Impaction using Polyurethane Foam Model and Finite Element Model

4.1 Introduction

Acetabular component deformation on impaction during THA has been reported in the literature [46, 47], with varying levels of occurrence from 16% [47] to 90 % depending on the implant used [46]. The previous chapter showed that rim loading may not be suitable for obtaining absolute values of deformation on impaction; therefore a regime more representative of the *in vivo* situation is required. Polyurethane foam has been previously used to simulate the impaction process *in vitro* [48, 49, 51, 128, 129, 155]. These studies generally follow the same procedure; hemispherical cavities are prepared in foam blocks to represent the reamed acetabulum, the cup is impacted into the cavities and the deformation is measured using a CMM (Coordinate Measuring Machine) or Vernier. Using cadavers to validate the their model, Jin *et al.* found that a hemispherical cavity with rectangular cut-outs gave the best approximation to the *in vivo* situation [51]. As a result the majority of the subsequent studies have used the same foam model [49, 155, 158].

An important factor to consider when investigating cup deformation is the actual size of the cavity produced by reaming. Studies have found that acetabular cavities are on average 0.5 mm larger than that of the reamer used [192-194]. These studies are all over 10 years old and it has been suggested that instrumentation for THA has improved and that the process is now more accurate and repeatable [195]. More recently mean variations of 0.3 mm have been reported [195].

The aims of this study were;

1. To investigate the accuracy of contemporary reaming techniques.
2. To investigate deformation on impaction of prototype PEEK cups using polyurethane foam blocks to represent the acetabulum.

3. To create a finite element model based on the experimental set up for further studies on performance prediction.

4.2 Materials and Methods

4.2.1 Materials

Prototype cups were machined from Motis PEEK injection moulded preforms (Invibio, Blackpool, UK) at Biomet UK Ltd (Figure 14 & Table 5). The cups were coated with Biomet's proprietary porous plasma sprayed titanium coating by Biomet UK Ltd, and the cups were measured using a CMM to gain accurate pre-impaction dimensions. The cup sizes were chosen to match the sizes used in the cadaver trial conducted as part of Chapter 5 (50, 52, 54, 56 mm OD).

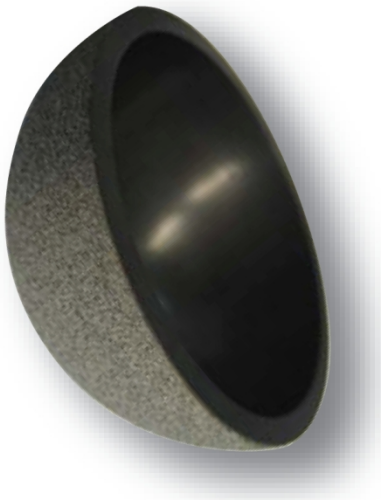

Figure 14 Machined cup with porous plasma sprayed titanium coating

Table 5 Cup sizes used in Sawbones testing

cup size	head size	ID (mm)	ID offset (mm)
50	44	45.8	3
52	46	47.8	3
54	48	49.8	3
56	50	51.8	3

Magnum cobalt chromium modular femoral heads (Biomet UK Ltd, Bridgend, UK) were used in this study. Although the final design will be used with the ceramic Magnum C head the dimensions of the ceramic and metal heads are the same, and

as no Magnum C heads were available at the time of testing, metal heads were used.

Selecting a block with the appropriate material properties was important so that the model simulated the pelvic bone as closely as possible. Sawbones polyurethane blocks are available with a wide range of material properties with densities from 5 to 50 pcf (pounds per cubic foot) and compressive modulus of 16 to 1148 MPa (Figure 15).

DENSITY		COMPRESSIVE		TENSILE	
		STRENGTH	MODULUS	STRENGTH	MODULUS
pcf	g/cc	MPa	MPa	MPa	MPa
5*	0.08	0.60	16	1.0	32
10*	0.16	2.2	58	2.1	86
15*	0.24	4.9	123	3.7	173
20*	0.32	8.4	210	5.6	284
30*	0.48	18	445	12	592
40*	0.64	31	759	19	1000
50*	0.80	48	1148	27	1469

Figure 15 Material properties of Sawbones polyurethane foam blocks [196]

Grade 30 has been previously shown to give results which agreed well with cadaveric tests in a similar set-up to the proposed study [51], however in another study [48] the 30 grade was found to be too stiff and the cavities had to be widened in order to impact the cups. Kosuge *et al.* [197] used Trident MHD 200 which has material properties between grade 10 and 15 of Sawbones. Previous testing by Biomet Inc and Biomet UK Ltd used grade 30 but did not ream the cavities in a standard way [198, 199]. The draft ISO standard on cup deformation suggests grade 30 based only on Jin's work [200].

Sawbones 4th generation composite bones have material properties designed to simulate bone; the compressive modulus for their simulated cancellous bone is 155 MPa and the compressive strength is 6 MPa. The properties are the same for all their composite bones regardless of the anatomical bone it represents (i.e. the composite femur has the same properties as the pelvis) [196].

The literature on the mechanical properties of pelvic trabecular bone is very limited. Thompson *et al.* measured the Young's modulus of human cancellous bone taken from the acetabulum at THA, they found a mean of 116.4 MPa (SD 86.7) [201]. It has been shown that bone volume fraction, trabecular volume and bone surface density decrease significantly with age (cancellous bone in the tibia) [202]; these changes were associated with a reduction in the Young's modulus of the bone [202].

There is a large variation in the mechanical properties of pelvic bone used in FE models of the pelvis. When apparent density from CT data is used to assign the Young's modulus of pelvic cancellous bone a wide range is found within the pelvis [103, 139, 146, 203]. This range also varies between studies, for example Majumder *et al.* and Anderson *et al.* both found a range of around 30-3500 MPa within one pelvis [139, 203], Thompson *et al.* found a range of 1.3 to 1600 MPa [146], however Dalstra reported that Young's modulus was generally not higher than 100 MPa with an occasional peak of 250 MPa [103].

In FE studies where constant material properties for trabecular bone have been assumed there is a lot of variation in the properties used. The values used range from 70 MPa [151, 154, 204] to 800 MPa [134, 137], the higher values appear to have been taken from data on femoral bone.

It seems that 20 pcf Sawbones blocks may be the most suitable to represent pelvic trabecular bone as it has material properties that closely match the material properties of pelvic trabecular bone. However from the literature 30 pcf is the most commonly used grade. Therefore in this study both grades were used to compare the results.

4.2.2 Experimental Method

To investigate the accuracy of reaming, spherical cavities were prepared by reaming polyurethane blocks (Sawbones, Washington USA). Two grades of foam were used, 20 pcf and 30 pcf to represent different bone densities. Two different types of greater reamers were used to compare the accuracy achieved with two different arrangements of cutting teeth, both supplied by Biomet UK Ltd (Bridgend, Wales). A size 56 mm reamer was used from each manufacturer. In order to prepare the foam

in a repeatable manner the reamers were attached to a vertical mill (preparation took place in the Biomet UK Ltd tool room). The prepared cavities were then measured by the quality control department at Biomet using a CMM (Talysurf, Taylor-Hobson). The test was repeated 3 times in each density to assess the repeatability of the reaming process.

For impaction testing Sawbones cavities were prepared as per Figure 16 using acetabular reamers (Orthogroup Inc., California, USA). Two different foam densities were used (GP20 and 30), 3 blocks were used for each condition. The geometry of the cavity was based on the work of Jin *et al.* [51] who found good agreement between cadaver testing and Sawbones testing using this configuration. As described in the previous chapter when a hemispherical acetabular cup is press-fitted into the acetabulum load transfer occurs predominantly near the rim of the cup and is maximum in the diagonal axis between the iliac and ischial bone [160].

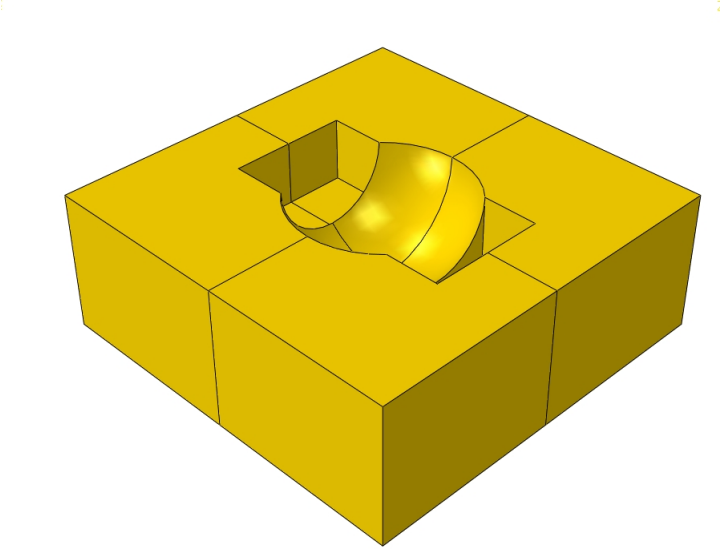

Figure 16 Diagram of Sawbones block used for impaction testing

The cups were impacted in to the prepared Sawbones block by hand using a ball impactor (Figure 17) as per previous publications [48, 51, 155, 158] and the standard operative technique; although the draft ISO standard suggests a monotonic loading it is not felt that this is representative of the *in vivo* situation.

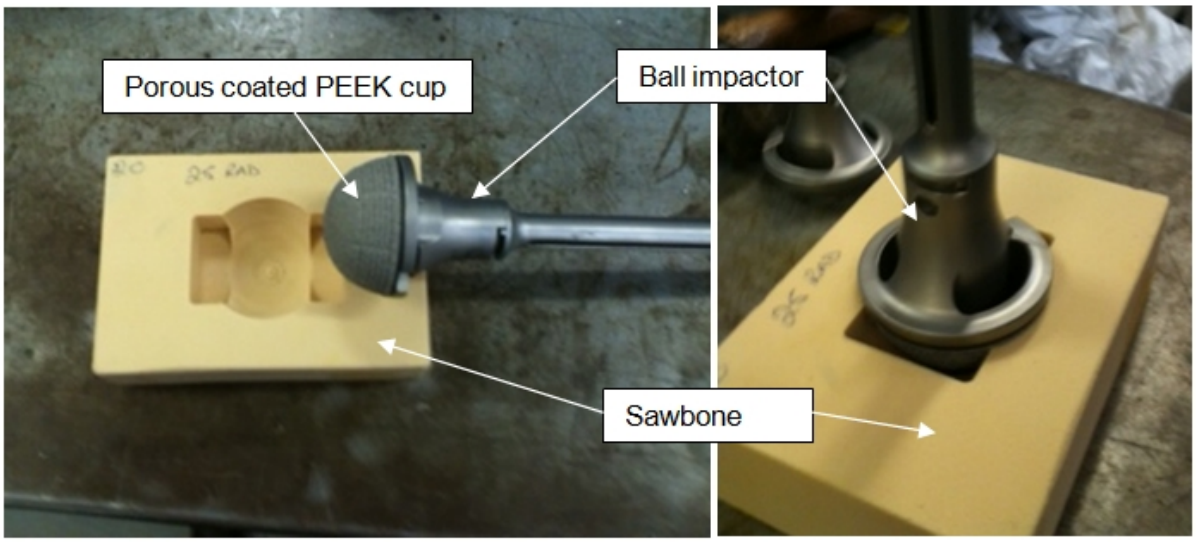

Figure 17 PEEK cups being impacted into prepared Sawbones cavity using ball impactor

DIC was used in the previous chapter to measure the deformation the cups underwent during rim loading. However this method was not suitable for the impaction testing as a ball impacted was used to impact the samples; restricting the field of view. Another possible measurement method is CMM (Coordinate Measuring Machine), which is an accepted method for measuring surfaces; while this would have been suitable for the cups impacted into Sawbones it would not be appropriate for use during the planned cadaveric testing (see chapter 5) for health and safety reasons. For consistency the same method was used for both the Sawbones and cadaveric test regimes. Various materials have been used to make replicas of acetabular cups and cadaver specimens [192, 193, 205], dental putty was chosen as medium for this study as it is easy to use and sets quickly. To validate the accuracy of the technique, dental putty (Provil Novo Putty, Heraeus Kulzer GmbH, Hanau, Germany) moulds were taken of a cup with known dimensions; a Recap shell (Biomet UK Ltd, Bridgend) was used, 4 moulds were taken of the same shell. The moulds were then laser scanned (Perceptron, Plymouth, UK) at Biomet UK Ltd by the quality control department and compared to CAD models of the original cup using Polyworks version 11 (Innovmetric, Québec, QC Canada).

Dental putty moulds were taken of the impacted cups *in situ* in the Sawbones block. The impacted cup was smeared with Engineer's blue and the matching femoral head rotated in the cup to check for normal articulation. The distribution of the dye on the cup was recorded. The cup was then removed from the Sawbones and measured

again to ensure that no permanent deformation had occurred. A new cavity was used each time to mitigate the risk that plastic deformation of the Sawbones had occurred. Each cup size was impacted into cavities with 1 and 2 mm under-ream in both 20 and 30 grade Sawbones; each condition was tested 3 times.

4.2.3 Finite Element Model

The Sawbones blocks were modelled using Abaqus CAE version 6.10-2 (Figure 18). The cup and block were meshed using a free meshing technique with a 4 node linear tetrahedron mesh (C3D4), the material properties for the Sawbones were taken from the Sawbones web site [196] and the CFR PEEK properties were provided by the manufacturer, Invibio [90] (Table 6). The porous coating was not modelled as it was not felt that this would significantly affect the stiffness of the cup, however the OD of the cup was assumed to include the porous coating. All materials were assumed to be linear elastic. Three different densities of Sawbones were modelled (with Young's modulus of 220, 445 and 900 MPa) to investigate the effect of bone quality on deformation and for comparison to the physical testing. Different levels of press-fit were also modelled (0.5, 1.0 1.5 and 2 mm diametric interference). Models of CoCr and titanium cups were also created for comparison to published literature. In addition to the cup sizes trialled in the Sawbones study two larger cups were also modelled for comparison to the cups modelled in the FE model of the pelvis (see Chapter 5).

Table 6 Material properties used in FE model

Material	Young's Modulus (MPa)	Poisson's ratio
CFR PEEK	15,000 [90]	0.4
CoCr	210,000 [54]	0.3
Titanium (Ti6Al4V)	100,000 [54]	0.34
Sawbones 20 pcf	445 [196]	0.3
Sawbones 30 pcf	210 [196]	0.3

Table 7 Cup sizes modelled in FE

cup size	ID (mm)	ID offset (mm)
50	45.8	3
52	47.8	3
54	49.8	3
56	51.8	3
59	55	0
59	54.8	3

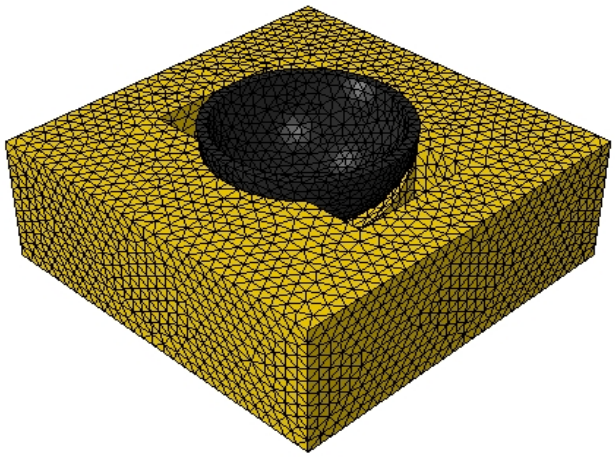

Figure 18 Abaqus model of Sawbones block and prototype cup

The contact between the cup and the Sawbones was modelled using finite sliding and a friction coefficient of 0.62 was applied to simulate the contact between bone and the porous coating of the acetabular cup [206]. A multiple-displacement control method was used to model the impaction. It has been suggested that a multiple-load control is more realistic [147] however Yew *et al.* have shown that displacement control reduces computation time without significantly affecting the results [130]. In the first step of the simulation a unidirectional displacement was applied to the inside surface of the cup to represent a ball impactor, the initial level of displacement was set by measuring the initial gap between the pole of the cup and the pole of the cavity (Figure 19). In the next step of the simulation the displacement was removed and the cup was allowed to recoil. The displacement was than reapplied and the value was increased by 1 mm. The process was repeated until further steps did not result in a reduction in the polar gap.

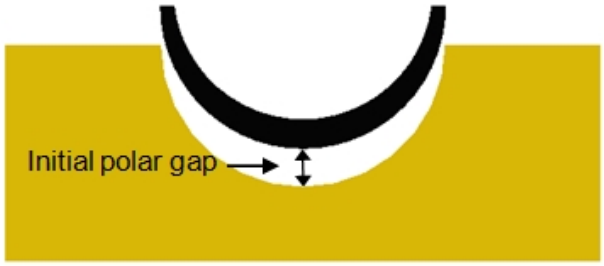

Figure 19 Initial polar gap

4.3 Results

Accuracy of Reaming

Table 8 shows the diameter of the Sawbones cavities prepared using the two types of 56 mm reamers in two densities of Sawbones. The mean size of cavity created with the Precimed reamer was 56.37 mm S.D. 0.21 (range 56.12 to 56.59 mm). The mean size of cavity created with the Othy reamer was 56.43 mm S.D. 0.18 (range 56.17 to 56.6). There was no significant difference between the size of cavities produced by the two reamer types (p=0.37). With the Precimed reamer the cavities produced in the 30 pcf foam were significantly larger than those in the 20 pcf foam (p=0.01), no significant difference was found between foam grades when the Othy reamer was used (p=0.27). It can be seen that the reamers always created a cavity larger than the size specified, by up to 0.59 mm (mean 0.4 mm range 0.12 to 0.59 mm).

Table 8 Diameter of Sawbones cavities prepared using pillar drill measured using CMM

	Block 20 pcf	**Block 30 pcf**
Reamer	**Diameter (mm)**	**Diameter (mm)**
Precimed	56.12	56.49
Precimed	56.33	56.59
Precimed	56.12	56.57
Othy	56.57	56.60
Othy	56.57	56.37
Othy	56.30	56.17
Mean	56.34	56.47
Standard deviation	0.20	0.17

4.3.1 Validation of Dental Putty

The dental putty moulds taken of the reference ReCap shell (of known dimensions) were scanned using the laser scanner previously described; the moulds were accurate to ±0.05 mm.

4.3.2 Experimental Results

After impaction into the Sawbones the matching modular femoral heads were placed inside the cups and it was observed that all heads articulated freely. Engineer's blue was smeared on the inside surface of the cups and the heads placed inside to check dome contact, all cups tested showed dye on the top of the head indicating dome contact. Figure 20 shows an example putty mould, compression and perpendicular expansion can clearly be seen.

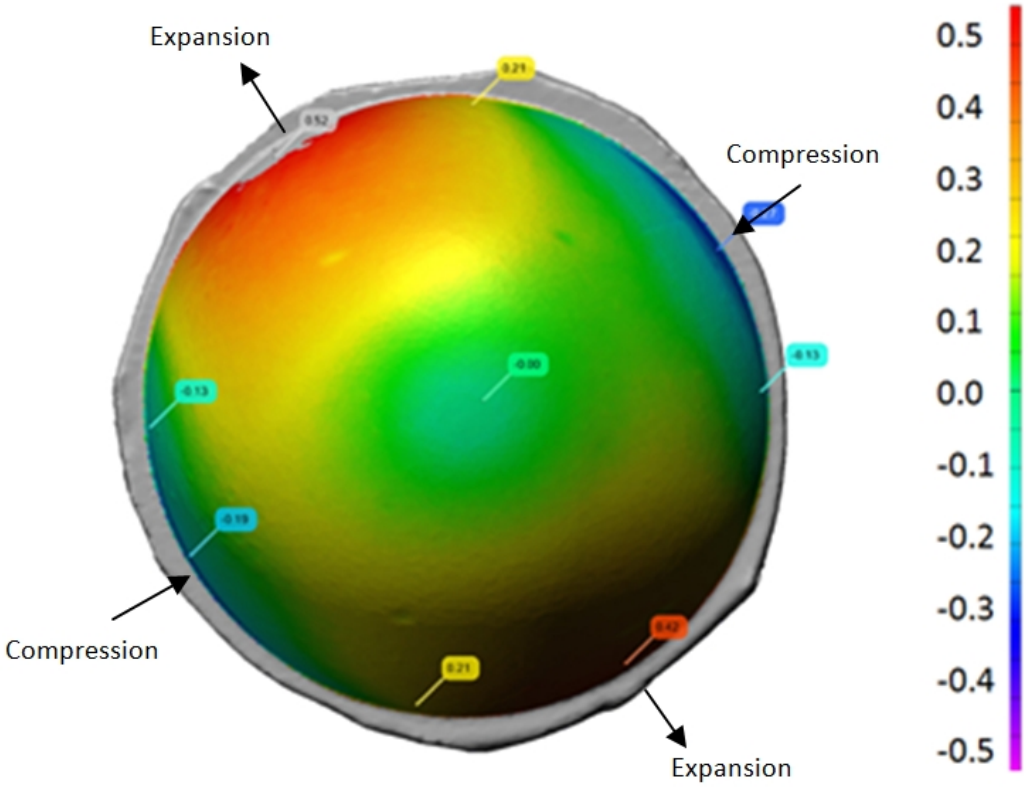

Figure 20 Example putty mould from Sawbones impaction testing, deformation in mm

Figure 21 and Table 9 show the results of the Sawbones impaction. It can be seen that the larger cups experienced a greater level of deformation, however this was not significant (Pearson's correlation $p>0.05$). When impacted into 30 pcf foam the cups experienced significantly greater deformation compared to the 20 pcf foam (paired T-

test; $p<0.05$). A 2 mm under-ream resulted in significantly greater deformation than 1 mm (paired T-test; $p<0.05$). It should be noted that the small samples size may not be sufficient for the statistical techniques used. No plastic deformation of the PEEK cups was observed.

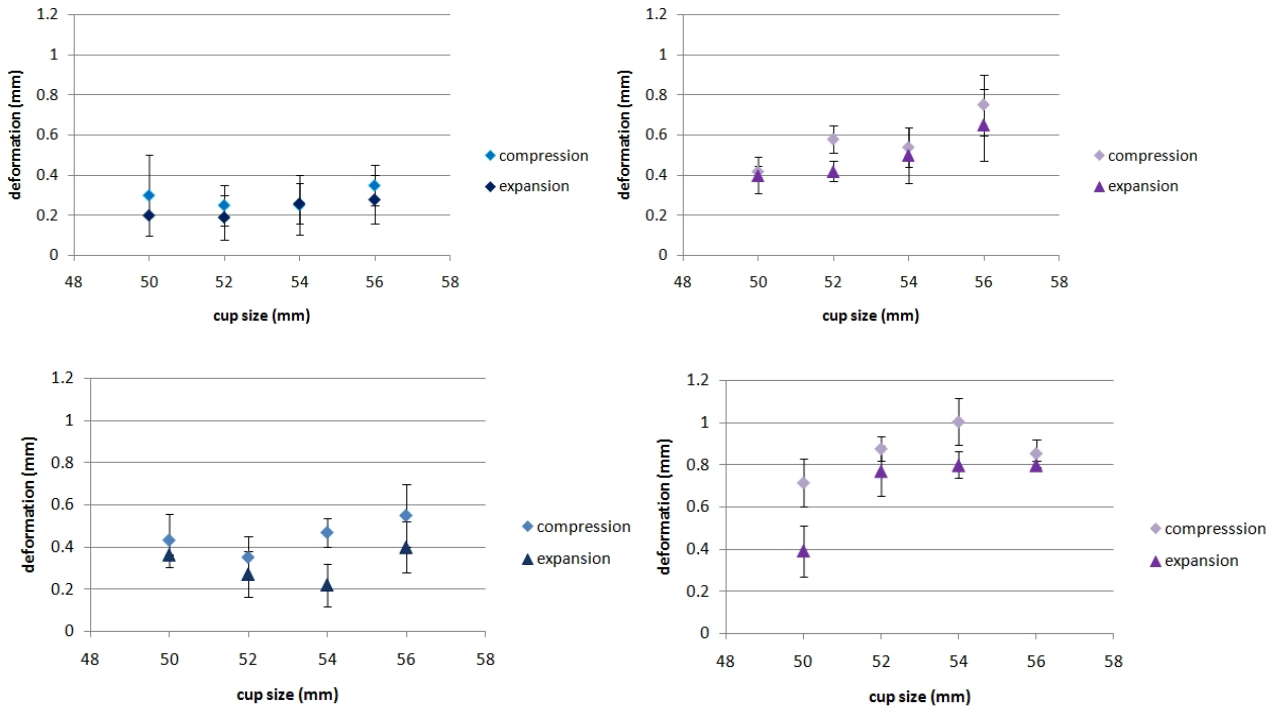

Figure 21 Deformation versus cup size; 20 pcf foam with 1 mm under-ream (top left), 30 pcf foam with 1 mm under-ream (top right), 20 pcf foam with 2 mm under-ream (bottom left), 30 pcf foam with 2 mm under-ream (bottom right).

Table 9 Deformation (in mm) on impaction into Sawbones (comp=compression, exp=expansion)

Density (pcf)	20				30			
Under ream (mm)	2		1		2		1	
Cup OD	comp	exp	comp	exp	comp	exp	comp	exp
50	0.43	0.36	0.30	0.21	0.71	0.39	0.42	0.40
52	0.35	0.27	0.25	0.19	0.87	0.77	0.58	0.42
54	0.46	0.22	0.25	0.26	1.01	0.80	0.54	0.50
56	0.55	0.40	0.35	0.28	0.85	0.80	0.75	0.65

4.3.3 Finite Element Results

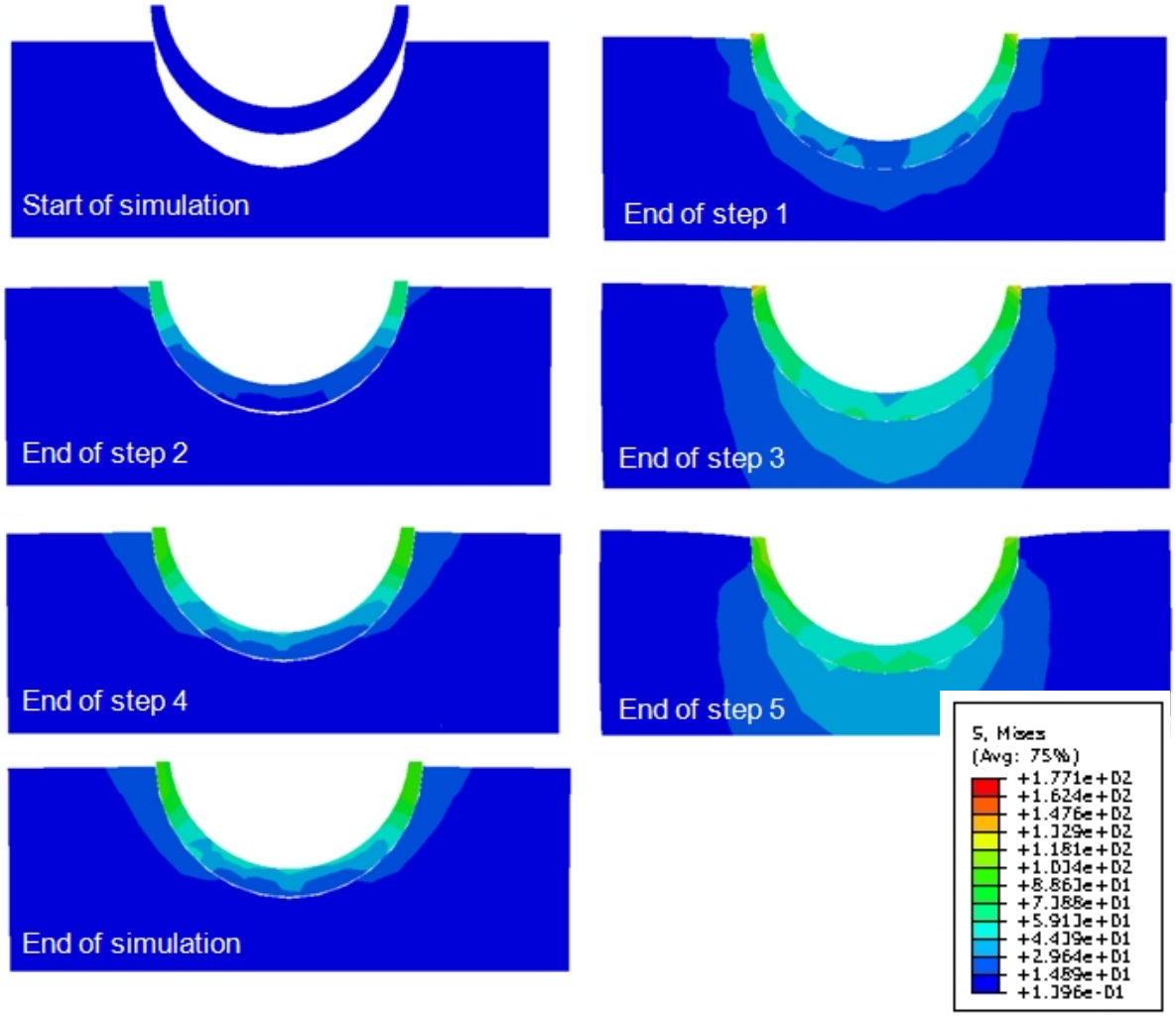

Figure 22 Cross section of FE results for 56 mm cup with 1.5 mm under-ream

At the end of step 1 (initial displacement applied) the cup is pushed into the cavity leaving a polar gap of 0.13 mm (example from model of 56 mm cup with 1.5 mm under-ream), at the end of step 2 (initial displacement removed) the cup has recoiled and the polar gap has increased to 0.54 mm. Application of a further displacements result in the cup being pushed progressively further into the cavity, with a smaller recoil each time (Figure 22 and Figure 23). With a greater under-ream the cups experienced more recoil; however the difference in final polar gap was small between the different levels of under-ream. This pattern was observed for all four cup sizes modelled. The polar gap was similar for all cup sizes (0.35 ±0.03 mm at

the end of the simulation), the polar gap was also similar for the CoCr and titanium cups modelled; approximately 0.35 mm.

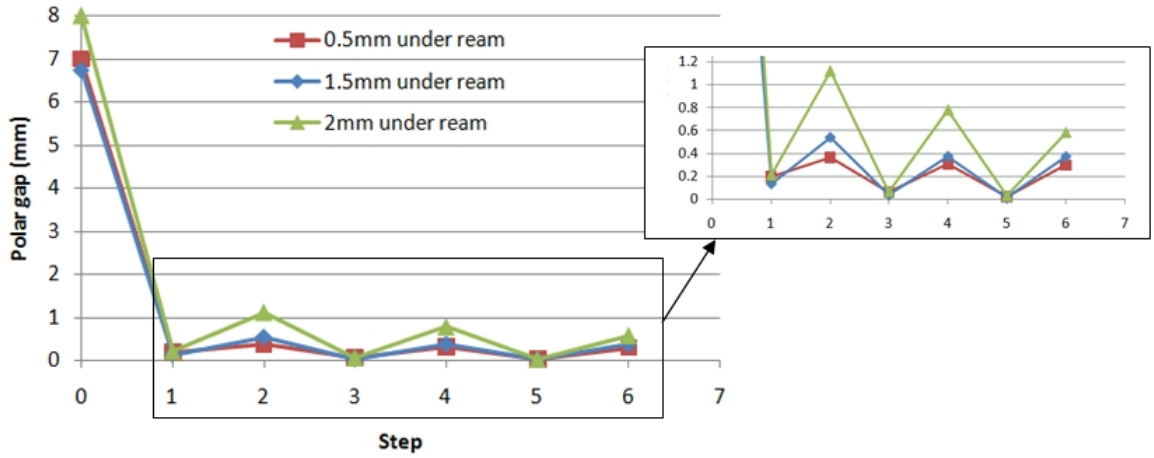

Figure 23 Polar gap remaining after each FE displacement step (54 mm cup, 30 pcf foam)

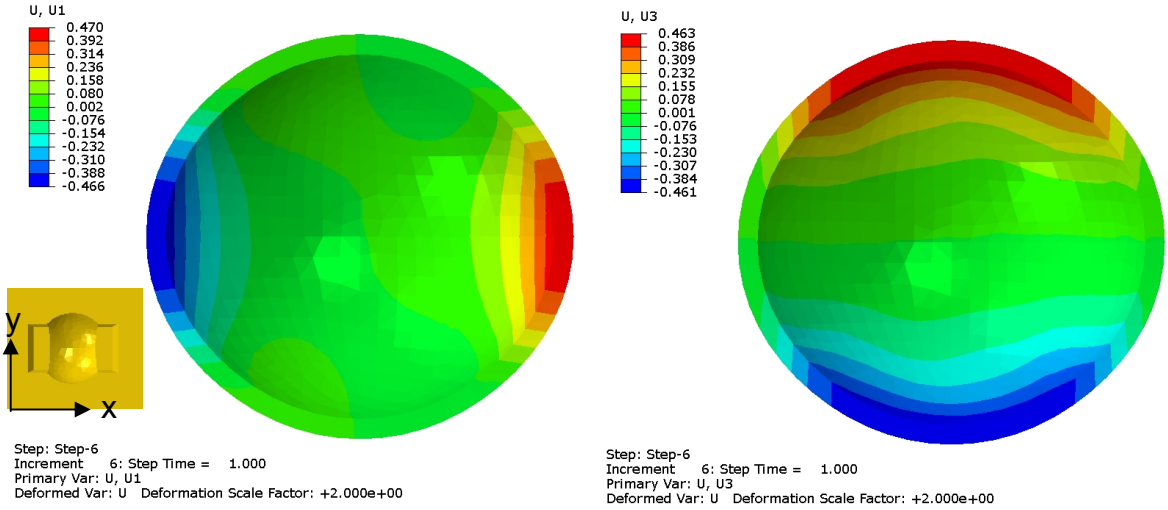

Figure 24 FE output for 56 mm cup with 1.5 mm under-ream in 30 pcf foam; deformation in x direction (u1) (left) and deformation in y direction (u2) compression (right) in mm

Figure 25 shows a typical deformation plot from the FE model, with compression in one direction and expansion in the perpendicular direction. The compression is symmetrical about the axis of expansion and *vice versa.*

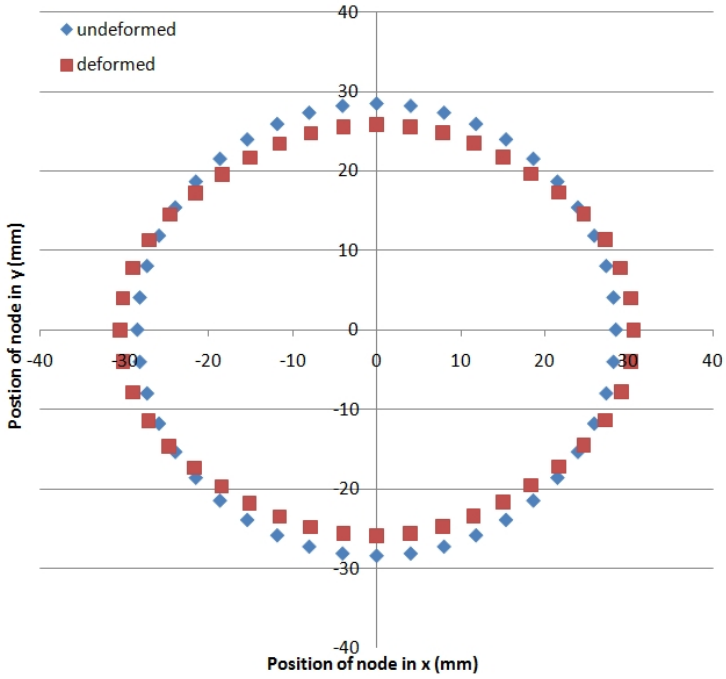

Figure 25 Example deformation plot for 54 mm cup with 1 mm under-ream, deformation scaled by a factor of 10

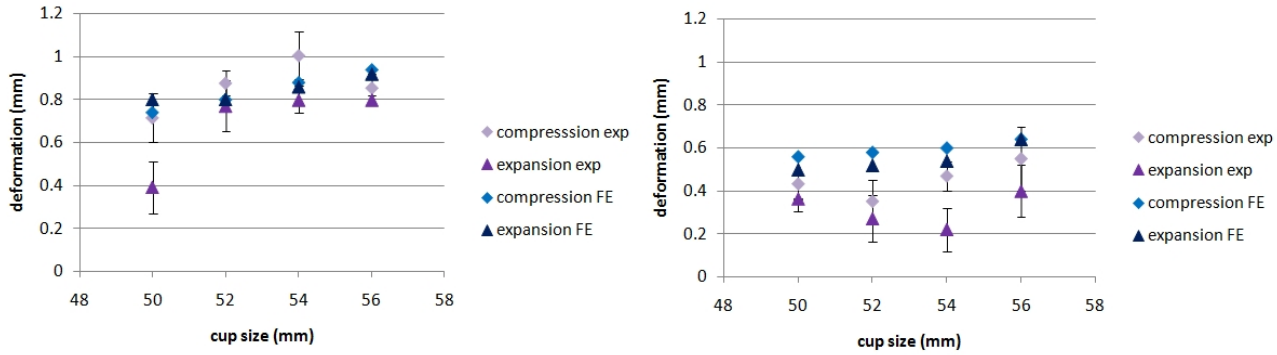

Figure 26 Deformation versus cup size for 2 mm under-ream in 30 pcf foam (left) 20 pcf foam (right), experimental and FE results (note FE model had diametric interference of 1.5 mm based on the results of the accuracy of the reaming)

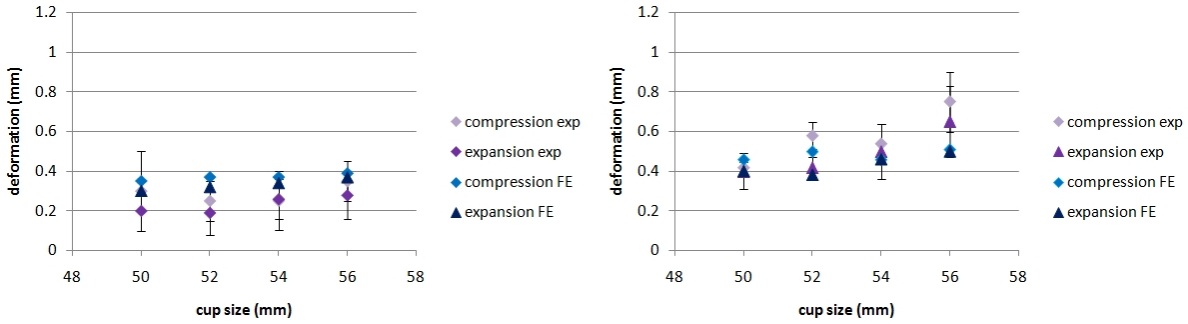

Figure 27 Deformation versus cup size for 1 mm under-ream in 30 pcf foam (right) 20 pcf foam (left), experimental and FE results (note FE model had diametric interference of 0.5 mm based on the results of the accuracy of the reaming)

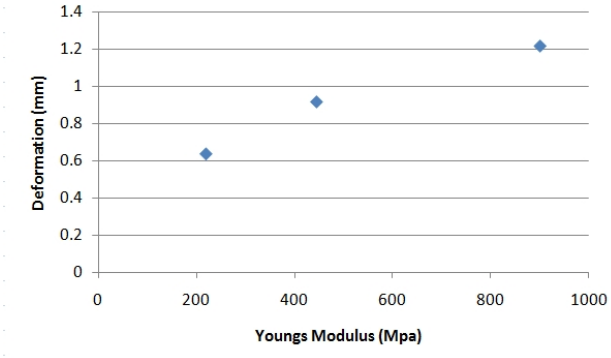

Figure 28 Deformation versus Young's Modulus of Sawbones block (56 mm cup with 1.5 mm under-ream)

Figure 28 shows the relationship between cup deformation and the stiffness of the Sawbones block; using a block with higher density (and hence greater stiffness) results in more cup deformation, demonstrating the importance of selecting the correct foam density.

Table 10 Compression and expansion of simulated cobalt chromium and titanium cups

Material	**Cobalt chromium**				**Titanium**	
Under Ream (mm)	**1.5**		**0.5**		**1.5**	
Cup size	**Exp (mm)**	**Def (mm)**	**Exp (mm)**	**Def (mm)**	**Exp (mm)**	**Def (mm)**
50	0.038	0.034	0.020	0.021	0.042	0.044
52	0.052	0.044	0.025	0.025	0.078	0.096
54	0.090	0.086	0.037	0.030	0.154	0.150
56	0.092	0.090	0.039	0.035	0.158	0.160

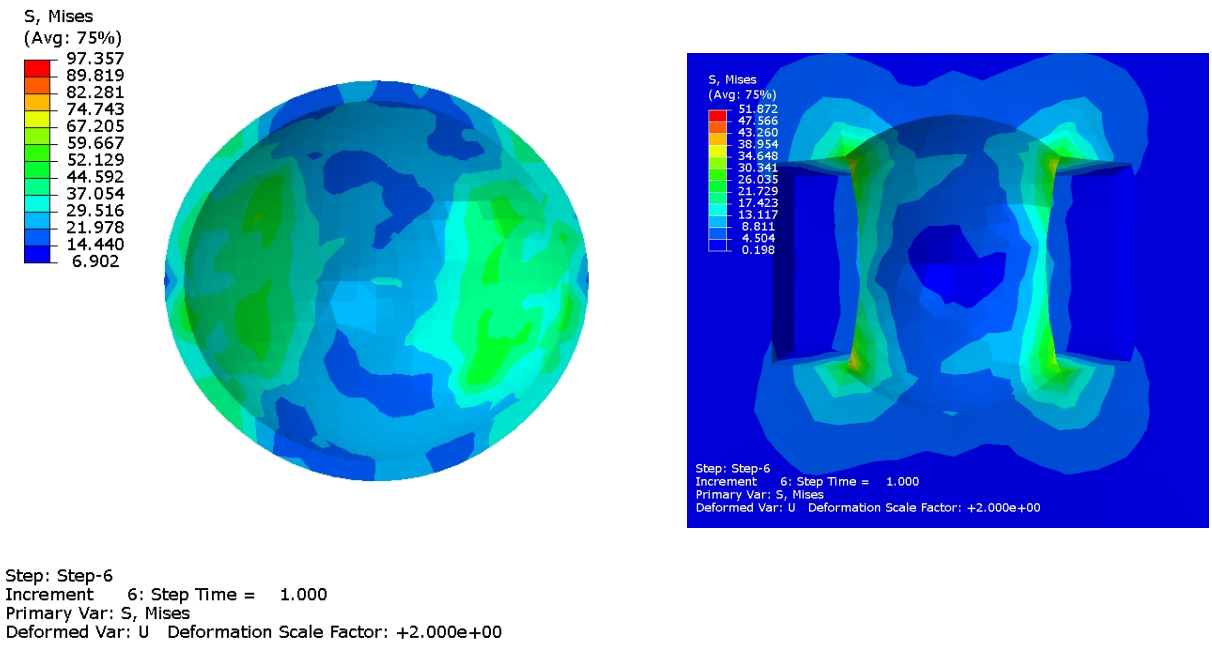

Figure 29 von Mises stresses (MPa) in 56 mm cup with 1.5 mm under-ream in 30 pcf foam, cup (left), Sawbones block (right)

The maximum von Mises stress predicted in the FE model was around 100 MPa in the cup and 50 MPa in the Sawbones block (Figure 29). Larger cups experienced more deformation and a corresponding increase in von Mises stress.

4.4 Discussion

The investigation into the accuracy of the reaming process demonstrated that the reamers always produced a cavity larger than the size specified; by up to 0.59 mm (mean 0.4 mm range 0.12 to 0.57 mm). This means that although a 1 mm press-fit is specified, the cavity produced is only actually giving around a 0.5 mm press-fit. The results are consistent with published data on cadaver specimens which also showed that the diameter of the cavity produced was larger than the nominal size of the reamer [51, 192, 193, 207]. The magnitude of the over ream is somewhat larger in the published data; Mackenzie *et al.* reported that the cavities were on average 0.56 mm larger than the reamer size, with a maximum of 1.63 mm [193]. Alexander *et al.* found deviations from sphere in some areas of the prepared acetabular of up to 4 mm, 11 out of 12 samples were over reamed, by an average of 0.5 mm [194]. This difference may be due to improvement in the design of greater reamers; the published data is at least 10 years old. More recently Jin *et al.* reported that the average size of Sawbones cavity produced by hand reaming for a nominal reamer

size of 59 mm was 59.56 ±0.15 mm [51] and Baad-Hansen *et al.* reported a mean deviation from best-fit sphere of 0.3 mm ±0.4 mm [195], which is comparable to the results of the current study.

The standard deviation in the size of cavity produced was 0.19 mm which is somewhat lower than the SD reported in the literature: 0.35 mm [207] and 0.5 mm [193], this could indicate that although modern reamers produce cavities which are larger than the nominal size of the reamer, the process is more repeatable. It should be noted that the published data is from cadaveric work and therefore more variables are present which could affect the repeatability of the process, such as bone density. However the current study showed no significant difference between the sizes of cavities produced in 20 pcf foam as compared to 30 pcf foam. The cavities produced in this study were produced using a pillar drill, which is an idealised situation, however the range of sizes produced is large compared to the level of press-fit specified in the operative technique. Mackenzie *et al.* [193] compared hand reaming and reaming using a press drill and found no significant difference in the size of the cavities produced.

The largest deformation measured in the impaction testing was 1.084 mm, which was recorded for a 56 mm cup impacted into 30 pcf Sawbones with 2 mm under-ream, the smallest deformation with a 2 mm under-ream was 0.22 mm, which was recorded for a 52 mm cup in 20 pcf foam. For 1 mm under-ream the largest deformation was 0.65 mm and the smallest was 0.25 mm. In general larger cups experienced more deformation than smaller cups, cups impacted into denser foam underwent a greater level of deformation than those impacted into less dense foam, and a 2 mm under-ream produced more deformation than a 1 mm under-ream. The relatively large standard deviation, the small number of cups tested of each cup size and the small range of sizes tested (i.e. 50 to 56 mm OD) mean that a clear relationship between cup size and defamation is not apparent.

The maximum von Mises stress predicted by the FE model was approximately 100 MPa for the PEEK cup, the compressive strength of Motis PEEK is 200 MPa and the tensile strength is 155 MPa [90], therefore failure of the material is not expected.

This is consistent with the experimental results where no plastic deformation of the cups was observed.

The experimental results from the 2 mm under-reaming are in agreement with the FE model of 1.5 mm under-ream, similarly the 1 mm under-ream experimental results agree well with the 0.5 mm FE results. The results of the accuracy of reaming study showed that the cavities produced were always over sized (on average 0.4 mm), therefore the 2 mm under-ream in the Sawbones is actually much closer to a 1.5 mm interference which explains the agreement with the 1.5 mm FE models.

A relatively large standard deviation (up to 0.15 mm) was found in the amount of deformation at each cup size. The reason for this variability in the results can be explained when the variation in the size of the cavity is considered, the standard deviation found in the accuracy of reaming study was also relatively large: 0.19 mm. Jin *et al.* also found a large standard deviation of 0.034mm compared to the mean value of deformation (0.08 mm) [51]. However Schmidig *et al.* found a maximum SD of 0.09 mm for a mean of 0.78 mm [155], this deviation appears to be very small; it is not specified how the foam cavities were created, but it is possible a more repeatable method for creating the hemisphere was used such as machining rather than reaming using surgical instruments. The results from the FE model confirmed that the amount of deformation was very dependent on the level of under-ream. Slight misalignment of the cups during impaction may also increase the variability of the experimental results; in addition the fact that the cups were impacted by hand meant that the force used to impact them was slightly variable. However this is representative of the situation in the operating theatre where the surgeon would impact by hand and slight misalignment between the cup and acetabulum would be possible.

In the experimental results it can be seen that for every cup tested the level of compression was greater than the expansion. However in the FE model the expansion and compression were very similar, this is in agreement with Yew *et al.* [130] who also found similar compression and expansion in their FE model of resurfacing cups impacted into Sawbones blocks. The reason for the discrepancy

between the FE and experimental results may be due to the way the contact has been modelled.

During the FE simulation the cup rebounded as the displacement was removed, this is in agreement with the experimental observations where several mallet blows were required to seat the cup and published data [51, 127, 130, 193]. The FE model showed that a polar gap remained even after several simulated mallet blows were applied; this is consistent with published literature [51, 127, 130, 155]. It was also found that with a greater under-ream a larger polar gap remained after each step, for example a 52 mm cup had a 0.29 mm polar gap with 0.5 mm under-ream, 0.34 and 0.58 mm with a 1.5 mm and 2 mm under-ream respectively, which is consistent with finding published in the literature [147]. The presence of polar gaps *in vivo* has been linked to poor bone in-growth onto the porous coating of acetabular cups [208]. The predicted polar gap for the CoCr and titanium cups modelled were very similar to those for the PEEK cups, suggesting that the PEEK cups would be no worse in terms of polar gap than cups currently on the market.

To the author's knowledge there are no reports in the literature on the level of deformation experienced by a PEEK cup on impaction, however there are a number of studies which have used polyurethane foam to model the impaction of metallic acetabular cups; Schmidig *et al.* conducted tests looking at the deformation of acetabular shells (Trident) on frictional torque; the maximum shell deformation was 0.78 mm at 2 mm under-ream [155]. Ong el at also investigated the deformation of the Trident shell on impaction into Sawbones (30grade) cavities as per Jin *et al.*; they found that with a 2 mm under-ream a 50mm shell experienced a maximum diametric deformation of 0.45 mm [158]. This seems a high level of deformation for a metallic cup and is much higher than the deformation predicted in the FE model of titanium cups (0.16 mm), however the Trident shell has a relatively thin wall for a titanium shell; 3.4 mm for the smaller diameters and 4.1 mm for the largest shell. Fritsche *et al.* report very small deformations for the Bicon-plus and EP Fit Plus cups (22 and 8 μm respectively), however they used hemispherical Sawbones cavities without cut-outs and had to enlarge the cavities to achieve seating of the implants [48]. The use of hemispherical cavities rather than cavities with cut-outs has been

shown not to be a worst case; Schmidig *et al.* compared using Sawbones cavities with hemispherical cavities and cavities with cut-outs and found that the cut-outs significantly increased the level of deformation [155].

The deformation of resurfacing cups Durom and BHR were compared by Grimes *et al.* who impacted 11 retrievals of each type into Sawbones; a mean diametric deformation of 89.8 ± 14.8 μm was found for the Durom, (this value is approaching the diametric clearance), whereas the BHR experienced deformation of 57.2 ± 25.8 μm [49]. No residual cup deformation was observed on removal of the cups from the foam [49]. The deformation of the Durcom resurfacing cup has also been investigated using an FE model; although the model considered body weight rather than impaction, the deformation was found to be greatest in the superior inferior direction and varied as a result of the press-fit technique (48.7 μm for 1 mm press-fit, 94.6 μm for the 2 mm press-fit, 7.5 μm for the line-to-line) [131]. Jin *et al.* reported diametric deformation of around 100 μm for the ASR (Depuy) when impacted into Sawbones [51]. The models created as part of the current study with material properties of cobalt chromium (E=210 MPa [54]) predicted cup deformations of up to 90 μm for 2 mm under-ream and 32 μm for 1 mm under-ream (Table 10), which is consistent with the range of values reported in the literature. The deformation in the CoCr cups is at the lower end of the values reported; the prototype cup is a simplified version of the Biomet ReCap resurfacing acetabular cup which has an ID offset designed to stiffen the cup.

In the Sawbones test, all the femoral heads were able to articulate freely in the impacted cups; Engineer's blue indicated dome contact in all cases. Jin *et al.* also looked at the ability of the femoral head to articulate within a deformed cup (ASR, DePuy) and suggested that the maximum deformation for an effective bearing system must be around 25μm less than the nominal clearance [51]. The large clearance of the Biomet PEEK cups enables the head to articulate despite the relatively high level of deformation. Grimes at al also used machinist's dye to check head-cup contact in impacted Durcom cups and found that with a deformation of around 90μm the cups had a 2cm band of dye extending from rim to rim, with no contact on either side [49].

In the current study displacement control was used to simulate impaction in the FE model. *In vivo* the acetabular cup is inserted into the prepared cavity by repeated mallet blows; previous studies have used load pulses to simulate this [147]. However, it has been shown that the load pulses required to achieve seating in the FE model did not correlate with the loads expected *in vivo* [130] and that only small differences in results are found when using load pulses compared to displacement pulses, especially when deflection is considered [209].

The assumption in the FE model that the material properties of CFR PEEK were linear elastic is valid as no plastic deformation was observed in the experimental results. However for the polyurethane foam this may not hold true; in the *in vitro* test it was possible to impact the cups until the rim of the cup was flush with the top of the Sawbones block, however in the FE simulation even when the polar gap was reduced to zero before the displacement was removed, the rim of the cup still remained proud. This indicates that plastic deformation of the Sawbones had occurred in the *in vitro* tests, allowing the cup to seat completely. The Sawbones are polyurethane foam; the porosity allowed local permanent deformation to occur, this deformation was not simulated in the FE model. The result of this may be that the FE model over estimates the deformation of the cup. It is also possible that the assumption of linear elastic properties accounts for the discrepancy between the FE and experimental results in terms of the magnitude of expansion and compression being similar in the FE model, whereas in the experimental results the level of compression was greater than the expansion.

The testing conducted in this chapter has shown that the Biomet PEEK cup undergoes a significant amount of deformation on impaction into a polyurethane model of the acetabulum. Due to the large clearance between the modular femoral head and the cup dome contact was indicated despite the cup deformation. However this does not necessarily show that the deformation will not adversely affect the bearing as the sensitivity of the bearing combination to changes in clearance is not known. Although polyurethane blocks have been widely used to simulate impaction of acetabular components into the prepared acetabulum they may not accurately

represent the *in vivo* conditions; the blocks have consistent material properties, whereas the cancellous bone of the pelvis is heterogeneous [103], in addition the dense cortical shell is not represented. Therefore it was important to conduct testing of the prototype cup in cadaveric specimens; this was the focus of chapter 5.

Chapter 5: Deformation on Impaction using Cadaveric Specimens and Subject Specific Finite Element Model

5.1 Introduction

In Chapter 4 the level of deformation on impaction of the Biomet PEEK cups into Sawbones was investigated. Although this technique has been widely reported in the literature [48, 49, 51, 128, 129, 210] it does not account for the heterogeneous material properties of cancellous bone and does not completely simulate the physiological conditions; therefore testing was conducted using cadaveric specimens as this is more representative of the *in vivo* situation.

The aims of this study were;

1. To investigate the level of deformation on impaction into cadaveric specimens of prototype PEEK cups.
2. To investigate the accuracy of reaming in cadavers.
3. To create a finite element model of the pelvis capable of simulating impaction.

It was essential that the FE model was able to provide absolute values of deformation; published work suggests that when absolute rather than comparative results are required, location dependant material properties based on CT attenuation and location dependent cortical shell thickness from the CT data are needed [135].

5.2 Materials and Methods: Experimental

5.2.1 Implants

Prior to the work undertaken in the cadaver experiment, which was held in the physiology department of the University of Vienna, a range of prototype cups were machined from Motis PEEK injection moulded preforms (Invibio, Blackpool, UK) at Biomet UK Ltd; the cups were porous coated by Biomet with their proprietary plasma sprayed titanium coating. A range of sizes was prepared to ensure the correct sizes would be available for each cadaver. Cobalt chromium Magnum modular femoral

heads (Biomet, Bridgend, UK) were used in this study; although ceramic heads will be used with the final design the dimensions of the ceramic and metal heads are the same, and as no Magnum C heads were available at the time of testing, metal heads were used.

5.2.2 Method

Five fresh frozen cadaveric specimens were thawed and then prepared by five orthopaedic surgeons using Exceed ABT instruments (Biomet UK Ltd, Bridgend) to give a 1 mm under-ream as per the Operative Technique. Quick set Provil Novo putty (Heraeus Kulzer GmbH, Hanau, Germany) was used to make putty moulds of the prepared acetabular cavities. The PEEK cups of the appropriate size were then impacted into the prepared acetabular cavities. Dental putty moulds were taken of the impacted cups *in situ* in the acetabulum (Figure 30). The articulating surface of the impacted cup was smeared with dye (Engineer's blue) and the matching femoral head was placed inside the cup and rotated. The head was then removed and photographed. The presence of Engineer's blue on the pole of the head indicated dome contact. The putty moulds were disinfected using Virkon (Antec International Limited, Sudbury, UK). The moulds were later laser scanned (Perceptron, Plymouth, UK) at Biomet UK Ltd and compared to CAD models of the original cups using Polyworks version 11 (Innovmetric, Québec, QC Canada). The software reports the distance between the CAD model and the surface created from the laser scanned point cloud.

Figure 30 Example dental putty mould of an impacted PEEK cup

5.3 Method: Finite Element Model

A fresh frozen cadaver of a 110 kg 69 year old male donor with no known bone disorders (cause of death was lung cancer) was CT scanned at The Royal National Orthopaedic Hospital (Stanmore, UK) with a 0.45 mm slice thickness and slice distance.

5.3.1 Location Dependent Material Properties

The relationship between apparent density and CT attenuation is dependent on the specific scanner being used [211]; therefore a CT phantom (Tissue Characterisation Phantom, Gammex, Nottingham, UK), covering a wide range of tissue densities from cortical bone (1.82 g/cm^3) to lung tissue (0.47 g/cm^3), was scanned along with the cadaveric pelvis (Figure 31).

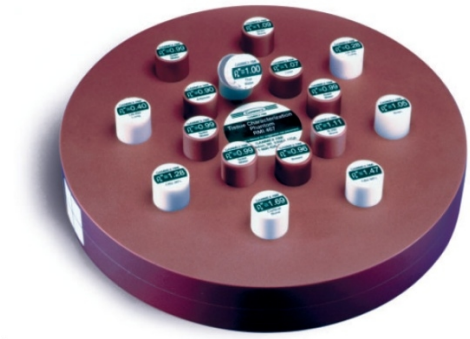

Figure 31 Tissue characterisation phantom

The resulting Dicom images were imported into Scan IP (Simpleware, Exeter, UK) using the full field of greyscale values. Initially only the phantom was considered in order to find the relationship between physical density (as specified by the manufacturer of the CT phantom) and the greyscale (attenuation) values from the CT data. The images of the CT phantom rods did not have a consistent greyscale value; to find the average greyscale value the images were cropped to give a cube in the centre of the rod (Figure 32 left). The statistics function of the software was used to create a histogram of the greyscale values for the cube (Figure 32 right), from which the modal value and standard deviation were taken. This process was repeated for all rods in the CT phantom. The greyscale values were then plotted against physical

density and linear regression was used to find the relationship between greyscale value and density.

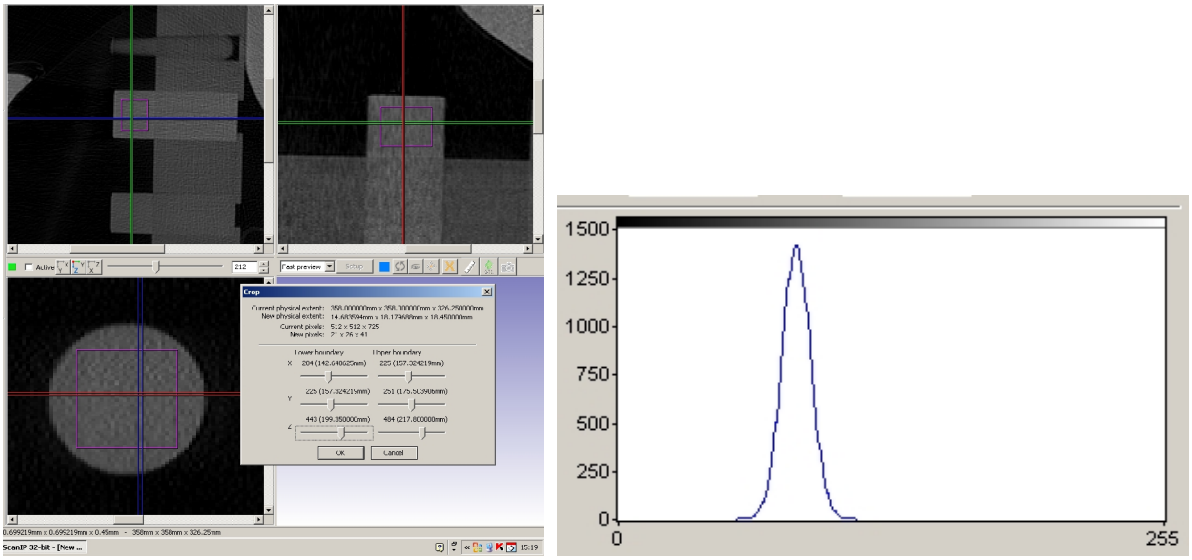

Figure 32 Cube cropped from centre of CT phantom rod (left), example histogram for CT rod (right)

5.3.2 Hemi Pelvis Model

The Dicom data of the pelvis was imported into Scan IP and the import parameters were adjusted to give good definition of the cortical bone; the software was then used to segment one hemi pelvis. Pixels with density of greater than 1.8 g/cm^3 were considered to be cortical bone (Figure 33) [138]. Separate masks of the cortical and cancellous bone were created using the thresholding method and visual inspection when required (Figure 34).

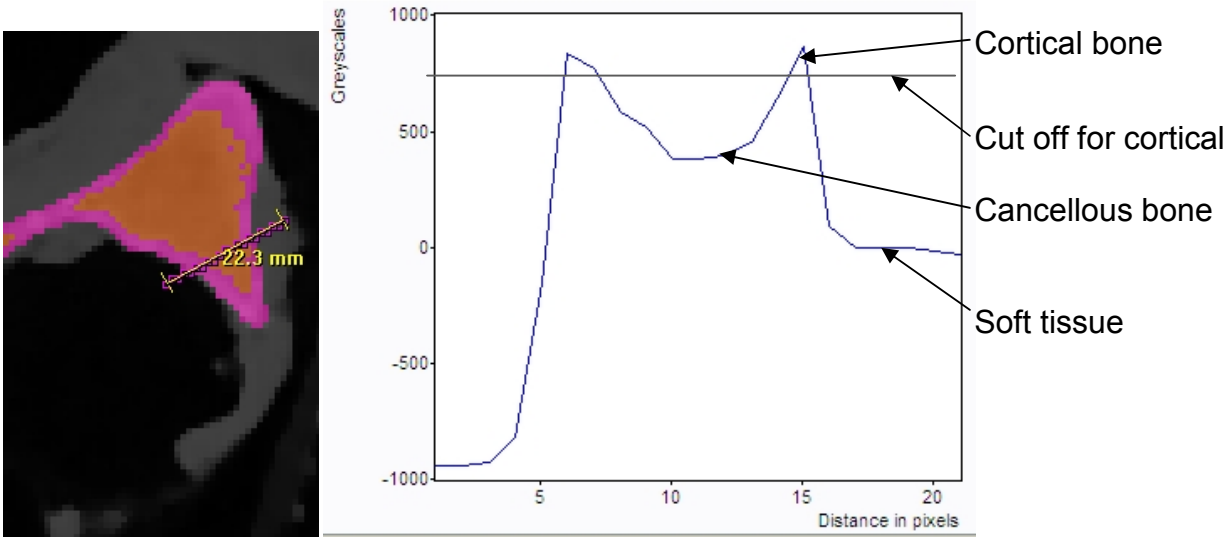

Figure 33 CT image through acetabulum (left) and graph of distance vs. greyscale for the profile line shown (right)

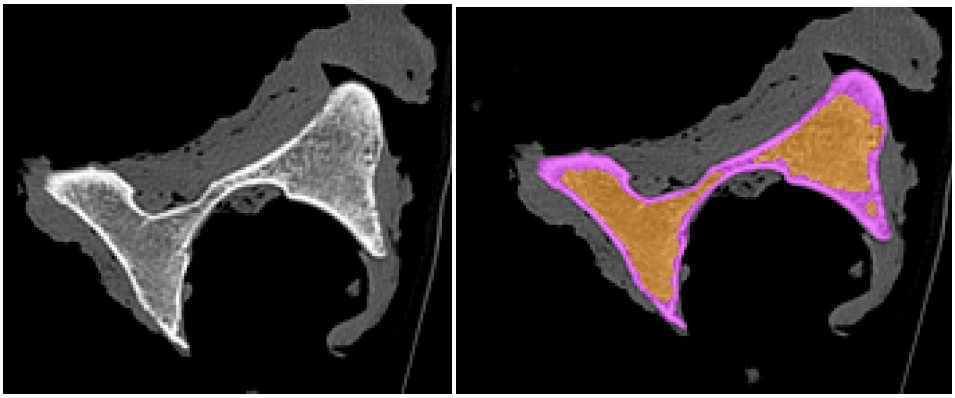

Figure 34 Segmentation of pelvis using Simpleware, pink = cortical mask, orange = cancellous mask

Scan IP was used to create a Finite Element mesh from the masks; the software has the facility to apply material properties based on greyscale value to each element in the mesh created. The following relationship between apparent density (ρ_{app}) and Young's modulus (E) was used:

$$E = 2017.3\rho_{app}^{2.46}$$ [103] Equation 1

Apparent density is given by:

$$\rho_{app} = \frac{\rho}{0.626}$$ [103] Equation 2

Where ρ (density) is calculated from the CT attenuation using the relationship derived using the CT phantom. Poisson's ratio for cancellous bone was assumed to be constant; 0.2 [103].

Cortical bone was assumed to be isotropic and homogeneous; Young's Modulus was taken to be 17 GPa and Poisson's ratio 0.3 [135]. The hemi pelvis model was used to investigate the thickness of the cortical bone and the distribution of bone density in the cancellous bone for comparison to published literature.

5.3.3 Acetabular Model for Impaction Modelling

A model of the acetabular area was created for investigation into cup deformation on impaction; the hemi pelvis model was cropped using Scan IP, this reduced the size of the model and simplified the boundary conditions (Figure 35).

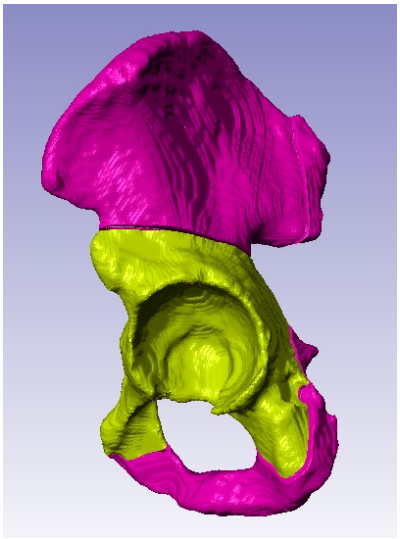

Figure 35 Acetabular model (pink areas were removed from hemi pelvis model)

In order to simulate the reaming process Scan CAD (Simpleware, Exeter, UK) was used. The approximate size of the acetabular cavity was measured using the "measure" function of the software; CAD spheres of various sizes were created in Abaqus CAE (version 6.8-, Simulia, Providence, USA) and imported into Scan CAD. After initial trials a 58 mm sphere was found to be the most suitable size. The 58 mm sphere was positioned using the software (Figure 36 left) as advised by operative technique; i.e. locate the bottom of acetabulum and ream to a hemisphere. The bone at the base of acetabulum was very thin in this cadaver; therefore care was taken not to perforate the bone (Figure 36 right).

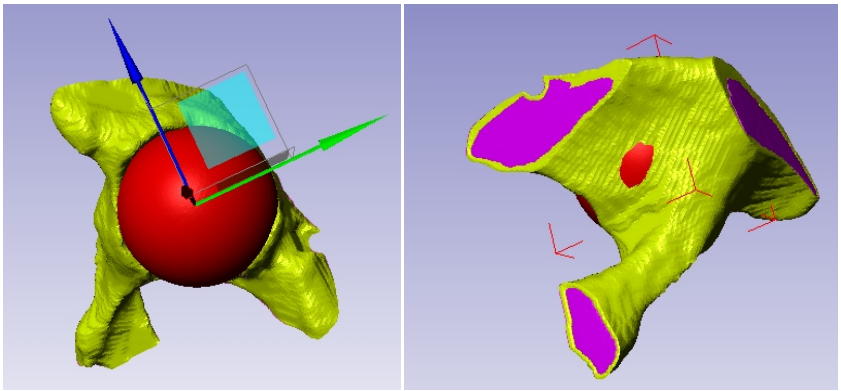

Figure 36 Positioning of sphere for reaming in ScanCAD (left) and example of perforating the acetabular wall (right)

A Boolean operation was performed in ScanCAD to subtract the sphere from the cortical and cancellous masks.

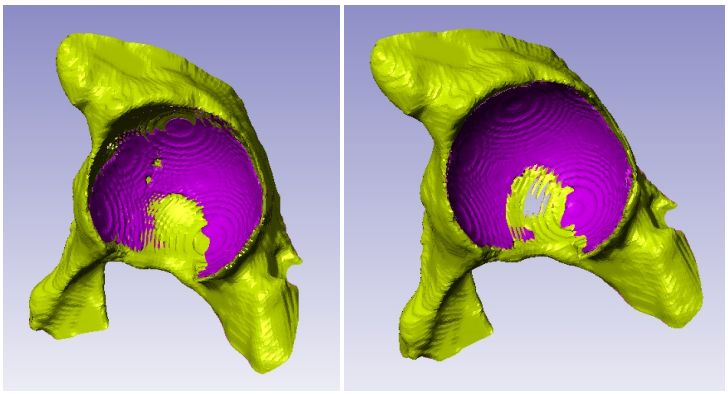

Figure 37 Acetabular model post reaming (left), acetabular model post reaming with incorrect position of sphere causing perforation of the acetabular wall (right)

To simulate impaction of the acetabular cup, CAD models were created in Abaqus CAE and imported in to ScanCAD (Table 11). In order for the contact simulation to solve in Abaqus it was very important to ensure that the cup and the acetabulum were not in contact at the start of the analysis, therefore in Scan CAD the cups were manually positioned so there was a gap between the bone masks and the cup mask (Figure 38).

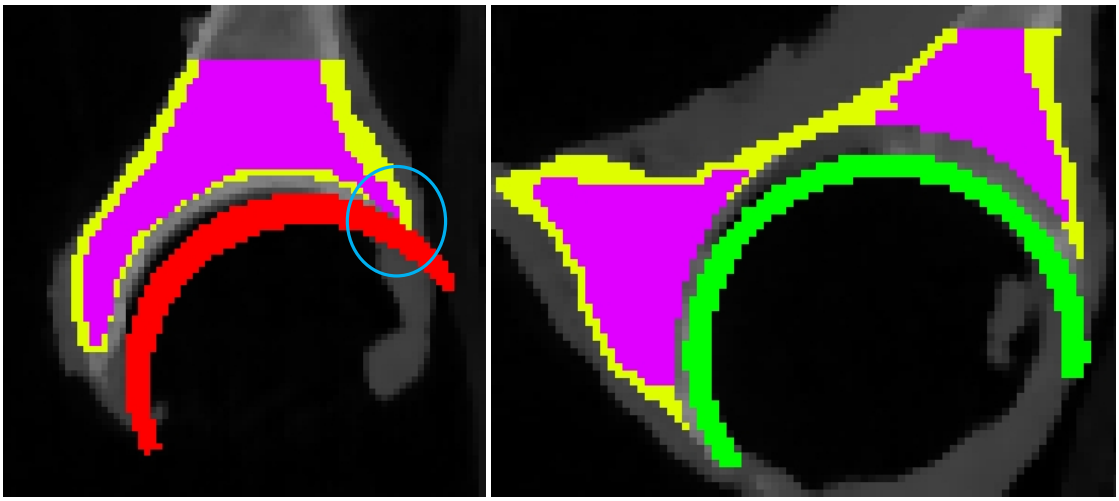

Figure 38 Incorrect position of cup with contact between cup and bone masks (left), correct position of cup with gap between cup and bone masks (right)

With the cup in the correct position the model was exported from Scan CAD to Scan IP to be meshed and material properties applied as described for the hemi pelvis, the resulting mesh was then imported into Abaqus CAE (Figure 39). The model contained around 300,000 tetrahedral elements. The mesh density was determined by the pixel size, in this case 0.45mm, although Scan IP enables the user to “down sample” the data to reduce the mesh density of the model produced, this option was not used as it would have resulted in loss of resolution of the cortical shell thickness. The cropped faces were fixed in all degrees of freedom (Figure 39), a surface-to-surface contact was used between the reamed acetabulum and the outside diameter of the cup with a coefficient of friction of 0.62 [206]. The porous coating was not modelled however the geometry of the cup models included the thickness of the coating, which is consistent with similar models in the literature [130, 131, 147-149]. Multiple displacements were applied to the inside surface of the cup to simulate impaction with a ball impactor as described in Chapter 4 (Figure 39). It has been suggested that load control could be more realistic [147] however Yew *et al.* have shown that displacement control reduces computation time without significantly affecting the results [130]. A small pre-load of 0.1 N was applied to the inside surface of the cup to stabilise the model. A Cartesian axis was set up using the cup as reference and the model was aligned to this axis to aid analysis of the results.

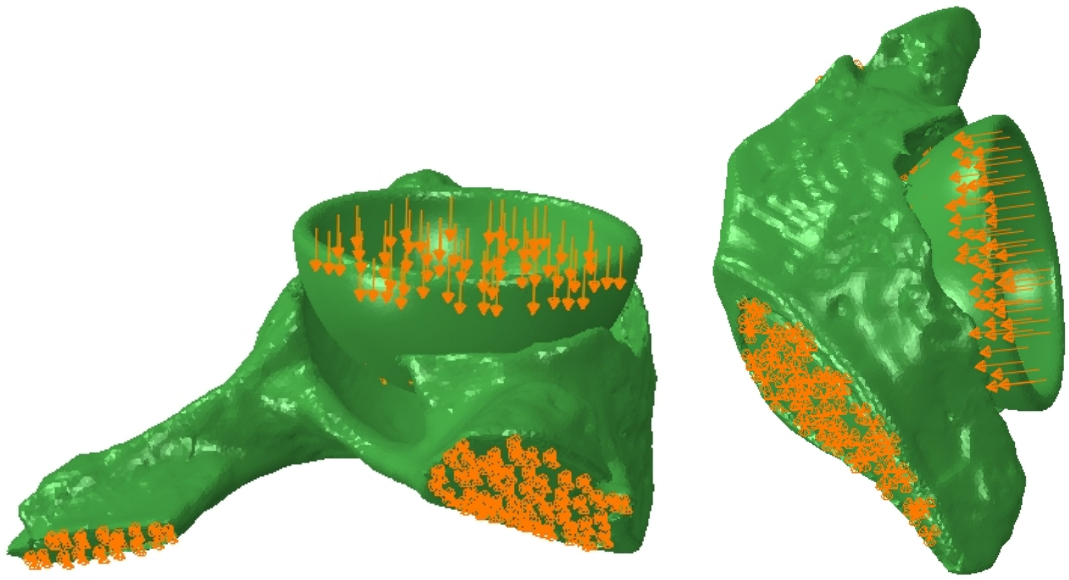

Figure 39 Acetabular model with cup in Abaqus showing fixed boundary conditions and direction of displacement

To assess the effect of the coefficient of friction between the cup and reamed acetabulum the thinnest cup was used as it represented a worst case; 4 different friction values were used: 0.2, 0.4, 0.62 and 0.8 all other variables in the model were kept constant. The lower values of μ may represent the effect of fluid in the reamed cavity, higher values represent novel tantalum porous coatings [212]. A model with homogeneous material properties was also created, again the thinnest cup was used, the cancellous bone was given a Young's modulus of 800 MPa and the cortical bone thickness was determined from the CT data. For comparison, a model was also created in which the cortical bone was assumed to have a constant thickness of 1 mm; refer to Table 11 for details of all the FE models created.

To measure the cup deformation the distance between 20 pairs of nodes on opposite sides of the rim of the cup was calculated at the beginning and end of the simulation (Figure 40).

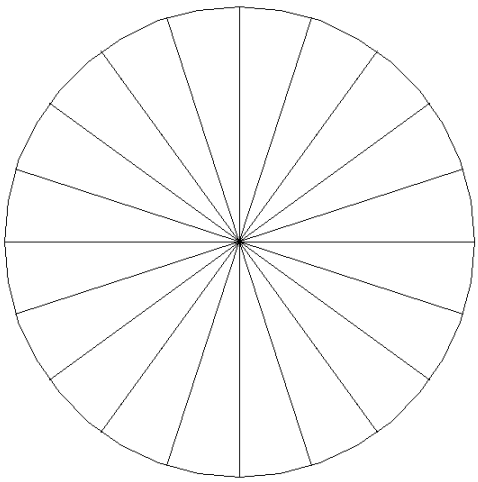

Figure 40 Diagram of the location of paired nodes for assessment of diametric deformation in FE model

Table 11 Cups modelled (LDT=Location Dependent Thickness, GS = Greyscale based)

Model	Cup size	Cup ID (mm)	ID offset (mm)	Press-fit (mm)	μ	Cortical bone	Cancellous bone
1	59	55	0	1	0.2	17000 MPa LDT	GS
2	59	55	0	1	0.4	17000 MPa LDT	GS
3	59	55	0	1	0.62	17000 MPa LDT	GS
4	59	55	0	1	0.8	17000 MPa LDT	GS
5	59	55	0	1	0.62	17000 MPa LDT	Homogeneous (800 MPa)
6	59	55	0	1	0.62	17000 MPa 1 mm thick	Homogeneous (800 MPa)
7	59	54.8	3	0.5	0.62	17000 MPa LTD	GS
8	59	54.8	3	1	0.62	17000 MPa LDT	GS
9	59	55	0	1	0.62	17000 MPa 1 mm thick	GS

Models 7, 8 were representative of the cups used in the cadaver experiment, i.e. with a 3 mm ID offset and a radial clearance of 930 μm between acetabular cup and femoral head. Different levels of press-fit were simulated by using different sized spheres to “ream” the acetabulum. Run times of approximately 5 hours were required for the cropped models described above.

5.4 Results: Experimental

5.4.1 Accuracy of Reaming

Table 12 Results from putty moulds of reamed acetabular cavities

Putty Sample	Reamer size (mm)	Laser Scan Results (mm)		Actual size of cavity (mm)
		Deviation (top to bottom)	**Deviation** (diameter)	
1	52	-0.9,	+0.5	51.1 to 52.5
4	54	Mould Not usable		
5	54	-0.39	-0.75	53.25 to 53.61
7	54	+0.4	+0.2	54.2 to 54.4
8	54	+0.5	-0.1	53.9 to 54.5
10	50	-0.1	-0.05	49.9 to 49.95
13	54	Very flat – maybe putty was not pushed in to cavity completely		

Table 12 shows the results from the laser scanning of the putty moulds taken from the reamed acetabular cavities. Figure 41 shows examples of the laser scan results; from these views it can be seen that mould 1 shows a deeper cavity compared to mould 7 which is somewhat shallow.

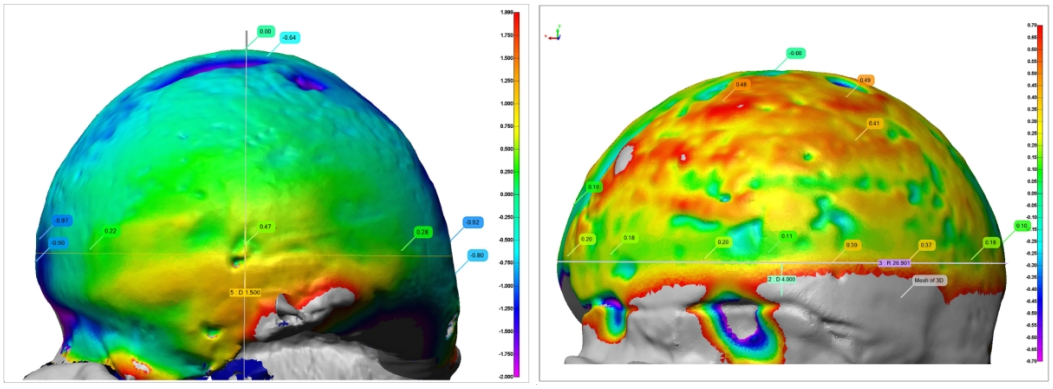

Figure 41 Example output from laser scanner for mould 1 (left) and mould 7 (right)

5.4.2 Deformation

Due to the sizes of cadaver available it was not possible to test the largest size cup; the cups tested were 1 x 50 mm cup, 1 x 52 mm cup and 3 x 54 mm cups. After impaction into the prepared acetabulum the matching heads were placed inside the cups; all heads articulated freely. Engineer's blue was smeared on the inside surface of the cups and the heads placed inside to check dome contact; all cups tested showed dye on the top of the head indicating dome contact (Figure 42 and Table 13). Moulds were taken of the impacted cups and laser scanned for comparison to CAD models of the cups (Figure 43). the results from the laser scanning are presented in Table 13.

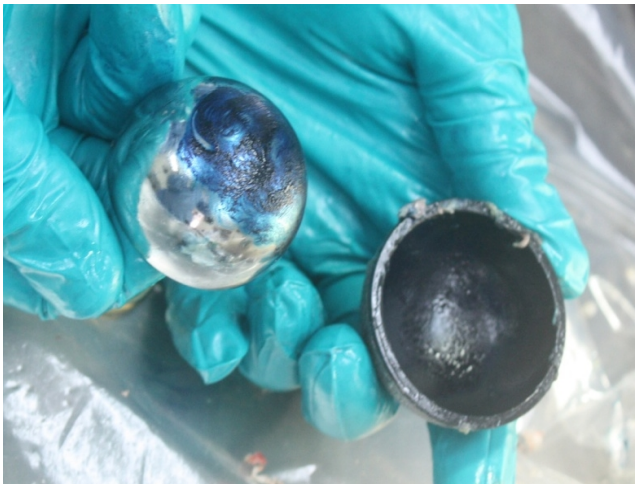

Figure 42 PEEK cup and metal head showing dome contact

Table 13 Results for impacted cups

Putty Sample	Cup size	Head articulated?	Dome contact?	Laser Scan Results (mm)	
				Max diametric compression	Max diametric expansion
2	52	yes	yes	-0.31	+0.46
3	52	yes	yes	-0.1	+0.25
6	54	yes but slightly stiffer	yes	-0.66	+0.46
9	54	yes	yes	-0.41	+0.31
12	50	yes	yes	-0.05	+0.11
14	54	yes	yes	-0.2	+0.4

All cups experienced compression in one direction and expansion in the perpendicular direction. A maximum diametric compression of 0.66 mm was recorded for one 54 mm cup, with a corresponding maximum expansion of 0.46 mm; in this case the head did not articulate as freely as the other cups; however dome contact was still indicated.

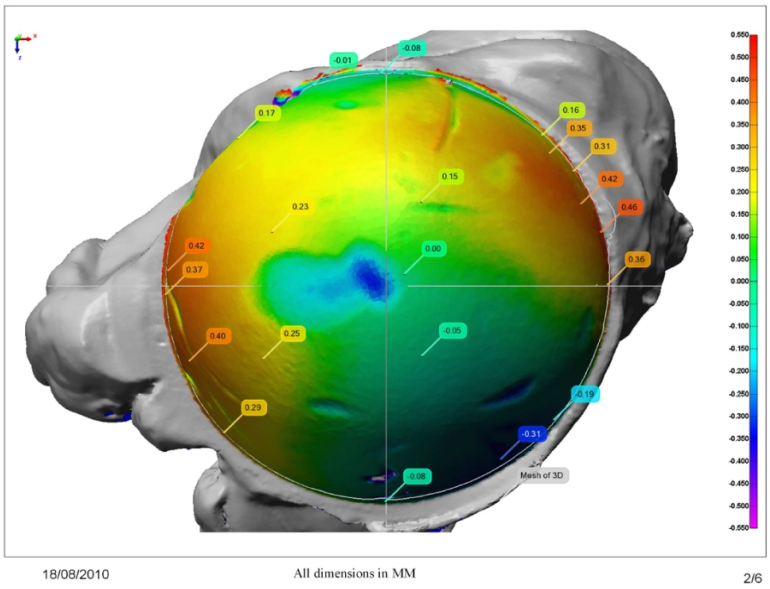

Figure 43 Example of laser scan and 3D CAD overlay

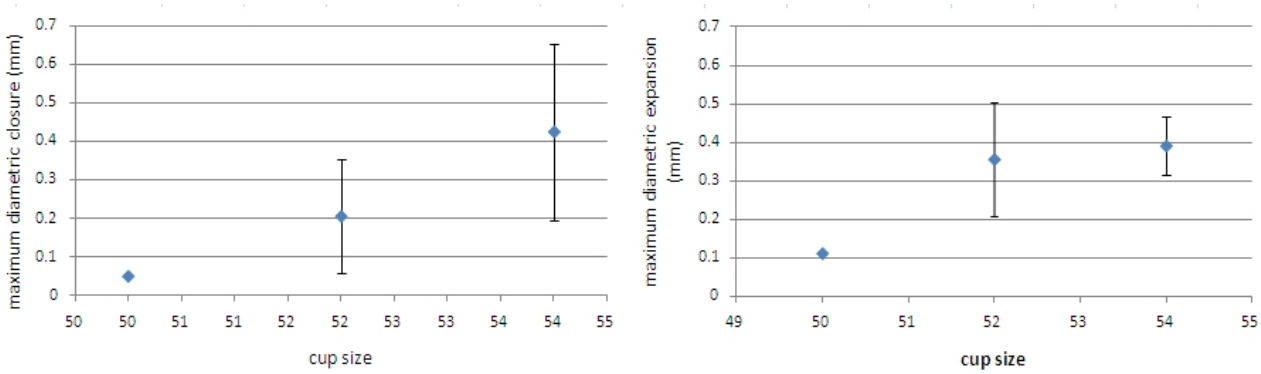

Figure 44 Graph of maximum diametric closure (left) and expansion (right) versus cup size

Figure 44 shows the relationship between cup size and maximum diametric closure. It can be seen that the level of deformation increased with increasing cup size, however there is a large standard deviation, and the sample size is too small to check for a significant difference.

5.5 Results: FE Model of the Pelvis

5.5.1 Material Properties

Linear regression was used to find the relationship between greyscale (GS) and density (ρ) (Figure 45). The following relationship was found;

$$\rho = 0.0008\,GS + 1.0398$$

Equation 3

The R^2 value of 0.984 shows a strong correlation between greyscale value and density (Figure 45).

Equation 3 was used to calculate the density of each pixel from the greyscale value using ScanIP; the software then assigns this density to the appropriate element in the finite element model. The range of densities found was 0.194 to 1.287 g/cm^3. Figure 46 shows the distribution of density in a cross section taken through the acetabular region. The trabecular bone is denser in the regions nearer to the cortical bone. Figure 47 shows the distribution of bone density in the cancellous bone (cortical shell not shown); higher density cancellous bone was found in the acetabulum, ischial tuberosity, iliac crest and body of ilium.

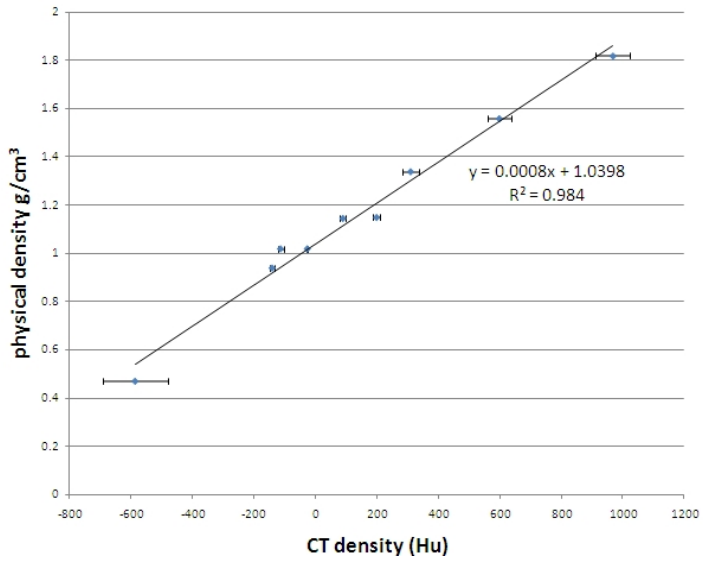

Figure 45 Graph of greyscale value vs. physical density of the CT phantom

Equation 1 was used to specify the Young's modulus of each element based on the calculated density value; range 35.7 to 3752.6 MPa, mean 911.6 MPa
The threshold tool in Scan IP was used to segment the cortical bone, the cortical bone had a maximum thickness of approximately 4.5 mm and a minimum of 0.45 mm; the minimum value was constrained by the slice thickness used in the CT

scanning process. The variation in the thickness of cortical bone can be seen in Figure 46.

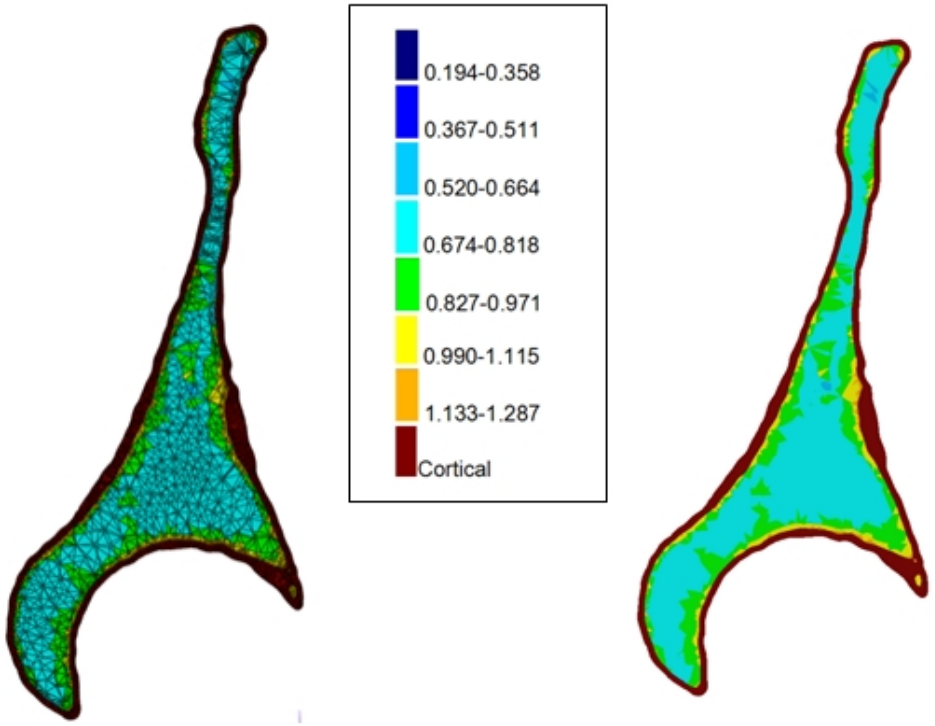

Figure 46 Distribution of material density (g/cm^3), section through acetabular region, with (left) and without (right) FE mesh

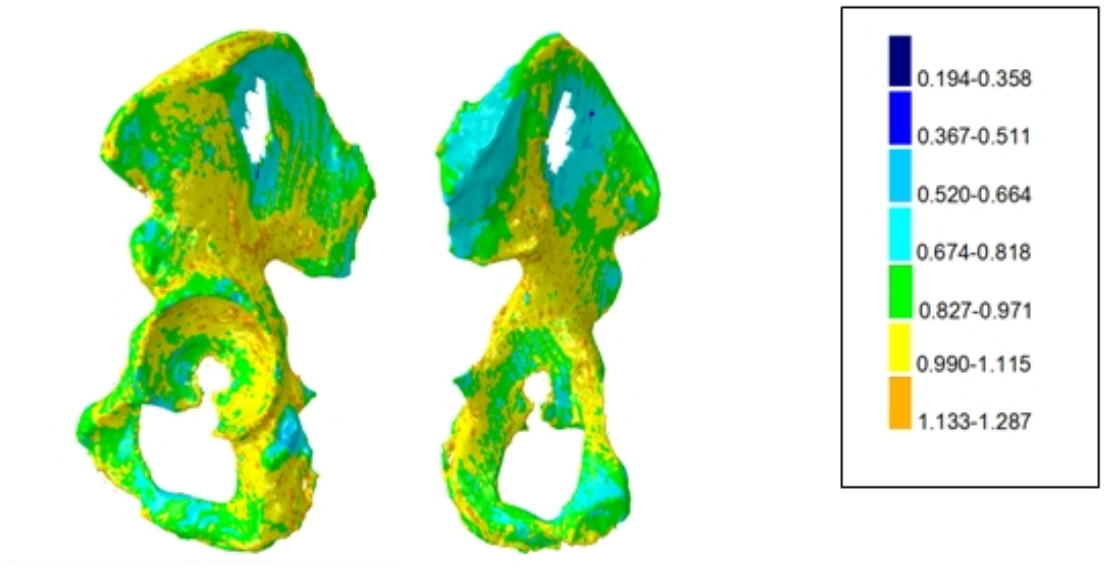

Figure 47 Distribution of bone density in cancellous bone, lateral (left) and medial (right) view

5.5.2 Deformation

Table 14 Results from FE model of pelvis created from CT data

Model	Cup size	ID	ID offset (mm)	Press-fit (mm)	μ	Cortical bone material properties used	Cancellous bone material properties used	Maximum diametric deformation (mm)	Maximum diametric expansion (mm)
1	59	55	0	1	0.2	17000 MPa LDT	GS	0.46	0.33
2	59	55	0	1	0.4	17000 MPa LDT	GS	0.51	0.32
3	59	55	0	1	0.62	17000 MPa Location depended thickness	GS	0.53	0.31
4	59	55	0	1	0.8	17000 MPa LDT	GS	0.56	0.34
5	59	55	0	1	0.62	17000 MPa LDT	Homogeneous (800 MPa)	0.42	0.24
6	59	55	0	1	0.62	17000 MPa 1 mm thick	Homogeneous (800 MPa)	0.42	0.20
9	59	55	0	1	0.62	17000 MPa 1 mm thick	GS	0.62	0.23
7(PEEK)	59	54.8	3	0.5	0.62	17000 MPa LDT	GS	0.30	0.10
7 (CoCr)	59	54.8	3	0.5	0.62	17000 MPa LDT	GS	0.15	0.08
8 (PEEK)	59	54.8	3	1	0.62	17000 MPa LDT	GS	0.41	0.17
8 (CoCr)	59	54.8	3	1	0.62	17000 MPa LDT	GS	0.22	0.17

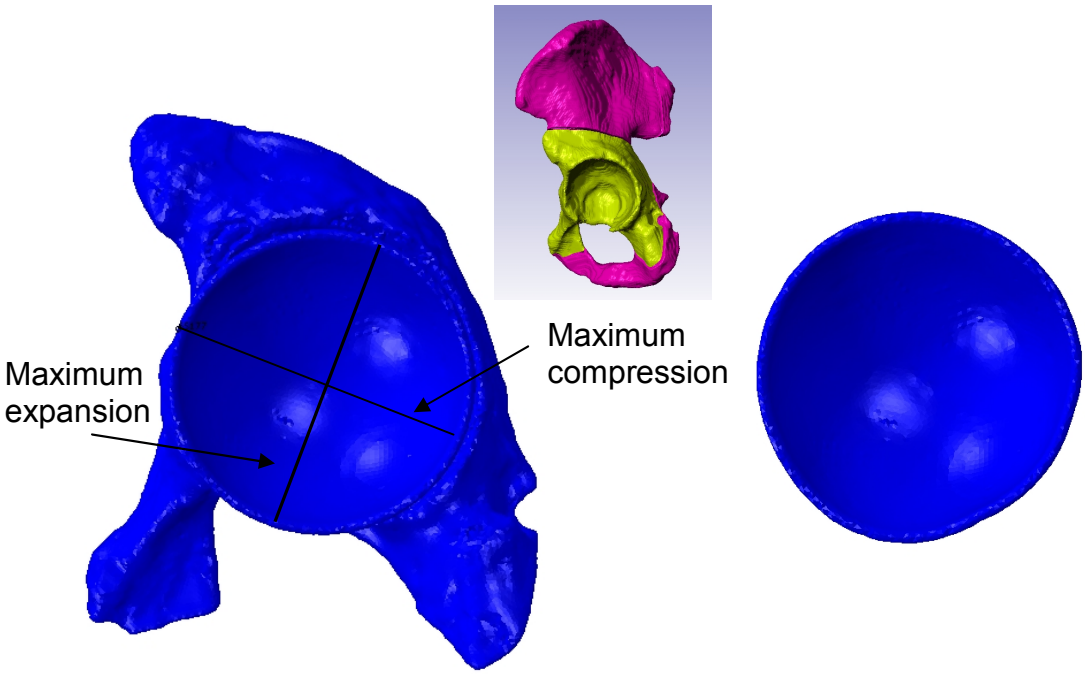

Figure 48 Direction of maximum cup compression and expansion in the FE model (left) exaggerated deformed cup (deformation scale factor = 4) (right)

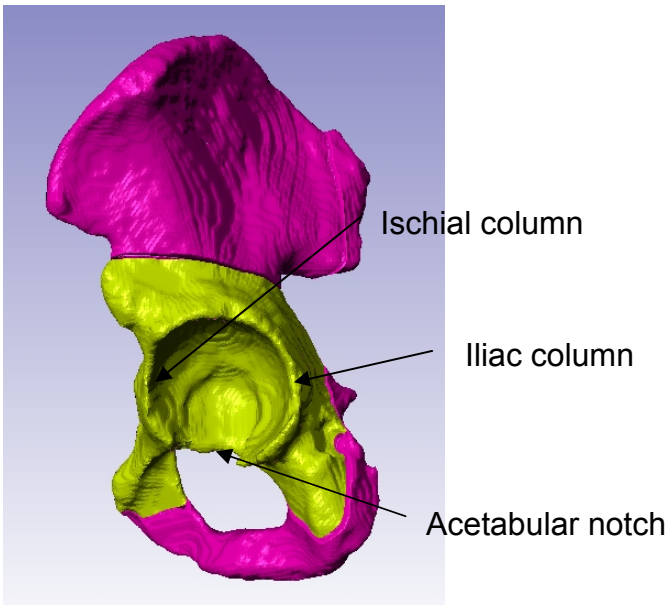

Figure 49 Lateral view of pelvis showing acetabular notch, iliac column and ischial column

At the end of the simulation the cups had undergone significant deformation (Table 14); experiencing compression in one direction and expansion in the perpendicular direction (Figure 48 left). The cups expanded through the acetabular notch where the cup does not have bony support, and were compressed between the iliac and ischial

columns (Figure 49). Exaggerating the deformation by a factor of 4 reveals an egg shaped deformation pattern (Figure 48 right).

Models 7 and 8 are representative of the cups used in the cadaver experiment. With 1 mm under-ream the cup experienced compression of 0.41 mm and expansion of 0.17 mm; with 0.5 mm under-ream the deformation was reduced to 0.30 mm and expansion was 0.10 mm. The thinner cup (model 3) experienced a greater level of deformation: 0.52 mm and expansion of 0.31 mm. For comparison with the literature on metallic resurfacing cups, models 7 and 8 were repeated with the cup having a Young's modulus of 210 GPa, the resulting deformation was 0.15 mm and 0.22 mm for models 7 & 8 respectively.

Models 1-4 were used to analyse the effect of the coefficient of friction (μ) between the cup and acetabulum on the deformation of the cup; four different coefficients were considered; 0.2, 0.4, 0.62 and 0.8. Only one cup size was considered for this section of the investigation; 58 mm cup with 2 mm wall thickness and 0 mm ID off set. Increasing the coefficient of friction from 0.2 to 0.62 resulted in a slight increase in diametric deformation for each pair of nodes (compression of 0.46 and 0.53 mm respectively). Increasing μ from 0.62 to 0.8 resulted in a decrease in deformation to 0.46 mm. The amount of cup expansion was also affect by the coefficient of friction; increasing μ resulted in a decrease in cup expansion, the model with μ=0.62 had a maximum expansion of 0.31 mm whereas the model with μ=0.2 had a maximum cup expansion of 0.33 mm.

When constant material properties were assumed for the cancellous bone (Young's Modulus of 800 MPa) the maximum deformation was reduced from 0.53 mm (Model 3) to 0.42 mm (model 5). Model 6, which had homogeneous material properties and constant cortical thickness, also predicted cup deformation of 0.42 mm. With constant cortical thickness and greyscale based material properties, model 9 predicted 0.62mm of deformation.

The maximum von Mises stress occurred predominantly near the rim of the cup (Figure 50, Figure 51 & Figure 52). Table 15 shows the maximum von Mises

stresses predicted in the cortical bone for each model as recorded by the Abaqus output data base.

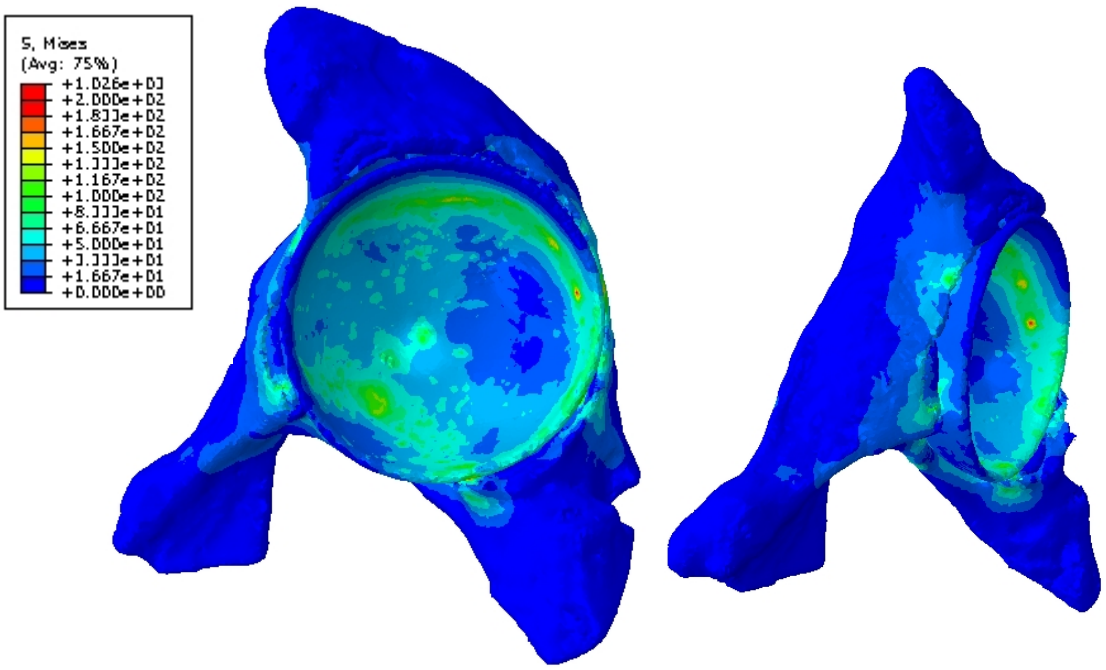

Figure 50 Plot of maximum von Mises stress for model 3

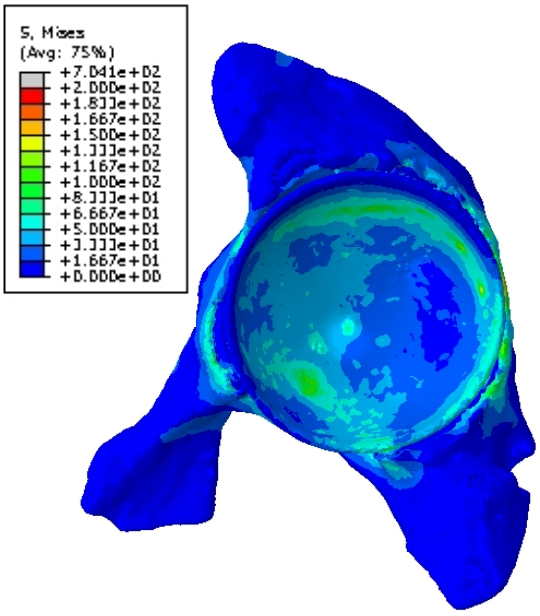

Figure 51 Plot of maximum von Mises stress in model 5

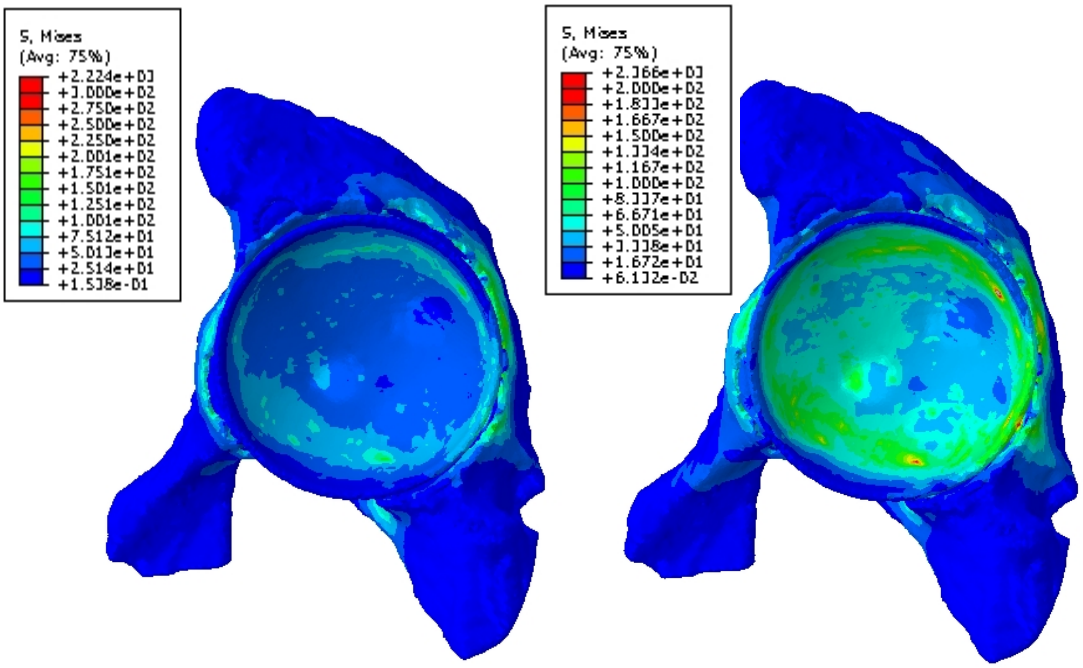

Figure 52 Plot of maximum von Mises stress model 6 (left), model 9 (right)

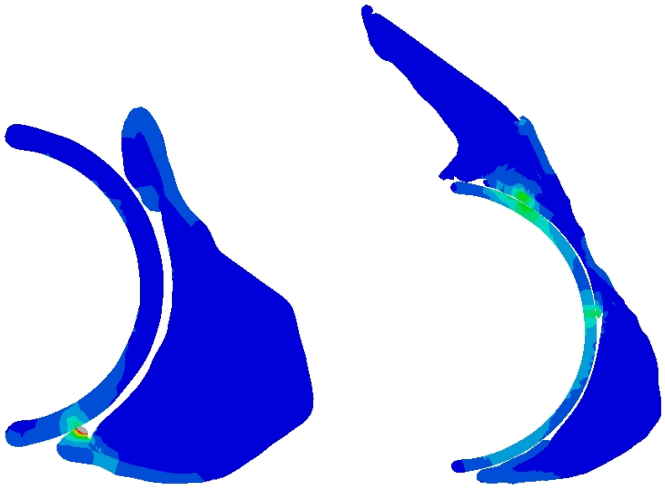

Figure 53 Example cross sections; point contact occurring part way though simulation (left) seated cup at end of simulation (right)

Table 15 Maximum von Mises stress in cortical bone

model	Maximum von Mises Stress in Cortical bone (MPa)
1	35
2	42
3	120
4	63
5	61
6	92
7	100
8	135
9	183
7 metal	200
8 metal	253

5.6 Discussion

The results of the laser scanning of the reamed acetabulum moulds showed that cavities were rather elliptical, in some cases being up to 0.5 mm larger than the nominal size of the reamer in one direction and in other cases being undersized by up to 0.75 mm. In the case where the cavity is undersized it is possible that the reamer was not pushed into the acetabulum properly due to a surgical technique error. The cavities produced were very uneven with high and low points evident on the moulds. There was also variation in the shape of the cavities produced with some being rather shallow and others deeper. The results are generally in agreement with other published data which show that reamed acetabula are uneven and generally larger than the size of reamer [27, 193, 195, 207, 213].

Kim *et al.* [192] and Mackenzie *et al.* [193] used artist's plaster to measure the size and shape of cavities prepared in cadaveric specimens. They found that the cavities produced were elliptical rather than hemispherical; in general the variation from hemisphere was in the depth [192, 193]. It was also found that the deviation from hemisphere was greater for smaller sized pelvis than larger (smaller pelvis had shallower cavities whereas larger ones were closer to hemispheres) [192]. In all cases the actual transverse diameter was larger than that specified on the reamer

[192, 193]. The cavities were on average 0.56 mm larger than the reamer size, with a maximum of 1.63 mm [193]. Alexander *et al.* carried out similar tests test on cadaveric pelvises, using high viscosity vinyl polysilicone impression material to make moulds of the prepared cavities [194]. They found deviations from sphere in some areas of the prepared acetabular of up to 4 mm; 11 out of 12 samples were over reamed, by an average of 0.5 mm [194]. MacDonald *et al.* reported inaccuracies of up to 2.9 mm in cavities produced during actual THA procedures [214]. In published data the difference between the reamed cavities and the reamer size is greater than the current study, with maximums of 4 mm [207], whereas in the current study there was a maximum over-ream of 0.5 mm. This difference may be due to improvements in the design of grater reamers; the published data is up to 10 years old. More recently Jin *et al.* reported that the average size of Sawbones cavity produced by hand reaming for a nominal reamer size of 59 mm was 59.56 ±0.15 mm [51]. Baad-Hansen *et al.* reported a mean deviation from best-fit sphere of 0.3mm ±0.4 mm using an optical 3D digitising system to scan prepared cavities of embalmed cadavers [195].

The variation in the size of cavities produced is likely to be a product of the large number of variables involved; surgical technique between the 5 surgeons, bone quality and how worn the reamers were.

In the impaction testing, as expected, larger diameter cups experienced greater deformation than smaller cups. The largest diametric deformation was 0.66 mm, which seems to be larger than expected given the size mismatch between the reamer and the cups (nominally 1 mm). This level of deformation can be explained when the actual size of the reamed acetabular cavity is considered; cup 6 was impacted into cavity 5 which was undersized by up to 0.75 mm. Despite the large deformations recoded all heads articulated freely and dome contact was indicated with Engineer’s blue. This is due to the large clearance between the femoral head and acetabular cup. The standard deviation in the results is quite large; this can be explained when the variability in the size of the cavity is considered. In addition there is likely to be variation in the bone density and stiffness between the cadaver

samples; Thompson *et al.* found a large variation in the Young's modulus of cancellous bone taken from THA patients [201].

Latif *et al.* briefly reported on impaction of the CFR-PEEK Mitch cup [27]. They reported that reaming with standard reamers gave large variations in the diameter of the cavity produced and that in some cases this lead to annular contact between the head and cup [27], the use of "finishing" reamers with improved manufacturing tolerances improved the quality of the bone surface. Unfortunately it is not explicitly reported if this alleviated the problem of annular contact; the magnitude of cup deformation was also not reported. There are no other reports in the literature on impaction/deformation of CFR-PEEK cups, however the deformation of metal acetabular components is widely reported; Squire *et al.* [46] reported that titanium Pinnacle shells had diametric compression deformity ranging from 0 to 0.57 mm (mean 0.16 mm ± 0.16) when inserted with a 1 mm press-fit technique *in vivo* [46]. Using polyurethane foam Fritsch *et al.* [48] found the Bi-Con plus cup exhibited a change in diameter of around 22 μm on impaction [48], however the foam cavities had to be enlarged to allow impaction. Trident shells (titanium shell) have been reported to deform by up 0.79 mm on impaction into polyurethane foam [128, 158]. Jin *et al.* found that a typical MOM resurfacing component deformed by up to 103 μm when impacted into polyurethane foam and cadaveric specimens [51]. Grimes [49] also used polyurethane blocks to compare the deformation on impaction of 11 retrieved Durom resurfacing cups (Zimmer, Warsaw, Indiana) and 11 BHR cups (Smith and Nephew, Memphis, Texas), a mean diametric deformation of 89.8 ± 14.8 μm was found for the Durom, and. 57.2 ± 25.8 μm for the BHR

As PEEK is a more flexible material than cobalt chromium or titanium it is not surprising that it experiences a greater level of deformation when impacted. However the deformation pattern (i.e. compression in one direction and expansion in the perpendicular direction) is in agreement with the work of Jin *et al.*'s work on impacting resurfacing cups into cadavers [51].

The results obtained from the segmentation of the CT data of the cadaveric specimen showed that the thickness of the cortical shell found in this study (min 0.45

mm, max approximately 4.5 mm) is similar to that reported in the literature; Dalstra *et al.*, Anderson *et al.*, Majumder *et al.* and Zhang *et al.* report cortical thicknesses of 0.7 to 3.2 mm, 0.44 to 4 mm, 0.74 to 4.061 mm and 0.5 to 4 mm respectively [135, 139, 140, 203, 215], Jansson *et al.* and Thompson *et al.* report slightly lower thicknesses of 0.7 to 3.2 mm and 0.96 to 2.06 mm respectively [146, 150]. As the models are subject specific, variations in bone density and thickness are to be expected between models. The locations of the thickest and thinnest cortical shell are also generally in agreement with the published results of Dalstra [135] and Anderson [139]; the other authors did not state the locations of the thicknesses found.

The relationship found between physical density and CT attenuation (ρ=0.0008CT+1.03) is similar to those found in the literature (ρ=0.0008CT-0.8037 [139], ρ=0.00099CT+0.0419 [203], ρ=0.0019CT+0.105 [153], ρ=0.000691CT+1.0267 [143]); differences are to be expected as the relationship depends on the specifications of the CT scanner being used [211]. When the Dicom images of the CT phantom were analysed it was noticed that the pixels within each phantom tube did not have uniform greyscale values, and therefore a modal value was used; this is consistent with the work of Anderson *et al.* who also reported using an average greyscale value from their phantom [139]. The density of the cancellous bone was found to range from 0.194 to 1.287 g/cm^3; this range of densities is in good agreement with the results of Vasu *et al.*, Dalstra *et al.* and Zhang *et al.*; Vasu *et al.* found apparent densities of 0.2 to 1.3 g/cm^3 around the acetabulum [133], Dalstra *et al.* found apparent densities of 0.101 to 0.9 g/cm^3 [103]. Other studies however have found lower ranges of densities; Majumder *et al.* found 0.042 to 0.541 g/cm^3 [203] and Thomson *et al.* [201] found apparent density of 0.348 ±0.173 g/cm^3 from imperial measurements taken from acetabular samples from THA patients. Variation between studies is expected as there are many variables influencing the bone density of individuals such as age [52, 202], diet [52, 216], weight [216] and disease [52]. Young's modulus was calculated from the density values and was found to be 35.7 MPa to 3752.6 MPa which is similar to the ranges reported in the literature [139, 140, 146]. The mean Young's modulus was found to be 911.7 MPa, which is rather higher than that published in other studies; Zhang *et al.* reported a mean of 151 MPa [140],

and Anderson *et al.* found a mean of 338 MPa [139], Thomson *et al.* found a mean E of 116.4 MPa from empirical measurements taken from acetabular samples from THA patients [201]. It is to be expected that the mean Young's modulus is higher from a donor with no know bone disorders as compared to THA patients. The areas of cancellous bone of high density and therefore high Young's modulus are generally in agreement with published data on pelvic cancellous bone density [135, 139]. The denser areas of bone also coincide with the areas reported to experience higher stresses during gait [134, 137, 141, 204] which is consistent with Wolff's Law [217].

The hemi pelvis created in this study has been shown to be generally consistent with other models created from CT data reported in the literature and is therefore suitable for investigating the level of deformation on impaction of the prototype cup. Although the model in this study has a higher modulus, this represents a worst case in terms of deformation. The hemi pelvis was cropped to reduce the number of elements (to speed up processing time) and to simplify the boundary conditions. Impacting the cup into the acetabulum was modelled using displacement control; this does not necessarily completely represent the clinical situation. During surgery the surgeon hits the impactor with a mallet, delivering a certain power (a high load in a short time), neither displacement control nor load control simulations accurately simulate this. The mechanical behaviour of bone is strain rate dependent [138], however linear elastic models do not account for this. Given a linear elastic model, load controlled or displacement controlled "impaction" should give the same result as the simulation is controlled by the seating of the cup and the interference between the cup and acetabulum.

Model 7 is representative of the prototype cups used in the cadaver experiment and has an under-ream of 0.5 mm based on the results of the reaming study. The FE model predicted that the cup would deform by 0.3 mm. As the cadavers used in the experiment were somewhat smaller than that used to create the FE model, direct comparison between the results is not possible. Although the deformation is in a similar range to that found in the cadaver experiment is it rather lower than might be expected by extrapolating from the line of best fit from the cadaver testing. The acetabulum of the cadaver used to create the FE model was rather shallow, resulting

in the rim of the cup not being in contact with the acetabulum even though the cup was fully seated, which may explain the slightly lower deformation than expected. Yew *et al.* also reported that their model tended to under estimate deformation on impaction compared to cadaveric tests [51, 130]. Increasing the level of press-fit from 0.5 mm to 1 mm (model 8) resulted in an increase in cup deformation to 0.41 mm which is consistent with the findings of the cadaver experiment.

Models 7 & 8 were repeated with cup material properties to represent cobalt chromium (Young's Modulus = 210 GPa); deformations of 0.15 mm and 0.22 mm were predicted respectively. This is rather higher that reported by Udofia *et al.* who predicted deformation of 0.096 mm for 2 mm under-ream, 0.048 mm for 1 mm under-ream and 0.069 for line-to-line for the Durom resurfacing cup [131], however the Durom cup has a wall thickness of 4 mm which is greater than the thickness of the cup in the current study and therefore less deformation is expected. The cup modelled in this study is comparable to the "thin" cup modelled in the work of Yew *et al.*, where it was reported that the 60 mm thin cup deformed by 0.11 mm when impacted with a 0.5 mm under-ream [130].

The coefficient of friction between the cup and bone used in FE models has been shown to have an influence on polar gap [147] and contact area [145, 147] and micromotion [145]. In the current study, increasing the coefficient of friction from 0.2 to 0.62 resulted in an increase in deformation, however further increasing μ to 0.8 resulted in a decrease in the cup deformation. This may be due to the cup not being pushed into the cavity as far. Spears *et al.* investigated the effect of coefficient of friction on polar gap and cup penetration and found that the cup penetrated deeper into the acetabulum when lower coefficients were assumed [147].

The maximum stresses in the cup occurred near the rim which is in agreement with the work of Udofia *et al.* [131]. The maximum stresses were not concentrated right at the rim of the cup but slightly below it; this is due to the rim of the cup not being in contact with the bone even though the pole of the cup is seated in the acetabulum.

Very high maximum von Mises stresses were predicted in the cortical (up to 2366 MPa) and cancellous bone (up to 50 MPa) in very small areas. The stresses are considerably higher than the compressive strength of bone; the compressive strength of cortical bone has been shown to be in the region of 100 to 350 MPa depending on strain rate [218]. These high stresses may occur due to hanging nodes, locally compressed elements or as a result of model abstraction. Away from these point loads the maximum stress in the cortical bone around the acetabulum in the heterogeneous models was around 135 MPa. The range of maximum von Mises stresses predicted in the cortical bone of 3D FE models in the literature is relatively wide: 17 MPa [137], 30 MPa [135], 44 MPa [139], 70 MPa [141, 146], however only Udofia *et al.* simulated press-fit and reported maximum von Mises stresses of 67 MPa with 1 mm under-ream and 125 MPa with 2 mm under-ream [131]. Differences between models are to be expected due to the different ways that the models were created (homogeneous from CT, heterogeneous), the boundary conditions used (fixed or muscular) and the loading. It is not unexpected that the current model would predict higher stresses than those reported in the literature; to the author's knowledge there has not been another model of impaction simulated in this way. Published studies of 3D pelvis models have simulated press-fit using "clearance" and "contact interference" formulations in FE packages; which push apart contact surfaces of the acetabulum and cup [131, 148-150]. In the current study it was not possible to use this method due to the high mesh density; the use of interference fit resulted in elements with zero volume. Thermal expansion has also been used to simulate press-fit [57], initial trials in the current study found that this was not a suitable method to find absolute values for deformation. Load pulses have been used in 2D models of the acetabular region [130, 147] and displacement pulses have been used in models of Sawbones Blocks [130]. Other 3D models of the pelvis have not considered press-fit, instead assuming line-to-line reaming (with cup outside diameter matching acetabular diameter) and assumed perfect contact between the cup and bone surfaces [136, 141, 142, 145, 146]. This is inconsistent with the findings of other studies which has shown polar gaps remaining after impaction in to cadaver specimens [193].

The maximum von Mises stresses predicted in the bone of the acetabulum in the model with heterogeneous material properties and location depended cortical thickness (model 3) were 120 MPa, when a constant cortical thickness of 1 mm was assumed the maximum stress increased to 99 MPa when heterogeneous cancellous bone was used (Model 9) and 183 MPa when constant material properties were used (Model 6). Model 5, which had location dependent cortical thickness and constant material properties had reduced maximum stresses compared to model 3; 61 MPa. The cup deformation predicted by models 3, 5, 6 & 9 were 0.53, 0.42, 0.42 and 0.62 mm respectively. Both models with homogenous material properties for cancellous bone (5&6) have similar levels of deformation which suggests that the properties of the cancellous bone are dominating the behaviour. The models with homogeneous cancellous bone material properties (regardless of location dependent cortical thickness) had reduced stress around the acetabulum and less cup deformation compared to the heterogeneous model. When constant cortical thickness but heterogeneous material properties were used, the model was significantly stiffer, with high stresses and greater deformation of the cup.

Dalstra *et al.* found that a homogeneous model (with constant cortical thickness and constant material properties) generally had higher stresses than the heterogeneous model with the same geometry [135]. Anderson *et al.* found that a homogeneous model (constant cortical thickness and constant material properties) was stiffer than a subject specific model with the same geometry; it was found that constant cortical thickness had a greater influence on the stiffness of the model than the material properties of the cancellous bone [139]. Zhang *et al.* found that the homogeneous model (constant material properties but variable cortical thickness) underestimated bone stresses compared to experimental results and their heterogeneous model [140], which are in agreement with the findings of the current study. The use of location dependent material properties is probably more important in models that are looking at acetabular implants because the cortical bone in the acetabulum has been removed and the implant is in direct contact with the underlying trabecular bone.

The model of the hemi pelvis was cropped to reduce the number of elements and to simplify the boundary conditions. This is potentially a limitation of the model,

however the stress (and deformation) in the model was confined to the area in the vicinity of the acetabulum; therefore it is not felt that cropping the model had a significant effect on the results. Muscle forces and body weight were not included in the model; however these would not be relevant during surgery, the damping effect of the soft tissue may influence the stress in the bone and this was not considered within the model.

The amount of cup deformation that occurs on impaction into the acetabulum is influenced by the level of press-fit as well as design parameters such as wall thickness. The results of this study highlight the importance of surgical technique; the variation in the size of reamed cavity may be in part due to surgical technique, although other variables also have an effect, such as bone density, the original anatomy of the acetabulum, surgical instrument design and wear.

Chapter 6 – Tribological Testing of Zirconia Toughened Alumina Femoral Head on CFR-PEEK Acetabular Cup

6.1 Introduction

The testing conducted in the previous chapters showed that the prototype PEEK cup experienced significant deformation on impaction into both cadaveric specimens and Sawbones cavities. Deformation of an acetabular cup will result in changes in the clearance between the modular femoral head and acetabular cup. It has been previously shown that bearing clearance affects the lubrication regimes of THA bearings [205, 219, 220]. If the lubrication regime of a bearing is very sensitive to changes in clearance, deformation of the cup could adversely affect the tribological behaviour of the system. The possible effect of changes to the lubrication regime of an acetabular bearing is a high wear rate, leading to a greater volume of wear particles which would elicit an increase in the body's foreign body reaction. The result of this reaction varies depending on the material; for example UHMWPE wear particles result in osteolysis [2-4], CoCr wear particles can lead to local accumulation and systemic distribution of cobalt chromium particles and ions [6, 58], hypersensitivity [11, 12], toxicity, carcinogenesis [3, 13] and aseptic lymphocytic vascular and associated lesions (ALVAL) [12, 14]. Very high friction could also result in micromotion at the bone-implant interface which can result in unfavourable conditions for bone growth in to porous coatings [221]. To assess the sensitivity of the Biomet ZTA-on-PEEK bearing to changes in clearance; friction testing was conducted on prototype cups with various clearances.

The aims of this study were;

1. To investigate the effect of clearance on the lubrication regime of the Biomet ZTA (Zirconia Toughened Alumina) ceramic-on-CFR-PEEK hip implant.
2. To investigate the effect of protein in the lubricant on the friction factor.

Theoretical predictions for minimum film thickness and lubrication regime were also made and compared to the experimental results.

6.2 Method

6.2.1 Clearances

In order to determine an appropriate range of clearances to be tested; the effective radius was considered, given by:

$$\frac{1}{R_{eff}} = \frac{1}{R_1} + \frac{1}{R_2}$$ Equation 4

[222]

where R_{eff} = effective radius (m)

R_1 and R_2 = radius of surface 1 and 2 respectively (m)

For convex surfaces R_1 and R_2 are positive, for a concave surface they are negative. Therefore for a ball and socket arrangement the formula becomes:

$$\frac{1}{R_{eff}} = \frac{1}{R_1} - \frac{1}{R_2}$$ Equation 5

Where:

R_1 = head radius (m)

R_2 = cup radius (m)

Ceramic-on-PEEK bearings have been previously shown to operate under mixed-boundary lubrication [118, 223]. In order to find a suitable starting point for the clearance of the Biomet PEEK cup a ceramic-on-polyethylene (Exceed ABT, Biomet UK, Ltd) was considered as this bearing combination has also been shown to operate under mixed lubrication [190, 191]. The effective radius of the COP (Ceramic on Polyethylene) bearing was calculated, this radius was then used to work back from the actual size of ceramic head to give a suitable cup size for the PEEK cup. The aim of this was to give both the COP and ceramic-on-PEEK bearings the same effective radius, thus ensuring mixed lubrication.

To give a range of clearances the largest effective radius was found from the tolerance combination which gave the smallest clearance, i.e. minimum head size - max cup size, and vice versa for the smallest effective radius.

The largest effective radius of a 28 mm polyethylene bearing was calculated as follows using Equation 5;

$$R_{eff} = \frac{1}{\frac{1}{R_1} - \frac{1}{R_2}} = \frac{1}{\frac{1}{R_{head\ min}} - \frac{1}{R_{cup\ max}}} = \frac{1}{\frac{1}{14mm} - \frac{1}{14.05mm}} = 3.93m$$ Equation 6

This effective radius was then used to calculate a maximum cup inside diameter (ID) given the head size (Magnum C, Biomet UK Ltd). The smallest effective radius was used to calculate the minimum cup diameter. Given these two values and the known size of the head; the maximum and minimum clearances were found. The PEEK cup ID was calculated so as to have a similar effective radius as the polyethylene bearing.

6.3 Samples

6.3.1 Clearance Testing; Phase 1

In the phase 1 testing, only one ceramic head was available; a 52 mm ZTA head (Biomet UK Ltd, Bridgend, UK), the head was measured using a CMM at Biomet to obtain the actual head size. Hemispherical cups with 52 mm articulating diameter and 58 mm outside diameter (OD) were machined from Motis PEEK (Invibio, Blackpool, UK) extruded bar by Biomet UK Ltd, to match the size of the ceramic head. 3 radial clearances were tested; 200, 300 and 400 μm.. The ID was polished by Biomet UK Ltd using methods similar to those used in the manufacture of ReCap resurfacing cups to achieve a surface roughness (R_a) of 0.1 μm (measured using a contacting profilometer (Talysurf, Taylor-Hobson μltra)). Due to an error in the manufacturing process the clearances tested in phase 1 were not actually 100, 200 and 300 μm but 257, 661 and 706 μm. The phase 1 testing was conducted at Durham University.

6.3.2 Clearance Testing: Phase 2 and 3

Due to the manufacturing error during the production of the samples for phase 1 a second set of cups were tested: four radial clearances were tested; 30, 330, 630 and 930 μm to gain a better understanding of the effect of clearance on Friction Factor (FF). The testing was conducted on cups with a 52 mm articulating diameter and 58 mm outside diameter manufactured from Motis PEEK extruded bar (Invibio, Blackpool, UK). The same 52 mm ceramic head was used for the clearance testing. Again the cups were machined to match the ceramic head to ensure the actual clearance was as close as possible to that specified. Testing was conducted at both

the University of Durham (phase 2) and the University of Bradford (phase 3). The cups had a machined finish on the inside diameter with a roughness (R_a) of 0.5 µm measured using a contacting profilometer (Talysurf, Taylor-Hobson µltra).

6.3.3 Stribeck Analysis

Stribeck analysis has been widely used to determine the lubrication regime in loading contacts [118, 224-228]. In this method friction factor (f) is plotted against the Sommerfeld number (z) (Figure 54), where:

$$f = \frac{T}{rL}$$ Equation 7

$$z = \frac{\eta u r}{L}$$ Equation 8

T = frictional torque between the bearing surfaces (Nm)
r = femoral head radius (m)
L= load applied (N)
η = viscosity of lubricant (Pas)
u = entraining velocity (average of the surface velocities of the two bodies in contact relative to the contact [224]) (m/s)

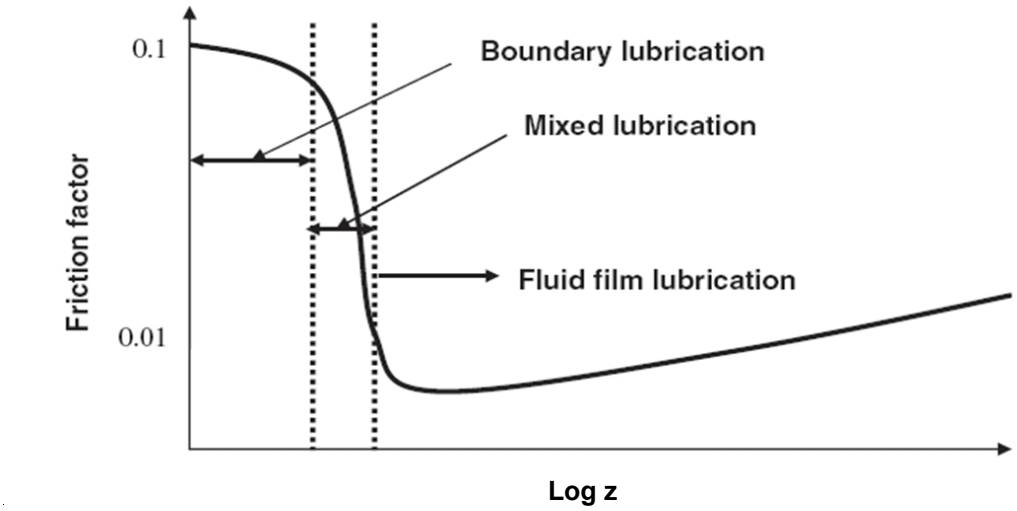

Figure 54 Idealised Stribeck plot

The Sommerfeld number is varied by altering the viscosity of the lubricant the entraining velocity, femoral head radius and load are kept constant. A falling trend in

the Stribeck plot indicates mixed lubrication, in which the load is carried by asperity contact and the lubricant pressure. As the curve reaches a minimum there is a transition from mixed to full fluid film lubrication and the friction factors are typically below 0.01 [225]. A rising trend with low overall friction indicates fluid film lubrication, where there is no asperity contact and the load is completely carried by the pressure in the lubricant [222], the raising trend due to the increasing force required to shearing the lubricant as its viscosity increases [225].

6.3.4 Prediction of Lubrication Regime

Hamrock and Dowson's theory was used to predict minimum film thickness [229]. The following formulae were used:

$$\frac{h_{min}}{R_x} = 2.798 \left(\frac{\eta u}{E' R_x}\right)^{0.65} \left(\frac{L}{E' R_x^2}\right)^{-0.21}$$

Equation 9

where

h_{min} = minimum film thickness (m)

R_x = effective radius (given by Equation 5) (m)

η = viscosity of lubricant (Pas)

u = entraining velocity (average of the surface velocities of the two bodies in contact relative to the contact [224]) (m/s)

L = load (N)

E' = equivalent modulus (given by Equation 10) (Pa)

$$\frac{1}{E'} = 0.5 \left(\frac{1 - v_1^2}{E_1} + \frac{1 - v_2^2}{E_2}\right)$$

Equation 10

E_1 = Modulus of head material (Pa)

E_2 = Modulus of cup material (Pa)

v_1 = Poisson's ratio of head material

v_2 = Poisson's ratio of cup material

Young's modulus of the head material (zirconia toughened alumina) was taken as 370 GPa [54], and 15 GPa [90] was used for the cup material (CFR-PEEK). The Poisson's ratios used were 0.22 and 0.4 for ceramic and CFR-PEEK respectively.

The load used in both University of Bradford and Durham testing was 2000 N [230], the entraining velocity of the Bradford simulator was 0.02 m/s and 0.015 m/s in the Durham friction simulator.

The lambda ratio was then calculated using Equation 11. Lambda is a dimensionless parameter calculated using the predicted minimum film thickness and the measured roughness values. Johnson *et al.* observed that if the lambda ratio is less than one, boundary lubrication is likely. If lambda is greater than three then full fluid film lubrication is likely and mixed lubrication is likely when lambda is between 1 and 3 [68].

[68].

$$\lambda = \frac{h_{min}}{\left(\sqrt{R_{q1}^2 + R_{q2}^2}\right)^{0.5}}$$

Equation 11

R_{q1} = roughness of head (m)

R_{q2} = roughness of cup (m)

The surface roughness (R_q) of the CFR-PEEK cups and Ceramic head was measured using a contacting profilometer (Talysurf, Taylor-Hobson µltra), three readings were taken and the average value used for the lambda ratio calculations.

6.3.5 Durham Friction Test Set Up

The Durham friction simulator consists of an oscillating upper frame in which the femoral head is mounted. The acetabular cup is fixed inverted to the anatomical position at 33° in the measuring carriage. A servohydraulic system applies a simple load profile comprising of a low load swing phase; the maximum and minimum forces exerted on the prostheses are 2000 and 100 N respectively, based on the work of English [230]. Sinusoidal motion was imposed on the femoral component in the flexion extension plane with amplitude of ±24° and a cycle frequency of 0.8 Hz. Load, frictional torque and angular displacement were recorded at the 1st, 21st and 41st cycle and used for final analysis.

The tests were performed with carboxymethyl cellulose (CMC) solution as the lubricant as well as CMC with bovine serum (BS) (25%). The viscosity ranged from 0.01 Pas to 1 Pas (±10% deviation) (0.01, 0.03, 0.1, 0.3 and 1 Pas). CMC fluids were used because of their similar rheological properties to synovial fluid [231]. Each cup was tested 3 times. The cups were held in a custom made UHMWPE fixture (Figure 55); the head was held on a tapered head holder. The phase 1 clearance tests were conducted using one design of cup holder; due to a machine breakdown and subsequent redesign of the carriage a new design needed to be manufactured for the phase 2 testing. The redesign ensured the same angle between the cup and head in both sets of testing.

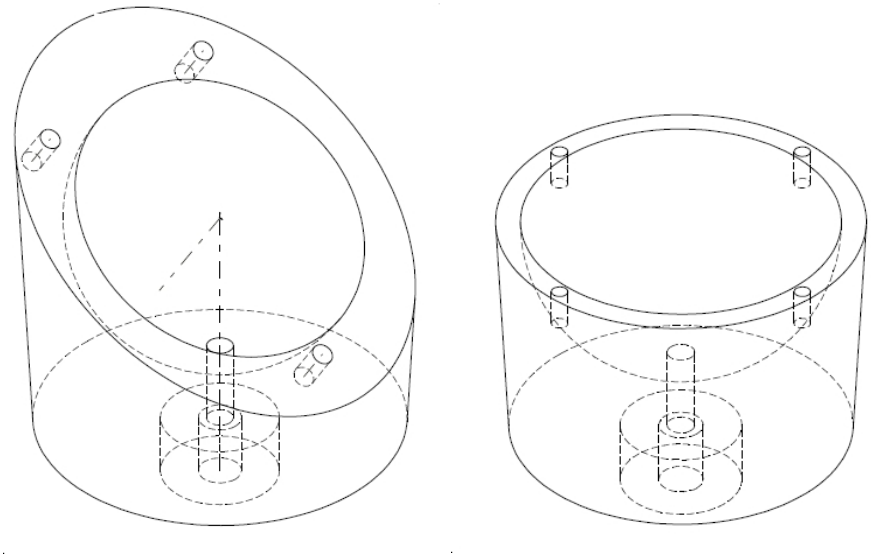

Figure 55 Durham cup holders for phase 1 testing (left) and phase 2 testing (right)

6.3.6 Bradford Friction Test Set Up

The frictional measurements at University of Bradford were carried out using a ProSim Hip Joint Friction Simulator (Simulation Solutions Ltd, Stockport, UK)) (Figure 56). The acetabular cups were positioned in a fixed low-friction carriage below and the femoral head in a moving frame above. The carriage sits on externally pressurized hydrostatic bearings generating negligible friction compared to that generated between the articulating surfaces. During the flexion-extension motion, the friction generated between the surfaces causes the pressurized carriage to move. This movement (or rotation) is restricted by a sensitive Kistler piezoelectric force transducer which is calibrated to measure torque directly. A pneumatic mechanism

controlled by a microprocessor generates a dynamic loading cycle and the load is also measured by the same piezoelectric force transducer.

Figure 56 ProSim Hip Joint Friction Simulator

Friction measurements were made in the ‘stable’ part of the cycle at 2000 N. The loading cycle was set at maximum and minimum loads of 2000 N and 100 N, respectively based on the work of English [230]. In the flexion/extension plane, an oscillatory harmonic motion of amplitude ±24° was applied to the femoral head with a frequency of 1Hz. The load was, therefore, applied to the femoral ceramic head with the artificial hip joint in an inverted position, i.e. femoral head on top of the acetabular component, but with a 12° angle of loading between the two bearings (12° medially to the vertical) as observed *in vitro*. Each cup was tested 3 times.

The testing was conducted using pure bovine serum, distilled water + 25% bovine serum, distilled water + 25% bovine serum + CMC in various amounts to give different viscosities (0.00157 Pas for pure BS, 0.00612 to 0.236 Pas for BS +CMC). The viscosities were measured at a shear rate of 3000 s^{-1} using the Anton Paar Physica MCR 301 Viscometer. Lubricants of lower viscosities were used in the testing conducted at University of Bradford to simulate the synovial fluid of a diseased joint. It is reported that viscosity of healthy human synovial fluid is around 0.01 Pas [232], however the synovial fluid of an arthritic joint is around a factor of 3 less viscous than that of a healthy joint [232]. The higher viscosity lubricants were used to give additional points for the Stribeck analysis.

6.4 Results

6.4.1 Phase 1 Testing

Figure 57 shows the Stribeck plot for the three cups tested in CMC fluid. The smaller clearance (257 µm) showed higher friction factors (0.062±0.005 to 0.071±0.007) than the larger two clearances (0.043±0.004 to 0.044±0.017 for the 661 µm clearance cup and 0.045 to 0.057 for the cup with 706 µm clearance). There is neither a rising or falling trend which suggests that the bearings were operating under boundary-mixed lubrication. A Pearson's correlation confirmed that there was neither a positive nor negative correlation between FF and Sommerfeld number for any of the cups (it should be noted that the small sample size means the correlation is for indication only).

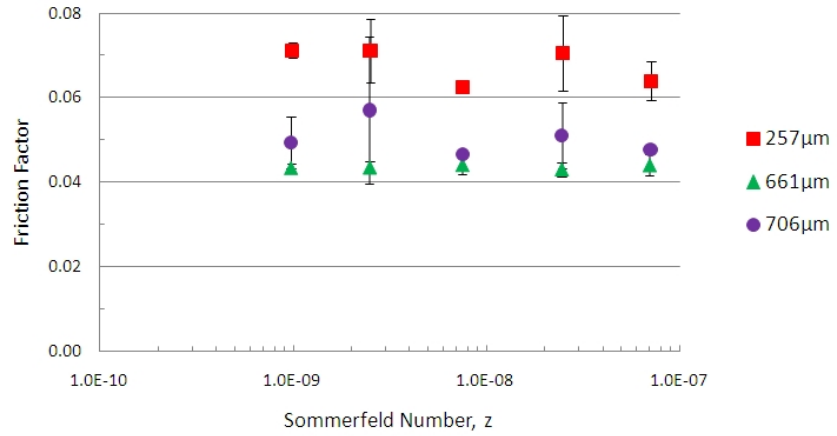

Figure 57 Stribeck plot for ZTA-on-CFR-PEEK in CMC fluid (phase 1 testing)

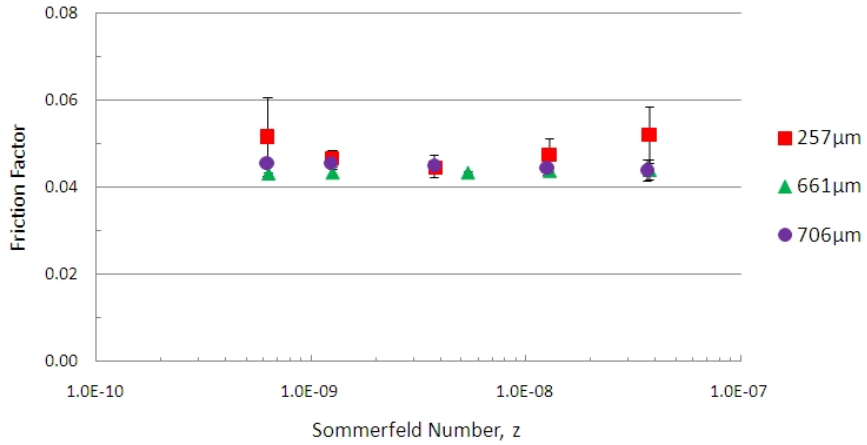

Figure 58 Stribeck plot for ZTA-on-CFR-PEEK in CMC fluid +25% bovine serum (phase 1 testing)

When lubricated with CMC + 25% bovine serum the smaller clearance had a slightly higher friction factor (0.045±0.001 to 0.052±0.009) than the larger clearances

(0.043±0.001 to 0.044±0.002 for 661 µm and 0.044±0.002 to 0.046±0.001 for 706 µm). The Stribeck plot (Figure 58) shows neither a rising nor falling trend which suggests that the bearings were operating under boundary lubrication. This lack of trend was confirmed using Pearson's correlation.

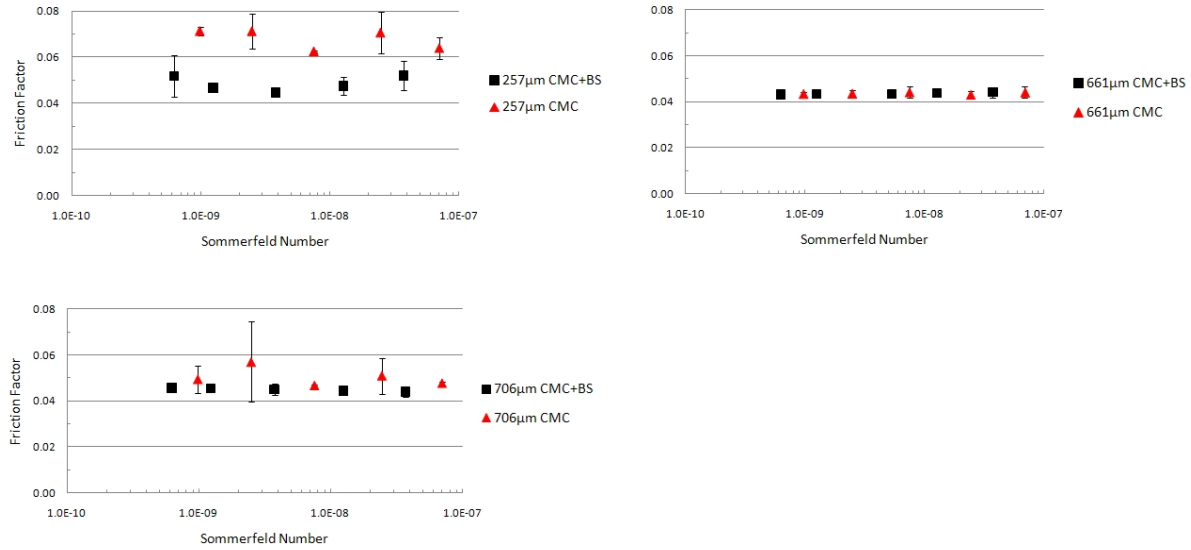

Figure 59 Stribeck plot for ZTA-on-CFR-PEEK in CMC fluid and CMC+25% bovine serum (top left 257 µm clearance, top right 661 µm clearance, bottom left 706 µm)

The addition of bovine serum to the lubricant significantly ($p=0.0009$ and $p=0.03$ respectively) reduced the FF of the 257 and 706 µm clearance cups (Figure 59). There was no significant difference between the FF for the 661 µm clearance with and without bovine serum.

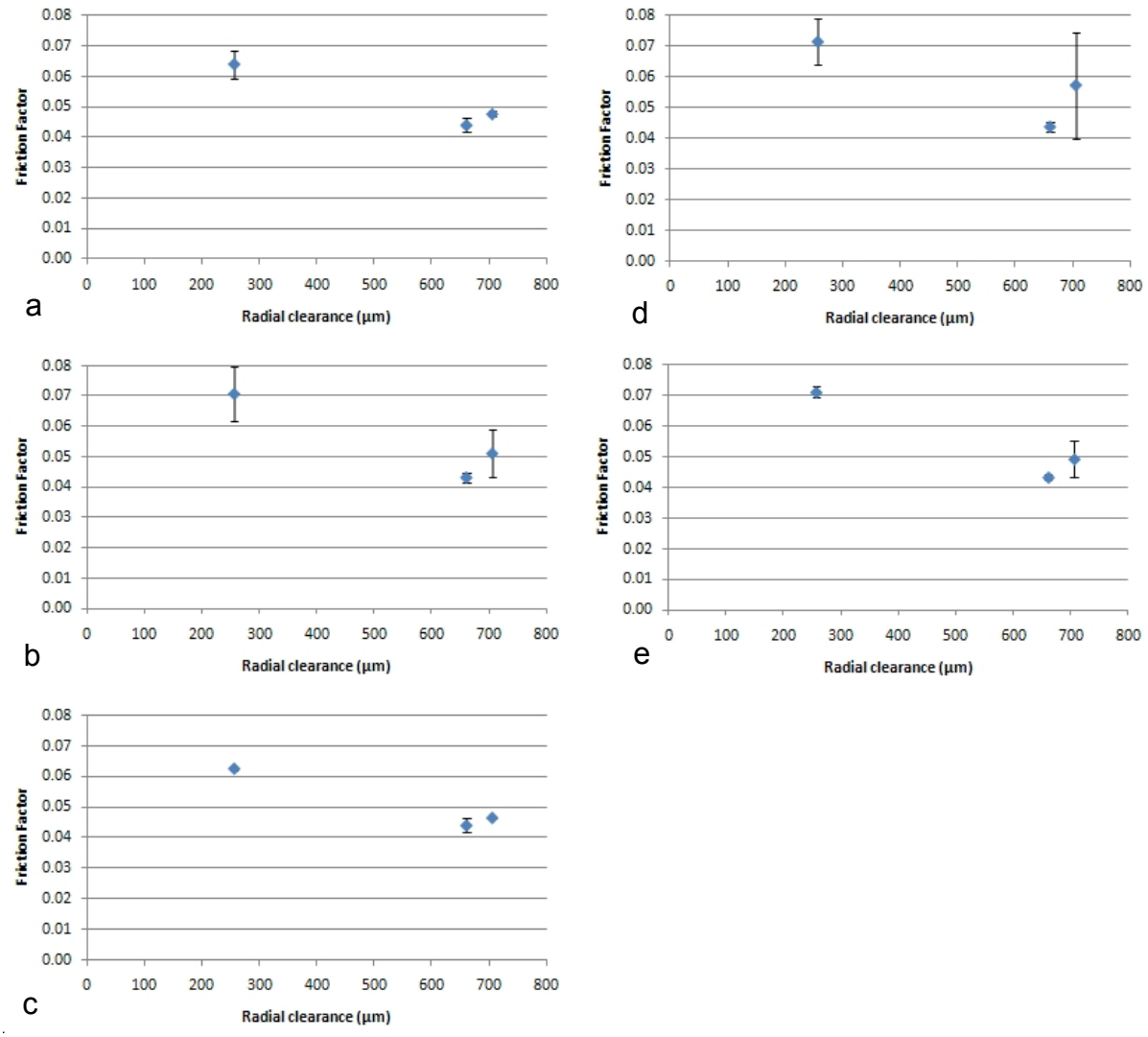

Figure 60 Friction factor versus radial clearance for different CMC lubricant viscosities a)1 Pas, b) 0.3 Pas, c) 0.1 Pas, d) 0.03 Pas, e) 0.01 Pas

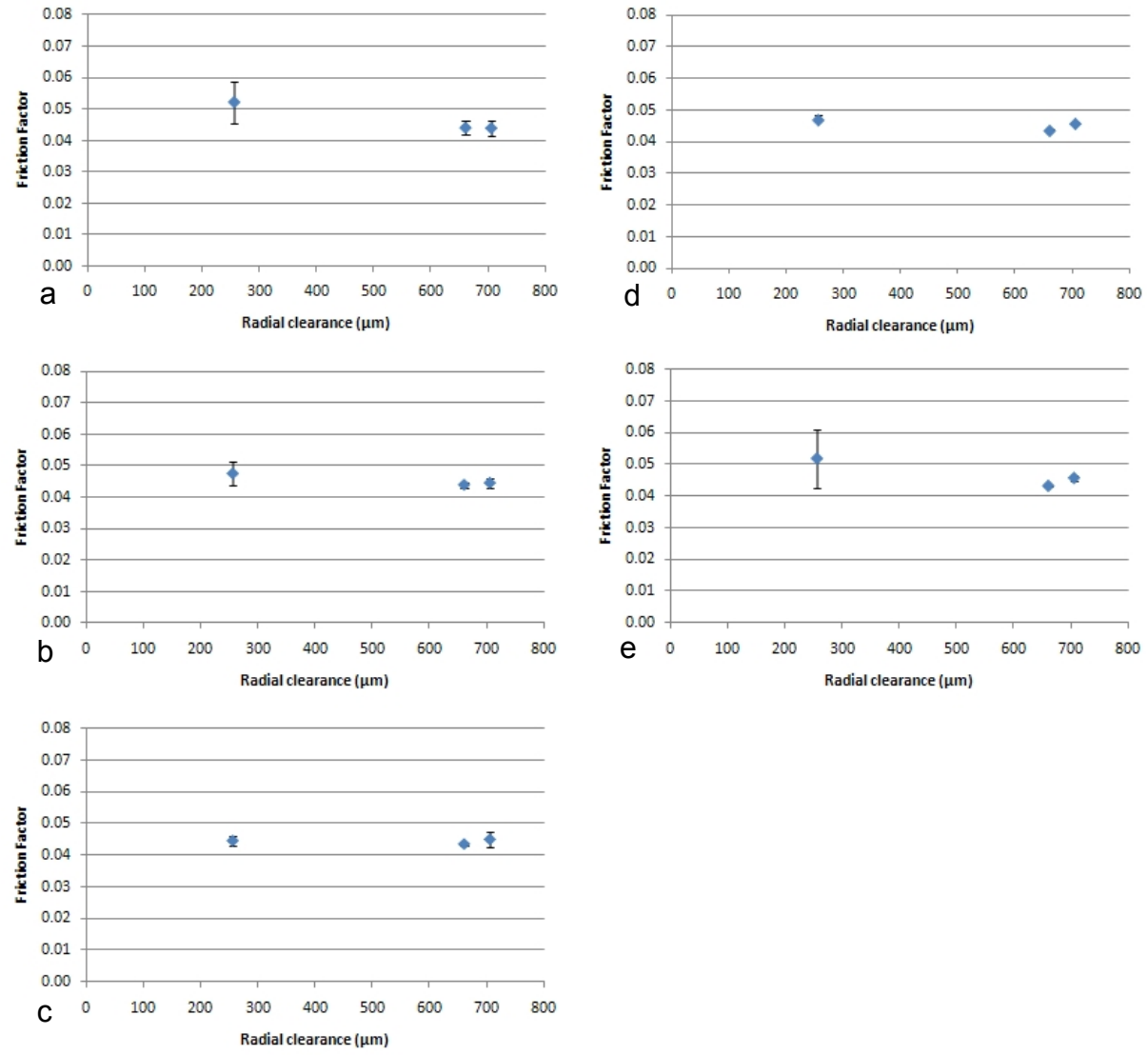

Figure 61 Friction factor versus radial clearance for different CMC+BS lubricant viscosities a)1 Pas, b) 0.3 Pas, c) 0.1 Pas, d) 0.03 Pas, e) 0.01 Pas

Figure 60 and Figure 61 show the effect of radial clearance on FF for CMC and CMC+BS lubricants. One way ANOVA (assuming normal data) was used to assess the significance of the differences in FF for the different clearances. In CMC, increasing the clearance reduced the friction factor; the cup with the 257 µm clearance had significantly (at the 0.05 level) higher FF than the 661 and 706 µm clearance cups at all lubricant viscosities except 0.03 Pas. With CMC as the lubricant there was no significant difference between the FF of the 661 and 706 µm at any lubricant viscosity ($p<0.05$). With CMC+BS as the lubricant increasing the clearance reduced the friction factor slightly but this was not significant ($p< 0.05$).

6.4.2 Phase 2 Testing

In the second phase of testing conducted at Durham, the 330 µm clearance showed a rising trend in FF with increasing Sommerfeld number (Figure 62) which was shown to be significant (p=0.015) using Pearson's correlation; this, in combination with the low friction factors (0.003 to 0.014) could indicate full fluid lubrication. The 930 µm clearance cup had the highest friction factors (0.05 to 0.07) and a falling trend (significant at p=0.000) indicating mixed lubrication. The 30 µm and 630 µm clearances cups also showed a slight falling trend however the trend was only a significant correlation for 30 µm clearance (p=0.018 & p=0.833 respectively).

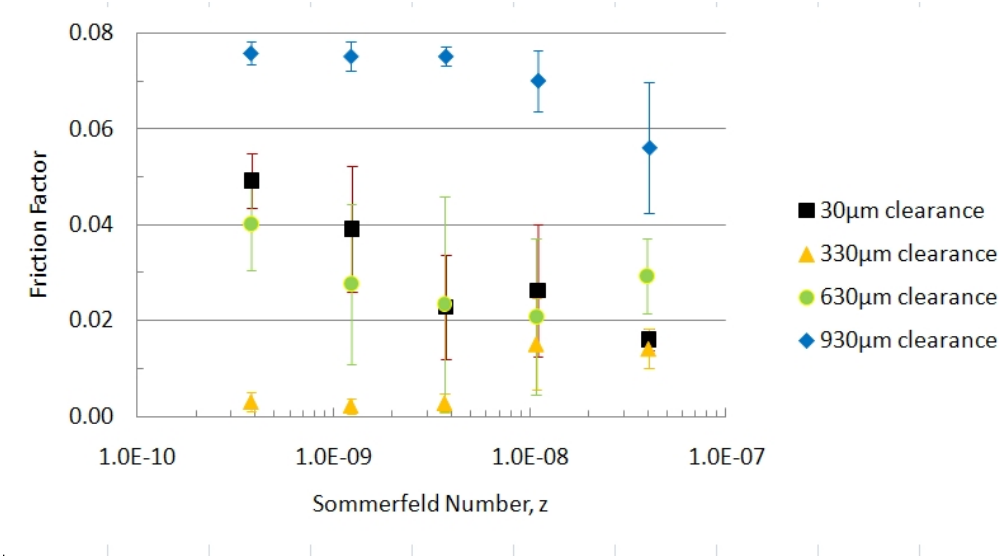

Figure 62 Stribeck plot for ZTA-on-CFR-PEEK in CMC fluid tested at Durham University

The Stribeck plot for testing in CMC + 25% BS showed a falling trend indicating mixed lubrication (Figure 63) for all clearances tested. The negative correlation between FF and Sommerfeld number was significant (p=0.001, 0.000, 0.027 for the 30, 660 & 930 µm clearance cups respectively) for all cups tested except the 330 µm clearance (p=0.42). The larger clearances tended to give the lowest friction factor.

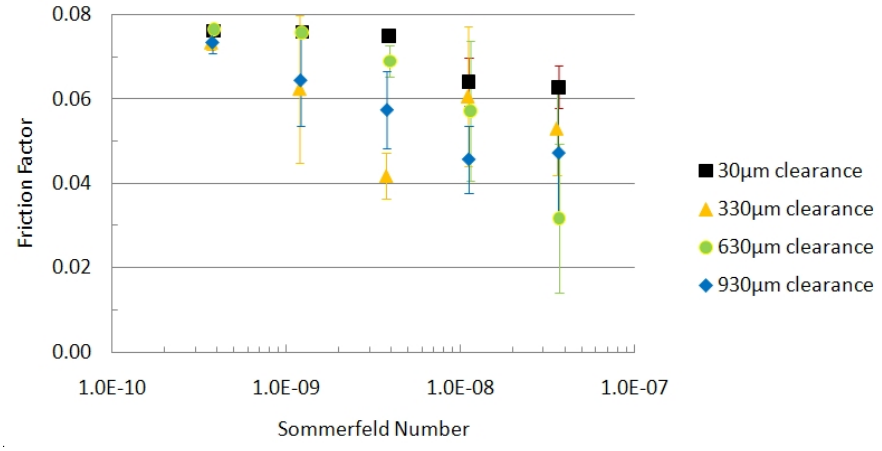

Figure 63 Stribeck plot for ZTA-on-CFR-PEEK in CMC fluid +25% bovine serum tested at Durham University

The effect of the addition of bovine serum to the lubricant for each clearance can be seen in Figure 64. For the three smaller clearances the friction factors increased with the addition of bovine serum to the lubricant. However the friction factor for the 930 µm clearance decreased with the addition of BS at all viscosities (0.056 to 0.075 in CMC and 0.045 to 0.073 in CMC+BS). A paired t-test was used to assess the significance of the differences; in all clearances tested the difference between the FF in CMC and CMC+BS was statistically significant (p=0.0008, 0.0012, 0.014 and 0.02 for 33, 330, 630 and 930 µm clearances respectively). When tested with lubricant containing BS all clearances tested showed a falling trend in friction factor with increasing Sommerfeld number, indicating mixed a lubrication regime.

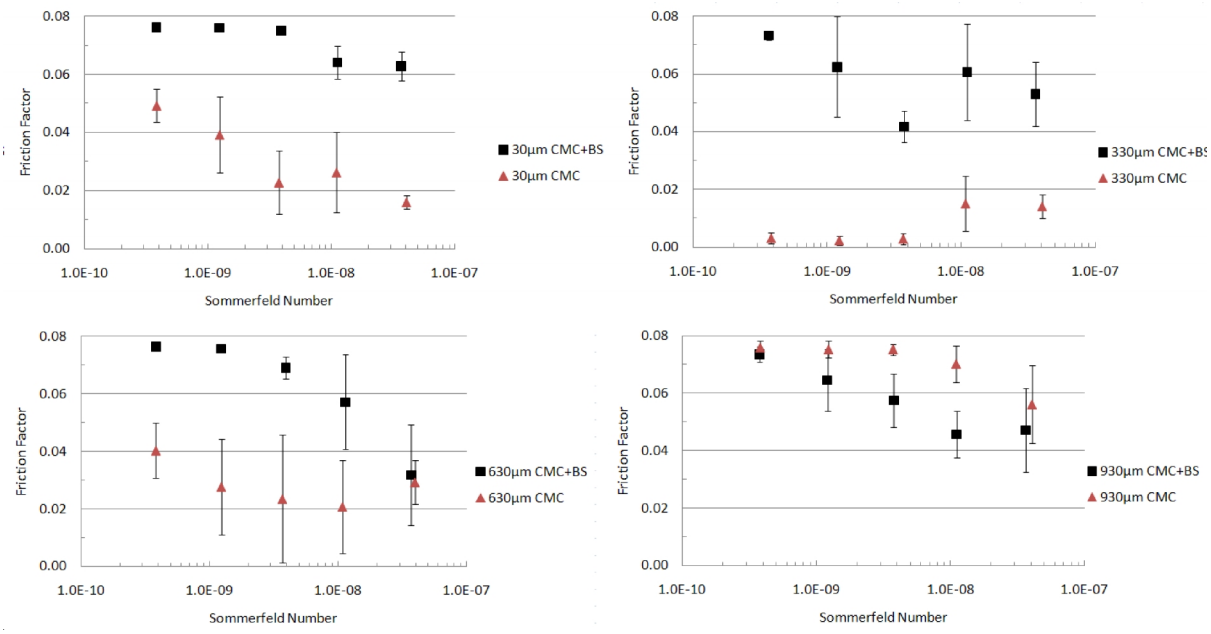

Figure 64 Stribeck plot for ZTA-on-CFR-PEEK in CMC fluid and CMC+25% bovine serum (top left 30 µm clearance, top right 330 µm clearance, bottom left 630 µm, bottom right 930 µm)

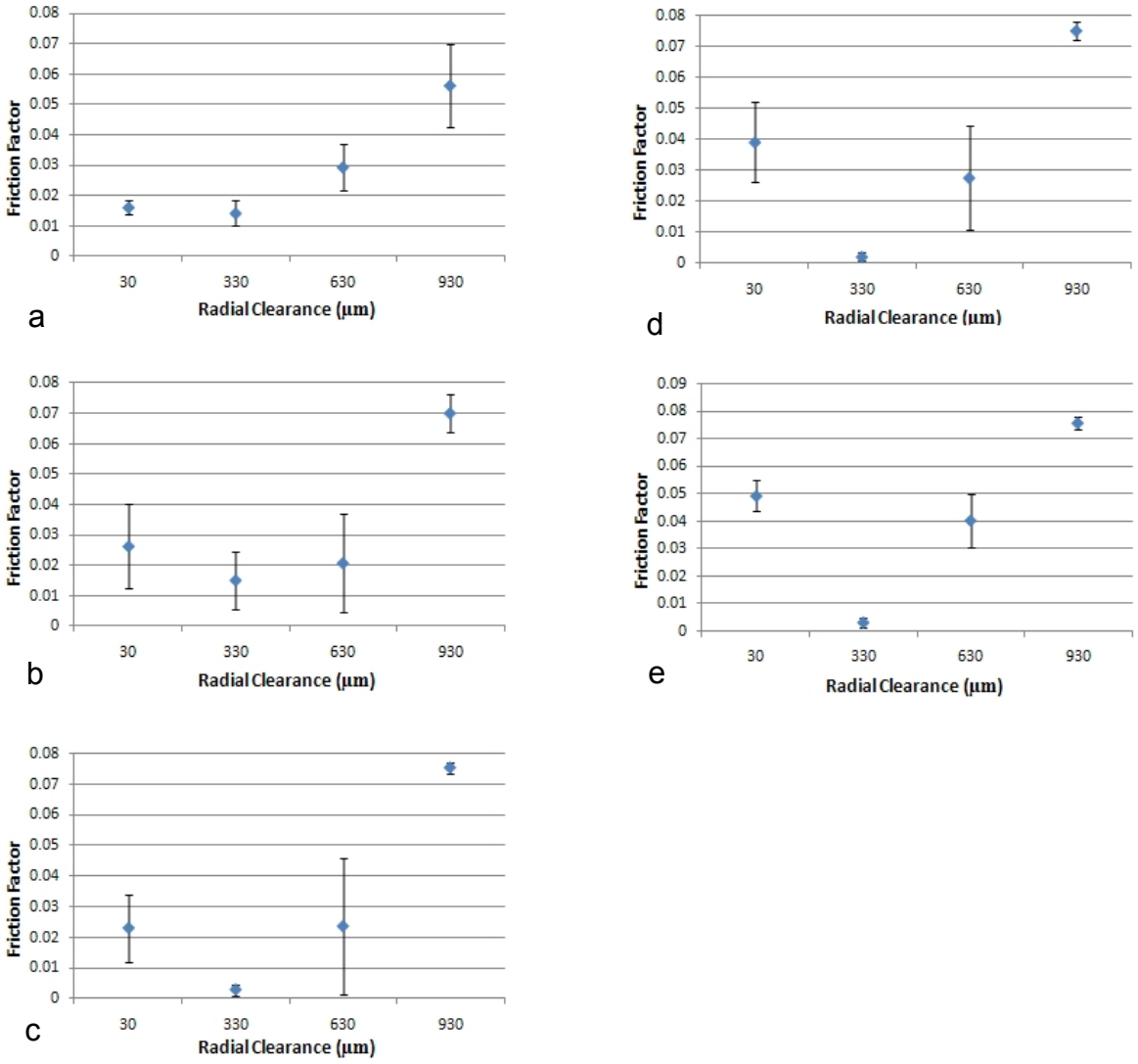

Figure 65 Friction factor versus radial clearance for different CMC lubricant viscosities a)1 Pas, b) 0.3 Pas, c) 0.1 Pas, d) 0.03 Pas, e) 0.01 Pas

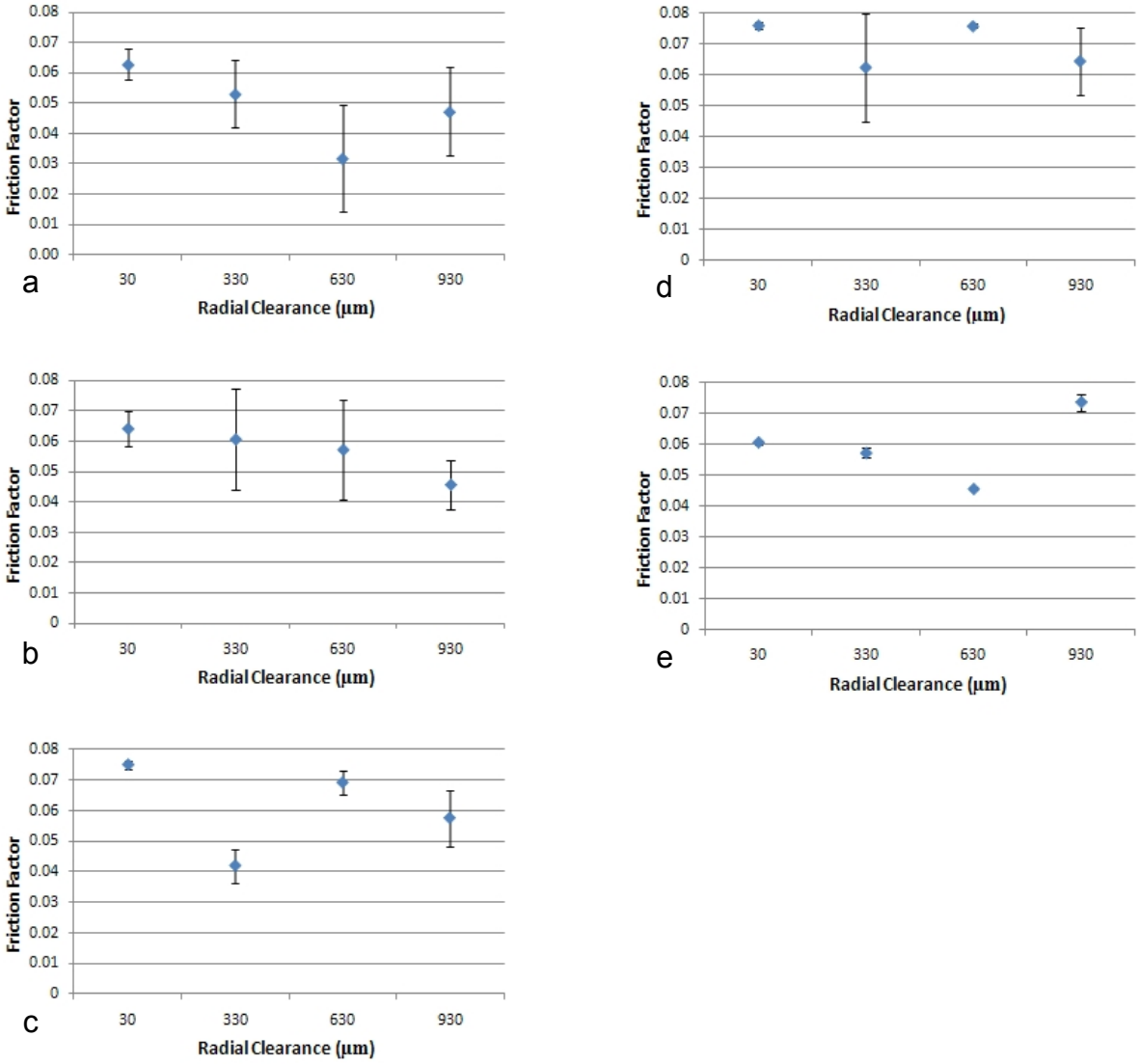

Figure 66 Friction factor versus radial clearance for different CMC+BS lubricant viscosities a)1 Pas, b) 0.3 Pas, c) 0.1 Pas, d) 0.03 Pas, e) 0.01 Pas

With CMC fluid as the lubricant, increasing the clearance of the bearing from 30 µm to 330 µm decreased the FF, further increasing the clearances then resulted in an increase in FF (Figure 65). In CMC fluid the 930 µm clearance cup had significantly ($p < 0.05$) higher FF than all the other clearances at all lubricant viscosities. The 330 µm clearance gave significantly lower FF than all other clearances in 0.01 Pas viscosity lubricant only.

With CMC + BS as the lubricant the effect of clearance was less uniform and was only significant with a lubricant viscosity of 0.1 Pas.

6.4.3 Phase 3 Testing

In the testing at Bradford all clearances tested showed a falling trend in friction factor as Sommerfeld number increased (Figure 67); indicating a mixed lubrication regime with some load supported by fluid film and some by asperity contact. The Pearson's correlation was used to assess the significance of the relationship between FF and Sommerfeld number; for the 330, 630 and 930 µm clearance cups, the negative trend was significant (p=0.002, 0.018, 0.003 respectively), however for the 30 µm clearance the relationship was not significant (p=0.139). In pure bovine serum the largest clearance showed the highest FF (0.25), with the 630, 330 and 30 µm clearances having FF of 0.14, 0.23 and 0.23 respectively. The addition of CMC to the bovine serum to increase the viscosity of the lubricant decreased the FF for all clearances tested. In the BS + CMC fluid the 930µm clearance gave FF of 0.02 to 0.13, 630 µm gave FF of 0.05 to 0.08, 330 µm had FF of 0.05 to 0.14 and 30 µm had FF of 0.08 to 0.14.

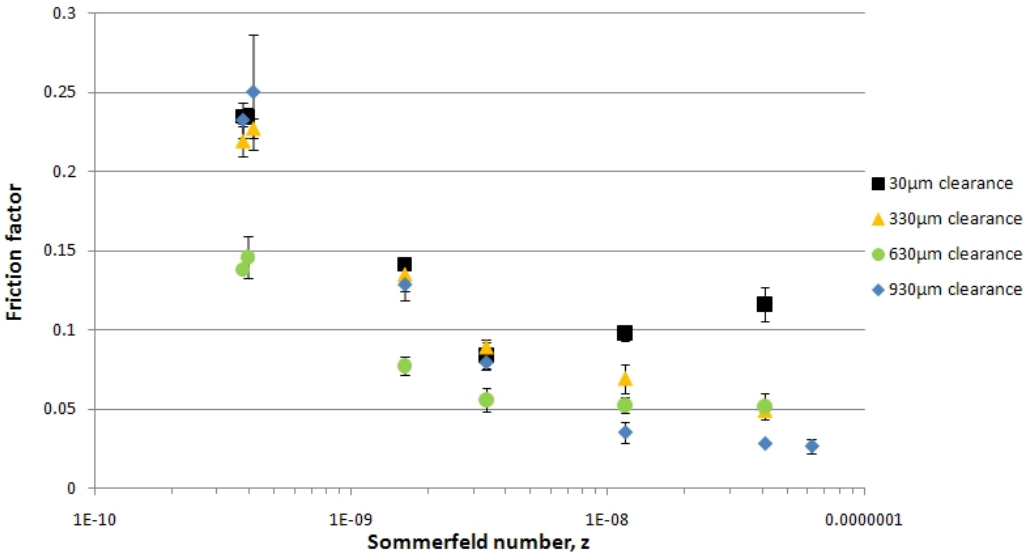

Figure 67 Stribeck plot for ZTA-on-CFR-PEEK tested at University of Bradford

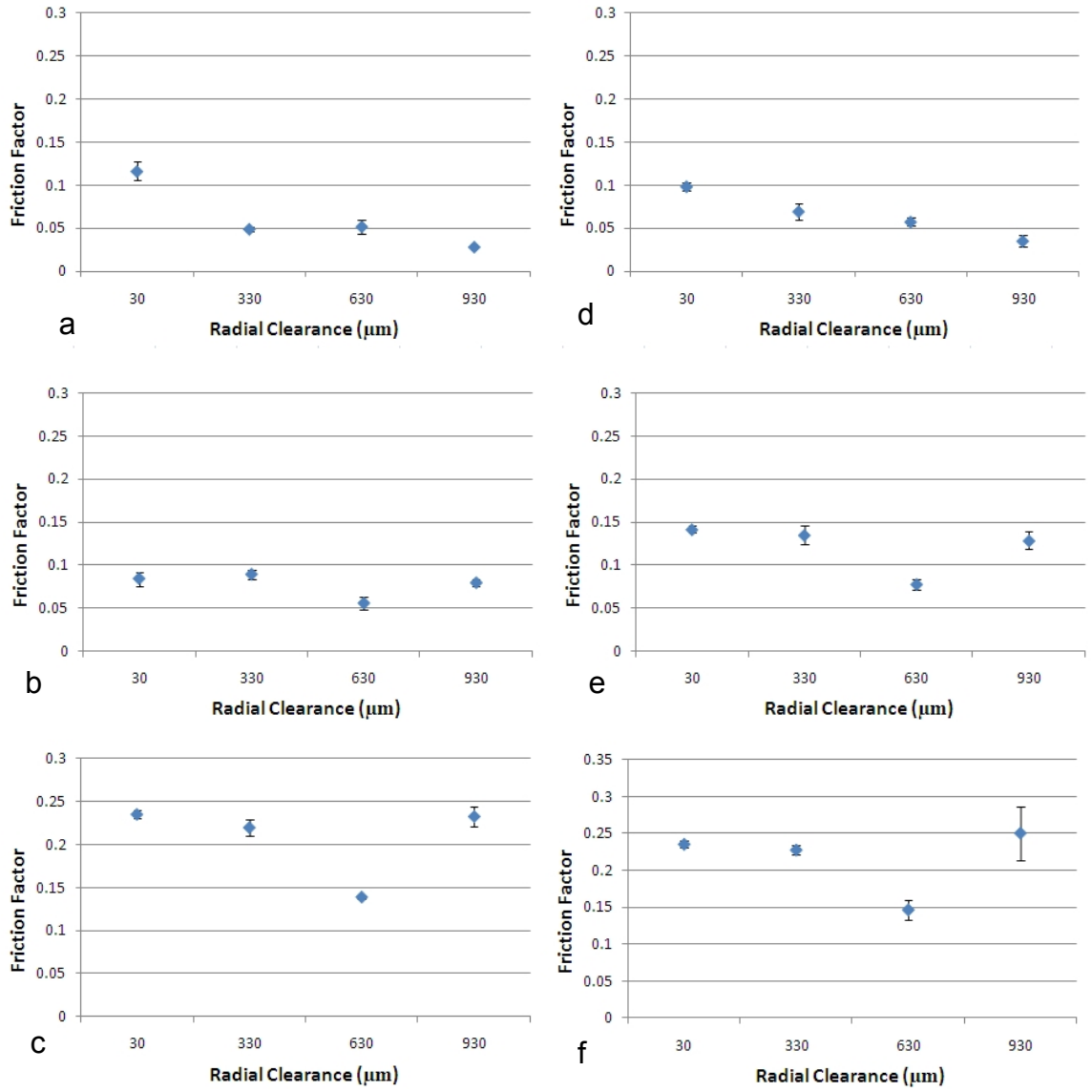

Figure 68 Radial clearance vs. friction factor for various viscosities a) 0.155 Pas (25%BS + CMC), b) 0.0442 Pas (25%BS + CMC), c) 0.0127 Pas (25%BS + CMC), d) 0.00612 Pas (25%BS + CMC), e) 0.00143 Pas (25% BS), f) 0,00157 Pas (pure BS).

Figure 68 shows the relationship between clearance and FF at various lubricant viscosities. It can be seen that in lower viscosity lubricants the 630 µm clearance had the lowest FF and that there is no clear relationship between clearance and FF; however at higher viscosities the 930 µm clearance gives lower FF.

The effect of clearance on FF was not significant in the less viscous lubricants (0.0015, 0.00143, 0.00612 and 0.01274 Pas). When tested in lubricants with viscosities of 0.0442 and 0.0155 the cup with a clearance of 30 µm produced

significantly higher FF than all the other cups; the 930 μm clearance gave significantly lower FF than the other clearances.

6.4.4 Prediction of Lubrication Regime

The lambda ratios were calculated using a viscosity of 0.01 Pas as this is representative of the viscosity of human synovial fluid [232]. If λ is less than one boundary lubrication is likely, when lambda is greater than three then full fluid film lubrication is likely and mixed lubrication is likely when lambda is between 1 and 3 [233]. The predictions for the phase 1 testing (Table 16) suggest the bearings would operate under boundary lubrication.

Table 16 Lambda ratio for phase 1 testing (conducted in Durham)

Clearance (μm)	**257**	**661**	**706**
Minimum film thickness (μm)	0.091	0.045	0.003
ʎ	0.90	0.44	0.03

The predicted minimum film thicknesses and therefore the value of the lambda ratios are slightly higher for the cups when tested in Bradford than in Durham. This is due to the difference in entraining velocity with the different test setups (0.015 m/s at Durham and 0.02 m/s at Bradford); however this difference has not affected the predicted lubrication mode. For all four clearances the lambda ratio radio was less than one; thus boundary lubrication was predicted (Table 16 & Table 17).

Table 17 Lambda ratio for phase 2 testing at Durham

Clearance (μm)	**30**	**330**	**630**	**930**
Minimum film thickness (μm)	0.485	0.075	0.046	0.035
ʎ	0.67	0.10	0.06	0.05

Table 18 Lambda ratio for the phase 3 testing (Bradford)

Clearance (μm)	**30**	**330**	**630**	**930**
Minimum film thickness (μm)	0.585	0.091	0.056	0.042
ʎ	0.81	0.13	0.08	0.06

6.5 Discussion

In phase 1 testing friction factors of 0.071, 0.043, 0.049 were recorded for the 257, 661 and 707 μm clearances with CMC fluid as the lubricant representative of physiologically relevant viscosity (0.01Pa s [231]). The addition of bovine serum to the lubricant reduced the FF of the 257 μm and 707 μm clearances to 0.053 and 0.046 respectively; the FF for the 661 μm clearance remained the same. The reduction in FF with the introduction of BS is not consistent with the results of Flanagan *et al.* who found that the introduction of bovine serum increased the friction factor [223]. Flanagan suggested that local heating resulting in denaturing of the proteins in the bovine serum may play a role. Since in the current study much lower friction factors were recorded the local heating should be reduced which may explain the difference between the two studies.

Due to a manufacturing error in the cups for phase 1 the clearances tested were not those intended (257, 661 and 707 μm rather than 100, 200 and 300 μm); however this showed that a larger clearance than expected may be suitable. Therefore a second set of testing was conducted to further investigate the effect of clearance on FF with radial clearances of 30, 330, 630 and 930 μm. In testing conducted at the University of Durham at physiologically relevant viscosities (0.01Pa s [231]) of CMC lubricant the cups tested showed FF of 0.049, 0.003, 0.040 and 0.078 for the 30, 330, 630 and 930 μm clearances respectively. In this case the largest clearance gave the highest friction factor. However CMC does not contain proteins and is not representative of the *in vivo* situation. For CMC + 25% BS at physiologically relevant viscosities the friction factors for the 30, 330, 630 and 930 μm were 0.073, 0.073, 0.076 and 0.073 respectively. In this case the clearance did not significantly ($p<0.05$ level) affect the FF. With increasing viscosity the larger clearances tended to have lower FF when tested in CMC + 25% BS; however this was only significant with a lubricant viscosity of 0.1 Pas which is a higher viscosity than would be expected in synovial fluid [231].

In the Durham phase 2 testing the addition of bovine serum increased the friction factors for the smaller clearances tested, which is in line with results published by Flanagan [223] and Scholes [118] on the Mitch cup but different to the phase 1

testing conduced on the Biomet PEEK cup. However with the largest clearance of 930μm the friction factor was reduced with the addition of BS to the lubricant. It should be noted that Flanagan *et al.* did not compare bovine serum and CMC of the same viscosity [223]. Previous studies have found that for ceramic-on-UHWMPE (CoP) bearings at physiological viscosity there is no significant difference between the friction factors with bovine serum and CMC [225, 234]; however metal-on-metal (MoM) joints have demonstrated significant decreases in friction factor with bovine serum [219, 223, 225, 234-236] and ceramic-on-ceramic (CoC) bearings have shown significant increase in friction factor when bovine serum was added to the CMC fluid [225, 234, 236]. The FF of ceramic-on-metal (CoM) joints has been shown to slightly increase with the addition of BS to the lubricant [234, 237].

The proteins in bovine serum can be adsorbed on to the surface of the bearings creating a protein layer [191, 225]. Depending on the lubrication characteristics of the bearing, this layer can either increase or reduce the FF of the bearing [225]. In the current study it seems that the addition of BS to the lubricant can either increase or decrease the FF of a ZTA-on-CFR-PEEK bearing. A possible explanation is that the proteins in the lubricant equilibrate the FF. When the FF for the bearing is below around 0.04 the addition of BS resulted in an increase in the FF (as can be see seen for the 30, 330 and 630 μm cups). In this situation the adsorption of proteins results in protein-protein rubbing as well as ceramic-PEEK contact. The friction of the protein-protein contact is higher and therefore the FF of the bearing is increased. When the FF of the bearing in CMC fluid was above 0.04 the addition of BS reduced the FF (as can be seen in the 225 μm and 930 μm clearance cups and to a lesser extent the 706 μm). In this case the protein-protein contact results in a reduction in FF, the protein rubbing creates the same friction in both cases. In the case of the 661 μm clearance cup the FF in CMC is just over 0.04 for all viscosities and the FF is unaffected by the addition of BS to the lubricant. These results indicate that the dominant factor in the friction factor of the ZTA-PEEK bearing is protein-protein friction; highlight the importance of conducting friction and wear testing with lubricants containing proteins.

Friction testing has been carried out on uni condylar knee replacements (Oxford Partial, Biomet UK Ltd) with Pitch based CFR-PEEK meniscal bearings and CoCr tibial and femoral components [119]. Prior to wear testing FFs of up to 0.25 were reported; in CMC fluids the Stribeck plots showed neither a rising nor falling trend in FF; the addition of BS resulted in a slight decrease in FF. However post wear testing the FF was reduced and the Stribeck plots showed falling trends, and the addition of BS to the lubricant post wear testing resulted in a slight increase in FF [119].

Comparing the results from phase 1 and 2 conducted at Durham for the 661 and 630 μm cups; in CMC fluid the FF was significantly ($p=0.01$) higher in phase 1 than phase 2, however with CMC+BS as the lubricant the FF was lower in the phase 1 but the difference was not significant ($p=0.09$). The difference may be due to the different surface roughness between the two sets of cups tested.

At Bradford the testing was conducted with bovine serum based lubricants only; a range of viscosities were used which covered some lower viscosities than those used in Durham to simulate diseased synovial fluid, which has been shown to be significantly less viscous than that of a healthy joint [232]. In this series of testing the friction factors for the 30, 330, 630 and 930 μm were 0.08, 0.09. 0.06 and 0.08 respectively at physiologically relevant viscosities (0.01 Pas [231]) of CMC+BS. The FF for the 630 μm clearance cup was significantly ($p<0.05$) less than that of the other cups at this viscosity and there was no significant difference between the other cups. At this viscosity there was no significant difference between the results from Bradford and Durham. Only three viscosities were tested in both the Bradford and Durham studies (≈ 0.01, 0.3 and 0.1 Pas); the FFs are slightly higher in the Bradford tests than the Durham tests with the same cups, however the difference is only significant for the 630 μm clearance cup ($p=0.007$).

Relatively high FF were measured at Bradford when pure bovine serum was used as the lubricant (up to 0.25), and 0.23 in BS + 75% deionised water. Comparing these values to published data on the CFR-PEEK Mitch cup, Flanagan *et al.* also conducted testing in pure BS and BS + 75% deionised water (without CMC) and

found FF of 0.29 for the 52 mm cup in BS +75% deionised water (actual values with pure BS were not reported but plotted on a graph and appear to be nearly 0.4) [223].

Scholes *et al.* [118] reported on the friction testing of the CFR-PEEK Mitch cup when tested in bovine-serum-based (30%) CMC fluids (viscosities of 0.001, 0.004, 0.009, and 0.034 Pa s), they found FF of 0.3–0.23 [118]. In the testing conducted in Bradford the ranges of FF found when using bovine based CMC as the lubricants were 0.02 to 0.13, 0.05 to 0.08, 0.05 to 0.14 and 0.08 to 0.14 for 930, 630, 330 and 30 μm clearances respectively. For all clearances tested the FFs of the Biomet CFR-PEEK cup were lower than those of the Mitch cup. The friction factors found in the Durham phase 2 study (0.076 max) were also considerably lower than those published for the PEEK Mitch cup. The clearances of the Mitch cup are comparable to the 330 μm clearance tested in this study (400 to 355 μm radial clearance). The 52 mm Mitch cup had friction factors of around 0.3 when tested in 25% BS [223], the Biomet cup with 330 μm had a max FF of around 0.09 in 25% BS. The differences in FF between the Biomet and Mitch cup may be due to the different designs of the cup tested; the Mitch cup is a horseshoe shaped cup whereas the Biomet cup is substantially hemispherical. Although Flanagan states that the fixture used was designed to prevent pinching of the cup it is possible that the head was pinched by the Mitch cup [223]. It is also possible that due to the design of the Mitch cup the clearance was not uniform. It should be noted that the loading used in the three studies was not identical; in all the testing on the Biomet cup a maximum load of 2000 N was used, Flanagan used 1000 and 500 N [223] and Scholes used 2800 N [118]. However Flanagan found that the friction results were very similar for both loads tested [223]. Other than the applied load the test set-up used by Scholes *et al.* was identical to that used for the Durham testing of the Biomet PEEK cup [118]. The Mitch cup is also significantly rougher than the Biomet cup; The Biomet cups had surface roughness of 0.1μm and 0.5μm for phase 1 and phase 2&3 respectively, Scholes *et al.* measured the surface roughness of the cups testing prior to and during wear testing, they reported R_a values of 2.8-4.3 μm prior to testing which was reduced to 0.27-0.57 μm after 25 million cycles of wear testing [118]. However it was reported that this polishing-in effect had little effect on the lubrication regime of the cup [118].

Comparing the friction factor of the Biomet ZTA ceramic against CFR - PEEK to published work on other bearing couples used in THA; large diameter (54 mm) metal-on-metal systems have been shown to have friction factors of around 0.1 to 0.2 depending on the clearance [219, 223], ceramic-on-ceramic systems (28 mm) have friction factors of 0.001 to 0.007 [225, 226], metal-on-polyethylene (28 mm) have FFs of 0.01 to 0.07 reported [225, 226] and 0.035 for 32 mm MOP bearings [227], ceramic-on-metal bearings have been reported to have FF of 0.027 [237].

The Stribeck plots for the clearance testing in both Durham and Bradford generally showed downward trends when BS was present in the lubricant; this indicates that the bearings are operating in a mixed lubrication regime with the load partly supported by fluid film but with some asperity contact. This is consistent with Scholes *et al.* who found a slight downward trend when the Mitch cup was tested in CMC + BS [118]. However the phase 1 testing showed neither a raising nor falling trend. Flanagan *et al.* found neither a rising or falling trend and due to the high FF concluded that the bearings were operating under a severe mixed lubrication regime with very little fluid film [223].

Flanagan *et al.* suggested decreasing the clearance to reduce the friction factor [223]. In the Durham study when the cups were tested in CMC lubricant reducing the clearance did result in a reduced FF, however when BS was added to the lubricant this was no longer the case. The effect of clearance on FF has been previously investigated for large diameter MOM joints; Brockett *et al.* found that the largest clearance (194μm diametric) gave a lower FF than smaller clearances (53μm and 94 μm) for a 54 mm ASR (DePuy) resurfacing implant tested in 25% BS [219]. Afshinijavid *et al.* also investigated the effect of clearance on large (50 mm) diameter MoM bearing, it was found that in clotted and whole blood larger clearances (306, 243, 200 μm) gave a lower FF than the smaller clearances tested (80 & 135 μm), however in BS+CM the smaller clearances had lower FFs [220]. The friction testing of novel bearings has also looked at the effect of clearance on lubrication regime; Scholes *et al.* performed friction tests on 32 mm metal-on-polyurethane cups with

various radial clearances (0.12 to 0.54), and found that a clearance of between 0.1 to 0.25 mm produced a performance approaching full fluid lubrication [205].

The flat shape of the Stribeck plot for the phase 1 testing seems to indicate boundary lubrication, which is in agreement with the theoretical predictions which gave a lambda ratio of less than one suggesting boundary lubrication. For the phase 2 and 3 testing the Hamrock and Dowson equations suggested that the 30 μm clearance cup would give better lubrication than the other three clearances. This did not agree with the experimental results from either Bradford or Durham. The lambda ratios for the all clearance testing cups were less than 1, suggesting boundary lubrication, however the falling trends in the Stribeck plots indicated mixed lubrication.

The Hamrock and Dowson equations [229] have been previously used to predict the lubrication regimes of hip joint bearings [226, 234, 235]. Brockett *et al.* used the theory to investigate the lubrication regimes of 28 mm MoM, MoP, CoP, CoC and CoM bearings. The lambda ratios found seemed to correlate with the experimental results [234], however a Stribeck analysis was not conducted thus conclusions about the lubrication regime were not made. Scholes *et al.* also used the equations to predict the lubrication regimes of 28 mm MoM, MoP and CoC; they found good agreement between experimental results and theory when synthetic lubricants were used but not with BS [226]. In larger diameter MoM resurfacing joints the theoretical predictions predicted full fluid film lubrication [223, 235], however experimental results have not shown this [223, 235]. The lack of agreement with theoretical predictions shows the importance of physical testing to investigate the lubrication and wear of large diameter hip bearings.

In all three sets of friction tests on the Biomet cup, at physiologically relevant viscosities with CMC + BS as the lubricant, the clearance of the bearing had little effect on the FF recorded. Therefore a large clearance should be chosen to allow for deformation on impaction without clutching of the femoral head.

The testing conducted in this chapter has shown that the lubrication regime of the Biomet ZTA-on-PEEK is relatively insensitive to changes in clearance at

physiologically relevant lubricant viscosities, which is a good indication that deformation of the cup will not adversely affect the lubrication of the bearing. However, the testing was conducted on un-deformed cups and therefore the clearance was uniform, whereas a deformed cup would give a non-uniform clearance. Further testing should therefore be conducted on deformed cups.

Chapter 7: Summary and Discussions

The aim of this project was to investigate the deformation characteristics of the Biomet UK Ltd prototype CFR-PEEK cup as a result of impaction and to examine the influence of this deformation on the lubrication of the bearing.

In order meet this aim the following objectives were completed;

1. **Explore the validity of rim loading as a model to investigate deformation on impaction of acetabular cups.**

Rim loading was used a simple method for investigating the stiffness of PEEK cups and for comparison to commercially available cobalt chromium and UHMWPE cups. The FE model created was able to predict the deformation to within 10%. Using the load found by Squire *et al.* the predicted deformation of the 52 mm PEEK cup was 2.85 mm at 1539 N and 0.76 mm at 414 N.

This project has shown that rim loading is not a valid method for investigating the deformation on impaction of acetabular shells. Under rim loading the small PEEK cup had a deformation of 1.78 mm with a rim load of 300 N; with a 1 mm under ream it would be impossible for this amount of deformation to occur. In order to use rim loading, the load equivalent to that experienced on impaction would have to be calculated for each cup design and size via empirical measurement. Rim loading can be used to assess the impact of design changes on the stiffness of the cup; however absolute values of likely deformation cannot be obtained. In order to determine the effect of deformation on the lubrication of a bearing true values of deformation are required, particularly for bearing couples which are very sensitive to clearance such as metal-on-metal joints.

2. **Investigate the use of polyurethane foam blocks a method to model the acetabulum.**

Using a Sawbones model the PEEK cups deformed by a maximum of 0.75 mm at 1 mm under ream and 1.084 mm at 2 mm under ream in 30 pcf foam; despite this deformation all femoral heads rotated freely within the impacted cups and Engineer's blue indicated dome contact. The FE model created was in agreement with the experimental results although there was a large standard deviation in the experimental results.

3. **Create a three dimensional finite element model of the pelvis which can be used to simulate acetabular component impaction.**

A very accurate representation of a cadaveric pelvis was created using Simpleware to segment high resolution CT data; the use of a CT phantom meant that the relationship between attenuation and density was correct for the specific CT scanner used. The use of high resolution data meant that the thickness of the cortical bone could be accurately segmented and material properties could be assigned using gray scale values. The model consisted of around 300,000 elements; the small mesh size limited how the impaction could be simulated; for example contact algorithms could not be used as the size of interference is greater than the mesh size resulting in elements with zero volume. Therefore displacement control was used to simulate impaction and the model predicted a maximum deformation of 0.53 mm. The modelling of the impaction by using displacement control rather than interference fit function of software is also more representative of the *in vivo* situation, as demonstrated by the fact that a polar gap remained after impaction (which is consistent with clinical findings). This means that an accurate prediction of the deformation likely to occur on impaction into this specific patient was achieved. However the model does not necessarily represent a worst case and may only be valid for the specific pelvis used to create the model.

4. **Measure the deformation of prototype cups on impaction into cadaveric specimens.**

The results of the cadaver experiment showed that the cup would deform by a maximum of 0.66 mm. There was a very high standard deviation in the amount of deformation the cup experienced, which corresponded to a high variability in the size of the reamed acetabulum. Other variables such as bone density, surgical technique and the original anatomy of the acetabulum could contribute to the high standard deviation. Dome contact was indicated in all impacted cups and the femoral heads articulated freely.

5. **Investigate the accuracy of modern reaming techniques.**

The results of the Sawbones reaming study showed that the cavities were always over sized compared to the nominal size of the reamer; by on average 0.4 mm ±0.18 mm, this is comparable to published data, with a smaller standard deviation than the older studies [193, 207] and similar SD to a more recent study [51]. This demonstrates that although the cavities produced were always larger than the nominal size of the reamer there was an acceptable level of variability compared to other reamers currently on the market.

The reaming study conducted during the cadaver experiment showed a high degree of variability in the size of cavity produced (with one cavity undersized by 0.75 mm and others being over sized by 0.5 mm). The variation in cavity size was far greater in the cadaver trials than in the Sawbones study; this is to be expected as there were fewer variables in the Sawbones study than the cadaver trial. However the variability found in the cadaver trial was also far larger than that reported in the literature [193, 207]. In the published data the reaming was performed in idealised conditions; the cadavers were stripped of soft tissue and the pelvises imbedded in resin. In the current study the reaming was performed in intact cadaveric specimens using a standard surgical technique. In addition, each cavity was prepared by a different orthopaedic surgeon with a different set of instruments (all of the same model but different sets, some sets may have been more worn than others), although this

introduces many variables and does not strictly investigate the ability of the reamer to produce a cavity of a specified size it is very representative of the *in vivo* conditions. There is a huge amount of variability in the size of cavity due to the many variables involved: operative technique, bone density, reamer wear. When modelling impaction, either in FE or *in vitro* it is important to consider this variability and ensure that a worse case is considered.

The variability in the size of cavity produced could result in different clinical outcomes; for example in an extreme case an over sized cavity may not provide the press-fit required for initial stability, or an under sized cavity may result in excessive deformation of the acetabular component resulting in problems seating modular components or clutching of the femoral head and excessive wear. The variability may be more critical to the clinical success of thin walled more flexible acetabular cups than stiffer designs, it will also influence the success of hard-on-hard bearings which are more sensitive to bearing clearance than hard-on-soft bearings such as UHMWPE.

The high level of variability in the size of cavity produced in the cadaver trials resulted in a corresponding high variation in the amount of deformation which occurred on impaction. The standard deviation in the deformation in the cadaver trials was far higher than that of the Sawbones tests. In addition to the variability of the level of under-ream, variations in bone density between specimens and operative technique will have affected the amount of deformation which occurred.

6. **Conduct friction testing with Ceramic-on-PEEK bearings with a range of clearances to assess the impact of clearance on the lubrication regime.**

Friction testing of the ceramic-on-PEEK bearings showed that the friction factor and lubrication regime were relatively insensitive to clearance over the range of clearances tested (30μm to 930μm radially). It also showed that the friction factors of the Biomet cup were far lower than the published data on the CRF-PEEK Mitch cup (Stryker), with mixed lubrication indicated from the slight downwards trends of the Stribeck plots.

7. **Make a recommendation based on the findings of objectives 1-6 for the most suitable methodology for impaction deformation testing**

The deformation patterns of both the rim loading and the Sawbones studies were very similar, with compression in one direction and expansion in the perpendicular direction (which is in agreement with published data [130]). However in the cadaver testing and pelvis FE model the shape of the deformed cup was more egg shaped; although the compression and expansion are in perpendicular directions the expansion was not symmetrical about the direction of maximum compression. The reason for the inconsistency between the deformation shape of the cadaver testing and the Sawbones testing is the different shape of the cavities the cup is impacted into. Although Jin *et al.* [51] found that a hemisphere with rectangular cut-outs give good agreement with cadaveric tests, and that that the cup was only supported by the iliac crest and iscially column [51], the FE model of the pelvis showed that the cup was only unsupported in the acetabular notch.

The rim loading study showed that increasing the cup size resulted in a significant decrease in cup stiffness (which is in agreement with the finding of Squire *et al.* [46]). However the Sawbones study and associated FE model showed that the deformation which occurred on impaction increased slightly with cup size but the pattern was much less pronounced with the larger sizes. The reason for this is that the amount of deformation the cup undergoes is limited by the under-ream, for example with an under ream of 1 mm the impacted cup cannot deform by more than 1 mm diametrically. Applying a specified load to the rim of the cup as in Chapter 3 will not give an accurate prediction of deformation on impaction for the *in vivo* situation and is likely to overestimate the level of deformation, particularly for larger cup sizes. The load that Squire *et al.* calculated is specific to the particular cup (size and material) that they tested [46].

The testing conducted using the Sawbones model generally showed larger deformations than those found in the cadaver study; there is good agreement between the pelvis model and Sawbones FE model of 30 pcf foam, however the mean Young's modulus found from the CT attenuation relationship was around 900

MPa; when this value was used for $E_{sawbone}$ the predicted deformation was 0.6 mm for 1 mm under ream (model 8 in pelvis mode) and 0.36 mm for 0.5 mm under ream (model 7 in pelvis model), which is higher than that in the pelvis model (0.41 mm for model 8 and 0.30 for model 7). The reason for this difference is likely to be that in the cadaver and pelvis model the cup is more supported than the Sawbones model.

The results of this project suggest that the use of the Sawbones model (hemispherical cavity with two rectangular cut-outs) is a more severe test than the cadaver testing. Although the Sawbones model may not represent the “average” person it is a simulation of a worst case scenario; in orthopaedics it is very important to consider the worst case rather than average. To investigate deformation on impaction a Sawbones model represents a worst case, and therefore in terms of product testing may be of more value than cadaveric testing where the bone density and shape of acetabulum (i.e. how supported the cup is) cannot be controlled. The variability in the size of cavity produced in the cadaver trial also highlights the importance of testing with a worst case.

The value of conducting cadaver trials to investigate cup deformation may be limited; a positive result (i.e. head articulation and dome contact) in a cadaver experiment will indicate the suitability of the cup for that particular pelvis but is unlikely to be representative of the population. A very large sample size would be needed to find the maximum deformation that could occur clinically due to the large number of variables, as demonstrated by the large standard deviation in the current results and also published literature. For a metal-on-metal or other hard-on-hard systems which are very sensitive to the clearance an accurate understanding of the maximum deformation would advantageous. Therefore the Sawbones model as a worst case is the more valuable test method.

To the author’s knowledge there has not previously been a study of the deformation on impaction of a press-fit CFR-PEEK cup. Latif *et al.* considered the effect that variability of reamed cavity size might have on the clearance between the femoral head and acetabular cup for the Mitch cup, however they did not investigate the

deformation which could occur on impaction and the Mitch cup is inserted line-to-line and relies on fins for stability [27].

7.1 Limitations

Throughout this project the viscoelastic and time dependent behaviour of bone has not been considered; clinically this would result in stress relaxation of the bone surrounding the implant and potentially a decrease in the compression of the implant (this has been described in the literature [47]). In addition the assumption of linear elastic properties for bone and Sawbones is a limitation of this project, plastic deformation of the Sawbones blocks occurred in the *in vitro* testing as demonstrated by the complete seating of the cup, which it was not possible to simulate in the FE model.

The high material cost of CFR-PEEK and the cost of porous coating meant that only a relatively small sample size of each cup size was tested in the Sawbones testing, and the number of cadavers available in the cadaver experiments prohibited a large sample size in that test. Larger sample sizes would be preferable to increase the accuracy of the results and to increase the statistical confidence in the results.

Chapter 8: Conclusions

The deformation experienced by a press-fit acetabular cup on impaction into the prepared acetabulum is an important consideration in the design of a new implant, particularly for more flexible materials such as CFR-PEEK. Excessive deformation could adversely affect the tribological behaviour of the bearing; it could also lead to equatorial and edge contact, and implant stability and long term fixation could be affected.

The main findings of this study are:

1. Rim loading is not a valid method to obtain the absolute values of deformation which would be required to assess the effect of the deformation on the lubrication of the bearing.
2. The highly variable size of cavity produced in cadaveric specimens and additional variables (bone density, surgical technique) make cadaveric testing unsuitable for design verification of cup deformation where a controlled worst case is required.
3. It is possible to create a very accurate representation of a pelvis from CT data and to model impaction using displacement control; however the resulting model is only valid for that specific pelvis and again does not represent a worst case.
4. The most useful method for assessing the amount of deformation which occurs due to the impaction of a press-fit acetabular cup is a Sawbones model with a hemispherical cavity and rectangular cut-outs as this represents a worst case situation.
5. The large deformation (up to 1.084 mm diametrically) experienced by the Biomet CFR-PEEK cup was not associated with jamming of the modular femoral head.
6. Friction testing demonstrated that the Biomet ZTA-PEEK bearing is insensitive to changes in clearance at physiologically relevant viscosities. Therefore, provided the initial clearance is sufficient, the deformation caused by press-fitting should not have an adverse effect on the friction and lubrication of the system.

Chapter 9: Further Work

Prior to release onto the market the CFR-PEEK cup requires further design validation; although friction testing showed that the cup had lower FF than the Mitch cup, wear testing should be conducted on sterilised samples of the final design. Optimisation of the clearance versus wall thickness should also be considered to reduce the amount of deformation which occurs on impaction. Friction testing could also be conducted to investigate the effect of surface roughness on the lubrication regime. The effect of cup inclination on the friction and wear of the ZTA-PEEK cup could also be investigated. Sawbones testing with the final cup design should be conducted on a larger sample size with 30 pcf foam and a 2 mm under ream, and the largest cup size should be tested. Further work will also investigate the possibility of introducing screw holes into the design for additional fixation.

An important finding of this project was the large variation in the size of cavity produced using grater reamers. With the introduction of thinner acetabular shells and novel bearings (such as large diameter ceramic cups) investigation into potential methods for improving the accuracy of reaming techniques, and improvements to the design of surgical instruments, would be very valuable.

The current study investigated the level of deformation on impaction of a CFR-PEEK cup and the likely impact of this deformation on lubrication of the bearing. Although deformation on impaction is a major consideration for an acetabular component of a total hip arthroplasty it is likely that deformation also occurs due to the forces experienced during gait and other daily activities. Further work should focus on this. Although it was found that Sawbones model are very valuable for assessing deformation on impaction a more sophisticated model would be required to investigate the deformation due to body weight and gait. The FE model of the pelvis created in this study should be further developed to simulate gait. The method of simulating impaction used in the current study (repeated displacements) should be employed in the initial steps of the FE model, subsequent steps of the analysis should apply boundary conditions based on muscle forces and body weight. Loading conditions from different activities of daily living should be considered.

Due to the subject specific nature of the FE model created using CT data, to properly validate a model, *in vitro* testing, including the relevant soft tissues and musculature, should be conducted on the same pelvis used to create the FE model.

Chapter 10: References

1. Purdue, P.E., Koulouvaris, P., Potter, H.G., Nestor, B.J., and Sculco, T.P., The cellular and molecular biology of periprosthetic osteolysis. Clinical Orthopaedics & Related Research 2007. 454: p. 251-261.
2. Agarwal, S., Osteolysis: Basic science, incidence and diagnosis. Current Orthopaedics, 2004. 18(3): p. 220-231.
3. Ingham, E. and Fisher, J., Biological reactions to wear debris in Total Joint Replacement. Proceedings of the Institution of Mechanical Engineers, Part H: Journal of Engineering in Medicine, 2000. 214: p. 21-37.
4. NJR, National Joint Registry for England and Wales 4th Annual Report. 2008, The Department of Health.
5. Clarke, I., Good, V., Williams, P., Schroeder, D., Anissian, L., Stark, A., Oonishi, H., Schuldies, J., and Gustafson, G., Ultra-low wear rates for rigid-on-rigid bearings in total hip replacements. Proceedings of the Institution of Mechanical Engineers, Part H: Journal of Engineering in Medicine, 2000. 214(4): p. 331-347.
6. Savarino, L., Greco, M., Cenni, E., Cavasinni, L., Rotini, R., Baldini, N., and Giunti, A., Differences in ion release after ceramic-on-ceramic and metal-on-metal total hip replacement: medium-term follow-up. Journal of Bone and Joint Surgery British Volume, 2006. 88-B(4): p. 472-476.
7. Scholes, S., Green, S., and Unsworth, A., The wear of metal-on-metal total hip prostheses measured in a hip simulator. Proceedings of the Institution of Mechanical Engineers, Part H: Journal of Engineering in Medicine, 2001. 215(6): p. 523-530.
8. Firkins, P.J., Tipper, J.L., Ingham, E., Stone, M.H., Farrar, R., and Fisher, J., A novel low wearing differential hardness, ceramic-on-metal hip joint prosthesis. Journal of Biomechancis, 2001. 34(10): p. 1291-8.
9. Ishida, T., Clarke, I., Donaldson, T., Shirasu, H., and Yamamoto, K., Ceramic-on-metal simulator wear and ion comparisons: 32 mm vs. 38 mm diameter. Orthopeadic Research Society 53rd Annual Meeting, 2007.
10. Williams, S., Ingham, E., Isaac, G., Hardaker, C., Schepers, A., Jagt, D.v.d., Breckon, A., and Fisher, J., Ceramic-on-metal hip replacements: Part 1 - In vitro testing. MechE Engineers and Surgeons: Joined at the Hip Conference, 2007: p. 19-21 April 2007.
11. Hallab, N., Merritt, K., and Jacobs, J.J., Metal sensitivity in patients with orthopaedic implants. Journal of Bone and Joint Surgery American Volume, 2001. 83(3): p. 428-.
12. Carrothers, A.D., Gilbert, R.E., Jaiswal, A., and Richardson, J.B., Birmingham hip resurfacing: the prevalence of failure. Journal of Bone and Joint Surgery British Volume, 2010. 92(10): p. 1344.
13. Tharani, R., Dorey, F.J., and Schmalzried, T.P., The risk of cancer following total hip or knee arthroplasty. Journal of Bone and Joint Surgery American Volume, 2001. 83(5): p. 774-780.
14. Kwon, Y.M., Ostlere, S.J., McLardy-Smith, P., Athanasou, N.A., Gill, H.S., and Murray, D.W., “Asymptomatic” pseudotumors after metal-on-metal hip resurfacing arthroplasty prevalence and metal ion study. The Journal of Arthroplasty, 2010. 26(4): p. 511-518.

15. Khatod, M., Barber, T., Paxton, E., Namba, R., and Fithian, D., An analysis of the risk of hip dislocation with a contemporary total joint registry. Clinical Orthopaedics & Related Research, 2006. 447: p. 19-23.
16. von Knoch, M., Berry, D.J., Harmsen, W.S., and Morrey, B.F., Late dislocation after total hip arthroplasty. Journal of Bone and Joint Surgery American Volume, 2002. 84(11): p. 1949-1953.
17. Amstutz, H.C., Le Duff, M.J., and Beaule, P.E., Prevention and treatment of dislocation after total hip replacement using large diameter balls. Clinical Orthopaedics & Related Research, 2004(429): p. 108-16.
18. Burroughs, B.R., Brian, H., Gregory, J.G., Daniel, H., and William, H.H., Range of motion and stability in total hip arthroplasty with 28-, 32-, 38-, and 44-mm femoral head sizes: An in vitro study. Journal of Arthroplasty, 2005. 20(1): p. 11-19.
19. Crowninshield, R.D., Maloney, W.J., Wentz, D.H., Humphrey, S.M., and Blanchard, C.R., Biomechanics of large femoral heads: what they do and don't do. Clinical Orthopaedics & Related Research, 2004. 429: p. 102-107.
20. Hirakawa, K., Bauer, T.W., Hashimoto, Y., Stulberg, B.N., Wilde, A.H., and Secic, M., Effect of femoral head diameter on tissue concentration of wear debris. Journal of Biomedical Materials Research, 1997. 36(4): p. 529-535.
21. Jasty, M., Goetz, D.D., Bragdon, C.R., Lee, K.R., Hanson, A.E., Elder, J.R., and Harris, W.H., Wear of polyethylene acetabular components in total hip arthroplasty. An analysis of one hundred and twenty-eight components retrieved at autopsy or revision operations. Journal of bone & Joint Surgery American Volume, 1997. 79(3): p. 349-58.
22. Kabo, J.M., Gebhard, J.S., Loren, G., and Amstutz, H.C., In vivo wear of polyethylene acetabular components. Journal of Bone and Joint Surgery British Volume, 1993. 75-B(2): p. 254-258.
23. Howling, G.I., Sakoda, H., Antonarulrajah, A., Marrs, H., Stewart, T.D., Appleyard, S., Rand, B., Fisher, J., and Ingham, E., Biological response to wear debris generated in carbon based composites as potential bearing surfaces for artificial hip joints. Journal of Biomedical Materials Research, 2003. 67(2): p. 758-64.
24. Hunter, A., Archer, C.W., Walker, P.S., and Blunn, G.W., Attachment and proliferation of osteoblasts and fibroblasts on biomaterials for orthopaedic use. Biomaterials, 1995. 16(4): p. 287-295.
25. Katzer, A., Marquardt, H., Westendorf, J., Wening, J.V., and von Foerster, G., Polyetheretherketone--cytotoxicity and mutagenicity in vitro. Biomaterials, 2002. 23(8): p. 1749-59.
26. Kurtz, S.M. and Devine, J.N., PEEK biomaterials in trauma, orthopedic, and spinal implants. Biomaterials, 2007. 28(32): p. 4845-69.
27. Latif, A.M.H., Mehats, A., Elcocks, M., Rushton, N., Field, R.E., and Jones, E., Pre-clinical studies to validate the MITCH PCR Cup: a flexible and anatomically shaped acetabular component with novel bearing characteristics. Journal of Materials Science: Materials in Medicine, 2008. 19(4): p. 1729-1736.
28. Morrison, C., Macnair, R., MacDonald, C., Wykman, A., Goldie, I., and Grant, M.H., In vitro biocompatibility testing of polymers for orthopaedic implants using cultured fibroblasts and osteoblasts. Biomaterials, 1995. 16(13): p. 987-992.

29. Utzschneider, S., Becker, F., Grupp, T., and Sievers, B., Inflamatory response against different carbon fibre-reinforeced PEEK wear particles compared with UHMWPE in vivo. Acta Biomaterialia, 2010. 6: p. 4296-4304.
30. Brantigan, J.W., Neidre, A., and Toohey, J.S., The lumbar I/F cage for posterior lumbar interbody fusion with the variable screw placement system: 10-year results of a Food and Drug Administration clinical trial. The Spine Journal, 2004. 4(6): p. 681-688.
31. Brantigan, J.W. and Steffee, A.D., A carbon fiber implant to aid interbody lumbar fusion. Two-year clinical results in the first 26 patients. Spine, 1993. 18(14): p. 2106-7.
32. Akhavan, S., Matthiesen, M.M., Schulte, L., Penoyar, T., Kraay, M.J., Rimnac, C.M., and Goldberg, V.M., Clinical and histologic results related to a low-modulus composite total hip replacement stem. Journal of Bone & Joint Surgery American Volume, 2006. 88(6): p. 1308-1314.
33. Kärrholm, J., Anderber, C., Snorrason, F., Thanner, J., Langeland, N., Malchau, H., and Herberts, P., Evaluation of a femoral stem with reduced stiffness : A randomized study with use of radiostereometry and bone densitometry. Journal of bone & Joint Surgery American Volume, 2002. 84(9): p. 1651-1658.
34. Orthodynamics. Bradley Solution http://www.orthodynamics.co.uk/products/bradley.php. 2008 [page accessed on 01/12/2008].
35. Zimmer. Epoch hip prosthesis http://www.zimmer.com/z/ctl/op/global/action/1/id/345/template/MP/prcat/M2/prod/y. 2007 [page accessed on 01/12/2008].
36. Beauvais, S. and Cecaux, O., Plasma sprayed biocompatible coatings of PEEK implants. Proceedings of the Global Spray Coating Society 2007: p. 371-376.
37. Vedova, S., Effect of plasma spray coating HA process onto mechanical propeties of PEEK and CFR-PEEK. Transactions of the 8th World Biomaterials Congress, 2008.
38. Devine, D.M., Coating of carbon fibre reinforced PEEK implants with titanium by vapour plasma spraying for improved bone apposition. 54th Annual Meeting of the Orthopaedic Society 2008: p. Paper No. 394.
39. Jones, E., Validating the limits for a PEEK composite as an acetabular wear surface. Society for Biomaterials 27th Annual Meeting Transactions, 2001.
40. Wang, A., Lin, R., Stark, C., and Dumbleton, J.H., Suitability and limitations of carbon fiber reinforced PEEK composites as bearing surfaces for total joint replacements. Wear, 1999. 225-229(Part 2): p. 724-727.
41. Wimmer, M., The effect of accelerated aging on the wear of PEEK for use in disc arthroplasty. 54th Annual Meeting of The Orthopeadic Research Society, 2008: p. Poster No. 1922.
42. Pace, N., Clinical trial of a new CF-PEEK acetabular insert in hip arthroplasty. Hip International, 2004. 14(2): p. 132-3.
43. Pace, N., Primary total hip arthroplasty with carbon fibre reinforced poly-ether-ether-ketone composite acetabular cup component 36 month results. Transactions of the International Society for Technology in Arthroplasty, 2005. 18: p. P2-6.
44. Pace, N., Mario, M., and Stefania, S., Technical and histologic analysis of a retrieved carbon fiber reinforced poly-ether-ether-ketone composite alumina-

bearing liner 28 months after implantation. Journal of Arthroplasty, 2008. 23(1): p. 151-155.
45. Ong, K.L., Manley, M.T., and Kurtz, S.M., Have contemporary hip resurfacing designs reached maturity? A review. Journal of Bone and Joint Surgery American Volume, 2008. 90(Supplement_3): p. 81-88.
46. Squire, M., Griffin, W.L., Mason, J.B., Peindl, R.D., and Odum, S., Acetabular component deformation with press-fit fixation. Journal of Arthroplasty, 2006. 21(6, Supplement 1): p. 72-77.
47. Langdown, A.J., Pickard, R.J., Hobbs, C.M., Clarke, H.J., Dalton, D.J.N., and Grover, M.L., Incomplete seating of the liner with the Trident acetabular system: a cause for concern? Journal of Bone and Joint Surgery British Volume, 2007. 89-B(3): p. 291-295.
48. Fritsche, A., Bialek, K., Mittelmeier, W., Simnacher, M., Fethke, K., Wree, A., and Bader, R., Experimental investigations of the insertion and deformation behavior of press-fit and threaded acetabular cups for total hip replacement. Journal of Orthopaedic Science, 2008. 13(3): p. 240-7.
49. Grimes, J.B., Does deformation of metal-on-metal acetabular components contribute to early failure? The Journal of Arthroplasty, 2010. 25(3): p. e21-e21.
50. Kamali, A., Daniel, J.T., Javid, S.F., and Youseffi, M., The effect of cup deflection on friction in metal-on-metal bearings. Journal of Bone and Joint Surgery British Volume, 2008. 90-B(SUPP_III): p. 552-c-.
51. Jin, Z., Meakins, S., Morlock, M., Parsons, P., Hardaker, C., Flett, M., and Isaac, G., Deformation of press-fitted metallic resurfacing cups. Part 1: experimental simulation. Proceedings of the Institution of Mechanical Engineers, Part H: Journal of Engineering in Medicine, 2006. 220(2): p. 299-309.
52. Tortoro, G., Principles of Anatomy and Physiology 2006, New Jersey Whiley.
53. NJR, National Joint Registry for England and Wales 8th annual report. Department of Health, 2011.
54. Enderle, J., Blanchard, S., and Bronzino, J., Introduction to Biomedical Engineering. 2005, San Diago, CA: Elsevier Academic Press.
55. Ries, M.D., Harbaugh, M., Shea, J., and Lambert, R., Effect of cementless acetabular cup geometry on strain distribution and press-fit stability. Journal of Arthroplasty, 1997. 12(2): p. 207-212.
56. Dorr, L., Wan, Z., and Cohen, J., Hemispheric titanium porous coated acetabular component without screw fixation. Clinical Orthopaedics & Related Research, 1998. 351: p. 158-168.
57. Bellini, C.M., Galbusera, F., Ceroni, R.G., and Raimondi, M.T., Loss in mechanical contact of cementless acetabular prostheses due to post-operative weight bearing: A biomechanical model. Medical Engineering & Physics, 2007. 29(2): p. 175-181.
58. MacDonald, S.J., McCalden, R.W., Chess, D.G., Bourne, R.B., Rorabeck, C.H., Cleland, D., and Leung, F., Metal-on-metal versus polyethylene in hip arthroplasty: a randomized clinical trial. Clinical Orthopaedics & Related Research, 2003. 406(1): p. 282-296.
59. Catelas, I., Petit, A., Marchand, R., Zukor, D.J., Yahia, L.H., and Huk, O.L., Cytotoxicity and macrophage cytokine release induced by ceramic and polyethylene particles in vitro. Journal of Bone and Joint Surgery British Volume, 1999. 81-B(3): p. 516-521.

60. D'Antonio, J., William, C., Michael, M., and Benjamin, B., New experience with alumina-on-alumina ceramic bearings for total hip arthroplasty. Journal of Arthroplasty, 2002. 17(4): p. 390-397.
61. McCarthy, M.J.H. and Maher, H., Lining up the liner: 2 case reports of early ceramic liner fragmentation. Journal of Arthroplasty, 2007. 22(8): p. 1217-1222.
62. Park, Y.-S., Hwang, S.-K., Choy, W.-S., Kim, Y.-S., Moon, Y.-W., and Lim, S.-J., Ceramic failure after total hip arthroplasty with an alumina-on-alumina bearing. Journal of Bone & Joint Surgery American Volume, 2006. 88(4): p. 780-787.
63. Toni, A.T., S. Sudanese, A. Bianchi, G, Fracture of ceramic components in total hip arthroplasty. Hip International, 2000. 10(1): p. 49-56.
64. Walter, W.L., O'Toole, G.C., Walter, W.K., Ellis, A., and Zicat, B.A., Squeaking in ceramic-on-ceramic hips: The importance of acetabular component orientation. Journal of Arthroplasty, 2007. 22(4): p. 496-503.
65. Taylor, S., Manley, M.T., and Sutton, K., The role of stripe wear in causing acoustic emissions from alumina ceramic-on-ceramic bearings. Journal of Arthroplasty, 2007. 22(7, Supplement 1): p. 47-51.
66. Hing, C.B., Back, D.L., Bailey, M., Young, D.A., Dalziel, R.E., and Shimmin, A.J., The results of primary Birmingham hip resurfacings at a mean of five years: an independent prospective review of the first 230 hips. Journal of Bone and Joint Surgery British Volume, 2007. 89-B(11): p. 1431-1438.
67. Sieber, H.P., Rieker, C.B., and Kottig, P., Analysis of 118 second-generation metal-on-metal retrieved hip implants. Journal of Bone and Joint Surgery British Volume, 1999. 81(1): p. 46-50.
68. Williams, S., Schepers, A., Isaac, G., Hardaker, C., Ingham, E., van der Jagt, D., Breckon, A., and Fisher, J., The 2007 Otto Aufranc Award. Ceramic-on-metal hip arthroplasties: a comparative in vitro and in vivo study. Clinical Orthopaedics & Related Research, 2007. 465: p. 23-32.
69. Brown, S., Davies, W., DeHeer, D., and Swanson, A., Long-term survival of McKee-Farrar Total Hip Prostheses. Clinical Orthopaedics & Related Research 2002. 402: p. 157-163.
70. Treacy, R.B.C., McBryde, C.W., and Pynsent, P.B., Birmingham hip resurfacing arthroplasty: a minimum follow-up of five years. Journal of Bone and Joint Surgery British Volume, 2005. 87-B(2): p. 167-170.
71. Daniel, J., Pynsent, P.B., and McMinn, D.J.W., Metal-on-metal resurfacing of the hip in patients under the age of 55 years with osteoarthritis. Journal of Bone and Joint Surgery British Volume, 2004. 86-B(2): p. 177-184.
72. Steffen, R.T., Pandit, H.P., Palan, J., Beard, D.J., Gundle, R., McLardy-Smith, P., Murray, D.W., and Gill, H.S., The five-year results of the Birmingham Hip Resurfacing arthroplasty: an independent series. Journal of Bone and Joint Surgery British Volume, 2008. 90-B(4): p. 436-441.
73. Little, C.P., Ruiz, A.L., Harding, I.J., McLardy-Smith, P., Gundle, R., Murray, D.W., and Athanasou, N.A., Osteonecrosis in retrieved femoral heads after failed resurfacing arthroplasty of the hip. Journal of Bone and Joint Surgery British Volume, 2005. 87-B(3): p. 320-323.
74. de Smet, K., Durme, R.v., Jansegers, E., and Verdonk, R., Early resutls of primary Birmingham hip resurfacing using a hybrid metal-on-metal couple. Journal of Bone and Joint Surgery British Volume, 2004. 86-B(SUPP_IV): p. 400-d-.

75. Shimmin, A.J., Bare, J., and Back, D.L., Complications associated with hip resurfacing arthroplasty. Orthopedic Clinicians of North America, 2005. 36(2): p. 187-193.
76. Shimmin, A.J. and Back, D., Femoral neck fractures following Birmingham hip resurfacing: a national review of 50 cases. Journal of Bone and Joint Surgery British Volume, 2005. 87-B(4): p. 463-464.
77. Amstutz, H.C., Campbell, P.A., and Duff, M.J.L., Fracture of the neck of the femur after surface arthroplasty of the hip. Journal of Bone and Joint Surgery American Volume, 2004. 86(9): p. 1874-1877.
78. Depuy. ASR Recall http://www.depuy.com/ukprofessional. 2010 [page accessed on 2011 15/04/2011].
79. Langton, D.J., Jameson, S.S., Joyce, T.J., Hallab, N.J., Natu, S., and Nargol, A.V.F., Early failure of metal-on-metal bearings in hip resurfacing and large-diameter total hip replacement: a consequence of excess wear. Journal of Bone and Joint Surgery British Volume. 92(1): p. 38.
80. Browne, J.A., Bechtold, C.D., Berry, D.J., Hanssen, A.D., and Lewallen, D.G., Failed metal-on-metal hip arthroplasties: A spectrum of clinical presentations and operative findings. Clinical Orthopaedics and Related Research: p. 1-8.
81. Campbell, P., Ebramzadeh, E., Nelson, S., Takamura, K., De Smet, K., and Amstutz, H.C., Histological features of pseudotumor-like tissues from metal-on-metal hips. Clinical Orthopaedics and Related Research, 2010: p. 1-7.
82. NJR, National Joint Registry for England and Wales 7th annual report. 2010, The Department of Health.
83. Hay, J.N. and Kemmish, D.J., Thermal decomposition of poly(aryl ether ketones). Polymer, 1987. 28(12): p. 2047-2051.
84. Brown, S.A., Hastings, R.S., Mason, J.J., and Moet, A., Characterization of short-fibre reinforced thermoplastics for fracture fixation devices. Biomaterials, 1990. 11(8): p. 541-547.
85. Sasuga, T. and Hagiwara, M., Radiation deterioration of several aromatic polymers under oxidative conditions. Polymer, 1987. 28(11): p. 1915-1921.
86. Sinmazçelik, T. and Yilmaz, T., Thermal aging effects on mechanical and tribological performance of PEEK and short fiber reinforced PEEK composites. Materials & Design, 2007. 28(2): p. 641-648.
87. Williams, D.F., McNamara, A., and Turner, R.M., Potential of polyetheretherketone (PEEK) and carbon-fibre-reinforced PEEK in medical applications. Journal of Materials Science Letters, 1987. 6(2): p. 188-190.
88. Toth, J.M., Wang, M., Estes, B.T., Scifert, J.L., Seim Iii, H.B., and Turner, A.S., Polyetheretherketone as a biomaterial for spinal applications. Biomaterials, 2006. 27(3): p. 324-334.
89. Kurtz, S., PEEK Biomaterials Handbook (preprint manuscripts). 2011: Elsevier.
90. Invibo, Marketing Material. 2010.
91. Hamdan, S. and Swallowe, G.M., The strain-rate and temperature dependence of the mechanical properties of polyetherketone and polyetheretherketone. Journal of Materials Science, 1996. 31(6): p. 1415-1423.
92. Karger-Kocsis, J., Temperature and strain-rate effects on the fracture thoughness of poly (ether ether ketone) and its short glass-fibre reinforced composite. Polymer, 1986. 27: p. 1753-60.

93. Rae, P.J., Brown, E.N., and Orler, E.B., The mechanical properties of poly(ether-ether-ketone) (PEEK) with emphasis on the large compressive strain response. Polymer, 2007. 48(2): p. 598-615.
94. Brillhart, M., Fatigue fracture behaviour of PEEK: 1; Effects of load level. Polymer, 1991. 32: p. 1605-11.
95. Brillhart, M., Fatigue fracture behaviour of PEEK: 2. Effects of thickness and temperature. Polymer, 1992. 32: p. 5225-32.
96. Boinard, E., Pethrick, R.A., and MacFarlane, C.J., The influence of thermal history on the dynamic mechanical and dielectric studies of polyetheretherketone exposed to water and brine. Polymer, 2000. 41(3): p. 1063-1076.
97. Pritchett, J., Heat Generated by Hip Resurfacing Prostheses: An in Vivo Pilot Study. Journal of Long-Term Effects of Medical Implants. 21(1): p. 55-62.
98. Jones, D., Mechanical properties of poly(ether-ether-ketone) for engineering applications. Polymer, 1985. 26(18): p. 1385-93.
99. Sagomonyants, K.B., Jarman-Smith, M.L., Devine, J.N., Aronow, M.S., and Gronowicz, G.A., The in vitro response of human osteoblasts to polyetheretherketone (PEEK) substrates compared to commercially pure titanium. Biomaterials, 2008. 29(11): p. 1563-72.
100. Nisitani, H., Evaluation of fatigue strength of plain and notched specimens of short carbon-fiber reinforced polyetheretherketone in comparison with polyetheretherketone. Engineering Fracture Mechanics, 1992. 43(5): p. 685-705.
101. Kurtz, M., The UHMWPE Handbook; Ultra-High Molecular Weight Polyethylene in Total Joint Replacement 2004, Phiadelphia: Elsevier Academic Press.
102. Piconi, C., Maccauro, G., and Muratori, F., Alumina Matrix Composites in Arthroplasty. Key Engineering Materials, 2005. 284: p. 979-982.
103. Dalstra, M., Huiskes, R., Odgaard, A., and van Erning, L., Mechanical and textural properties of pelvic trabecular bone. Journal of Biomechanics, 1993. 26(4-5): p. 523-535.
104. Wang, A., Carbon fiber reinforced polyether ether ketone composite as a bearing surface for total hip replacement. Tribology International, 1998. 31(11): p. 661-667.
105. Cook, S.D. and Rust-Dawicki, A.M., Preliminary evaluation of titanium-coated PEEK dental implants. Journal of Oral Implantology, 1995. 21(3): p. 176-81.
106. Ha, S.W., Eckert, K.L., Wintermantel, E., Gruner, H., Guecheva, M., and Vonmont, H., NaOH treatment of vacuum-plasma-sprayed titanium on carbon fibre-reinforced poly(etheretherketone). Journal of Materials Science: Materials in Medicine, 1997. 8(12): p. 881-886.
107. Ha, S.W., Gisep, A., Mayer, J., Wintermantel, E., Gruner, H., and Wieland, M., Topographical characterization and microstructural interface analysis of vacuum-plasma-sprayed titanium and hydroxyapatite coatings on carbon fibre-reinforced poly(etheretherketone). Journal of Materials Science: Materials in Medicine, 1997. 8(12): p. 891-6.
108. Gillett, N., Brown, S.A., Dumbleton, J.H., and Pool, R.P., The use of short carbon fibre reinforced thermoplastic plates for fracture fixation. Biomaterials, 1985. 6(2): p. 113-121.

109. Bradley, J.S., Hastings, G.W., and Johnson-Nurse, C., Carbon fibre reinforced epoxy as a high strength, low modulus material for internal fixation plates. Biomaterials, 1980. 1(1): p. 38-40.
110. Pemberton, D.J., Evans, P.D., Grant, A., and McKibbin, B., Fractures of the distal femur in the elderly treated with a carbon fibre supracondylar plate. Injury, 1994. 25(5): p. 317-321.
111. Baker, D., Kadambande, S.S., and Alderman, P.M., Carbon fibre plates in the treatment of femoral periprosthetic fractures. Injury, 2004. 35(6): p. 596-598.
112. Davim, J.P., Marques, N., and Baptista, A.M., Effect of carbon fibre reinforcement in the frictional behaviour of PEEK in a water lubricated environment. Wear, 2001. 251(1-12): p. 1100-1104.
113. Scholes, S.C. and Unsworth, A., The wear properties of CFR-PEEK-OPTIMA articulating against ceramic assessed on a multidirectional pin-on-plate machine. Proceedings of the Institution of Mechanical Engineers, Part H: Journal of Engineering in Medicine, 2007. 221(3): p. 281-9.
114. Davim, J.P. and Marques, N., Evaluation of tribological behaviour of polymeric materials for hip prostheses application. Tribology Letters, 2001. 11: p. 91-94.
115. Scholes, S.C. and Unsworth, A., Wear studies on the likely performance of CFR-PEEK/CoCrMo for use as artificial joint bearing materials. Journal of Materials Science: Materials in Medicine, 2009. 20(1): p. 163-170.
116. Clarke, I.C., et al., Current status of zirconia used in Total Hip Implants. Journal of Bone and Joint Surgery American Volume, 2003. 85(suppl_4): p. 73-84.
117. Chevalier, J., Gremillard, L., and Deville, S., Low-temperature degradation of zirconia and implications for biomedical implants. Annual Review of Mateerials Research, 2007. 37: p. 1-32.
118. Scholes, S.C., Inman, I.A., Unsworth, A., and Jones, E., Tribological assessment of a flexible carbon-fibre-reinforced poly(ether-ether-ketone) acetabular cup articulating against an alumina femoral head. Proceedings of the Institution of Mechanical Engineers, Part H: Journal of Engineering in Medicine, 2008. 222(3): p. 273-83.
119. Scholes, S.C. and Unsworth, A., Pitch-based carbon-fibre-reinforced poly (ether–ether–ketone) OPTIMA assessed as a bearing material in a mobile bearing unicondylar knee joint. Proceedings of the Institution of Mechanical Engineers, Part H: Journal of Engineering in Medicine, 2009. 223(1): p. 13-26.
120. Lombardi, A.V., Mallory, T.H., Dennis, D.A., Komistek, R.D., Fada, R.A., and Northcut, E.J., An in vivo determination of total hip arthroplasty pistoning during activity. Journal of Arthroplasty, 2000. 15(6): p. 702-709.
121. Dennis, D.A., Komistek, R.D., Northcut, E.J., Ochoa, J.A., and Ritchie, A., "In vivo" determination of hip joint separation and the forces generated due to impact loading conditions. Journal of Biomechanics, 2001. 34(5): p. 623-629.
122. Fisher, J., Tribology of hard on hard bearing for hip prostheses under adverse clinical conditions. Bearing surfaces in hip replacement: past present and future, 2008.
123. Mak, M., Besong, A., Jin, Z., and Fisher, J., Effect of microseparation on contact mechanics in ceramic-on-ceramic hip joint replacements. Proceedings of the Institution of Mechanical Engineers, Part H: Journal of Engineering in Medicine, 2002. 216(6): p. 403-408.
124. Williams, S., Butterfield, M., Stewart, T., Ingham, E., Stone, M., and Fisher, J., Wear and deformation of ceramic-on-polyethylene total hip replacements with

joint laxity and swing phase microseparation. Proceedings of the Institution of Mechanical Engineers, Part H: Journal of Engineering in Medicine, 2003. 217(2): p. 147-153.
125. Williams, S., Leslie, I., Isaac, G., Jin, Z., Ingham, E., and Fisher, J., Tribology and wear of metal-on-metal hip prostheses: influence of cup angle and head position. Journal of Bone and Joint Surgery American Volume, 2008. 90(Supplement_3): p. 111-117.
126. Callaghan, J.J., The clinical results and basic science of total hip arthroplasty with porous-coated prostheses. Journal of Bone and Joint Surgery American Volume, 1993. 75(2): p. 299-310.
127. Kroeber, M., Michael, D.R., Yoshihiro, S., Glen, R., Frank, A., and Jeff, L., Impact biomechanics and pelvic deformation during insertion of press-fit acetabular cups. Journal of Arthroplasty, 2002. 17(3): p. 349-354.
128. Schmidig, G., Patel, A., Liepins, I., Thakore, M., and Markel, D.C., The effects of acetabular shell deformation and liner thickness on frictional torque in ultrahigh-molecular-weight polyethylene acetabular bearings. Journal of Arthroplasty, 2010. 25, Issue 4, June 2010, Pages (4): p. 644-653.
129. Ong, K.L., Rundell, S., Liepins, I., Laurent, R., Markel, D., and Kurtz, S.M., Biomechanical modeling of acetabular component polyethylene stresses, fracture risk, and wear rate following press-fit implantation. Journal of Orthopaedic Research, 2009. 27(11): p. 1467-1462.
130. Yew, A., Jin, Z., Donn, A., Morlock, M., and Isaac, G., Deformation of press-fitted metallic resurfacing cups. Part 2: Finite element simulation. Proceedings of the Institution of Mechanical Engineers, Part H: Journal of Engineering in Medicine, 2006. 220: p. 311-319.
131. Udofia, I., Liu, F., Jin, Z., Roberts, P., and Grigoris, P., The initial stability and contact mechanics of a press-fit resurfacing arthroplasty of the hip. Journal of Bone and Joint Surgery British Volume, 2007. 89-B(4): p. 549-556.
132. Carter, D.R. and Hayes, W.C., The compressive behavior of bone as a two-phase porous structure. The Journal of Bone and Joint Surgery, 1977. 59(7): p. 954.
133. Vasu, R., Carter, D.R., and Harris, W.H., Stress distributions in the acetabular region. Before and after total joint replacement. Journal of Biomechanics, 1982. 15(3): p. 155-164.
134. Dalstra, M. and Huiskes, R., Load transfer across the pelvic bone. Journal of Biomechanics, 1995. 28(6): p. 715-724.
135. Dalstra, M., Huiskes, R., and van Erning, L., Development and validation of a three-dimensional finite element model of the pelvic bone. Journal of Biomechanical Engineering, 1995. 117(3): p. 272-278.
136. Phillips, A.T.M., Pankaj, P., Usmani, A.S., and Howie, C.R., Numerical modelling of the acetabular construct following impaction grafting. Proceedings of Computer Methods in Biomechanics and Biomedical Engineering, 2004.
137. Cilingir, A., Three-dimensional anatomic finite element modelling of hemi-arthroplasty of human hip joint. Trends in Biometerials and Artificial Organs, 2007. 21(1): p. 63-72.
138. Mow, V.C. and Huiskes, R., Basic Orthopaedic Biomechanics & Mechano-Biology. 1991: Lippincott Williams & Wilkins.

139. Anderson, A.E., Peters, C.L., Tuttle, B.D., and Weiss, J.A., Subject-specific finite element model of the pelvis: development, validation and sensitivity studies. Journal of Biomechanical Engineering, 2005. 127(3): p. 364-373.
140. Zhang, Q.-H., Wang, J.-Y., Lupton, C., Heaton-Adegbile, P., Guo, Z.-X., Liu, Q., and Tong, J., A subject-specific pelvic bone model and its application to cemented acetabular replacements. Journal of Biomechanics, 2010. In Press, Corrected Proof.
141. Phillips, A.T.M., Pankaj, P., Howie, C.R., Usmani, A.S., and Simpson, A.H.R.W., Finite element modelling of the pelvis: Inclusion of muscular and ligamentous boundary conditions. Medical Engineering & Physics, 2007. 29(7): p. 739-748.
142. Kluess, D., Souffrant, R., Mittelmeier, W., Wree, A., Schmitz, K.P., and Bader, R., A convenient approach for finite-element-analyses of orthopaedic implants in bone contact: Modeling and experimental validation. Computer Methods and Programs in Biomedicine, 2009. 95(1): p. 23-30.
143. Leung, A.S.O., Gordon, L.M., and Skrinskas, T., Effects of bone density alterations on strain patters in the pelvis: application of a finite element model Proceedings of the Institution of Mechanical Engineers, Part H: Journal of Engineering in Medicine, 2009. 223: p. 965-980.
144. Shim, V.B., Pitto, R.P., Streicher, R.M., Hunter, P.J., and Anderson, I.A., Development and Validation of Patient-Specific Finite Element Models of the Hemipelvis Generated Form a Sparse CT Date Set. Journal of Biomechanical Engineering, 2008. 130: p. 051010.
145. Hsu, J.-T., Chang, C.H., Huang, H.L., Zobitz, M.E., Chen, W.P., Lai, K.A., and An, K.N., The number of screws, bone quality, and friction coefficient affect acetabular cup stability. Medical Engineering & Physics, 2007. 29(10): p. 1089-1095.
146. Thompson, M., Northmore-Ball, M., and Tanner, K., Effects of acetabular resurfacing component material and fixation on the strain distribution in the pelvis. Proceedings of the Institution of Mechanical Engineers, Part H: Journal of Engineering in Medicine, 2002. 216(4): p. 237-245.
147. Spears, I.R., Morlock, M.M., Pfleiderer, M., Schneider, E., and Hille, E., The influence of friction and interference on the seating of a hemispherical press-fit cup: a finite element investigation. Journal of Biomechanics, 1999. 32(11): p. 1183-1189.
148. Spears, I.R., Pfleiderer, M., Schneider, E., Hille, E., Bergmann, G., and Morlock, M.M., Interfacial conditions between a press-fit acetabular cup and bone during daily activities: implications for achieving bone in-growth. Journal of Biomechanics, 2000. 33(11): p. 1471-1477.
149. Spears, I.R., Pfleiderer, M., Schneider, E., Hille, E., and Morlock, M.M., The effect of interfacial parameters on cup-bone relative micromotions: A finite element investigation. Journal of Biomechanics, 2001. 34(1): p. 113-120.
150. Janssen, D., Zwartelé, R.E., Doets, H.C., and Verdonschot, N., Computational assessment of press-fit acetabular implant fixation: the effect of implant design, interference fit, bone quality, and frictional properties. Proceedings of the Institution of Mechanical Engineers, Part H: Journal of Engineering in Medicine, 2010. 224(1): p. 67-75.
151. Manley, M., Biomechanics of a PEEK horseshoe-shaped cup: comparisons with a predicated deformable cup. Institution of Mechanical

Engineers,“Engineers & Surgeons: Joined at the Hip, 2007. Paper C655/058(London).
152. Manley, M.T., Ong, K.L., and Kurtz, M., The potential for bone loss in acetabulr stuctures following THA. Clinical Orthopaedics & Related Research, 2006. 453: p. 246-253.
153. Yong-wei, J., A finite element analysis of the pelvic reconstruction using fibular transplantation fixed with four different rod-screw systems after type I rescection. Chinese Medical Journal 2008. 121(4): p. 321-326.
154. García, J.M., Doblaré, M., Seral, B., Seral, F., Palanca, D., and Gracia, L., Three-dimensional finite element analysis of several internal and external pelvis fixations. Journal of Biomechanical Engineering, 2000. 122: p. 516.
155. Schmidig, G., Patel, A., Liepins, I., Thakore, M., and Markel, D.C., The effects of acetabular shell deformation and liner thickness on frictional torque in ultrahigh-molecular-weight polyethylene acetabular bearings. Journal of Arthroplasty, 2010. 25, Issue 4, June 2010, Pages (4): p. 644-653
156. Hothan, A., Huber, G., Weiss, C., Hoffmann, N., and Morlock, M., Deformation characteristics and eigenfrequencies of press-fit acetabular cups. Clinical Biomechanics, 2000. In Press, Corrected Proof.
157. Massin, P., Vandenbussche, E., Landjerit, B., and Augereau, B., Experimental study of periacetabular deformations before and after implantation of HIP prostheses. Journal of Biomechanics, 1996. 29(1): p. 53-61.
158. Ong, K.L., Rundell, S., Liepins, I., Laurent, R., Markel, D., and Kurtz, S.M., Biomechanical modeling of acetabular component polyethylene stresses, fracture risk, and wear rate following press-fit implantation. Journal of Orthopaedic Research, 2009. 27(11): p. 1467-1462.
159. Lazennec, J.Y., Laudet, C.G., Guérin-Surville, H., Roy-Camille, R., and Saillant, G., Dynamic anatomy of the acetabulum: an experimental approach and surgical implications. Surgical and Radiologic Anatomy, 1997. 19(1): p. 23-30.
160. Widmer, K.H., Zurfluh, B., and Morscher, E.W., Load transfer and fixation mode of press-fit acetabular sockets. Journal of Arthroplasty, 2002. 17(7): p. 926-935.
161. Stolk, J., Janssen, D., Huiskes, R., and Verdonschot, N., Finite element-based preclinical testing of cemented total hip implants. Clinical orthopaedics and related research, 2007. 456: p. 138.
162. Stolk, J., Maher, S.A., Verdonschot, N., Prendergast, P.J., and Huiskes, R., Can finite element models detect clinically inferior cemented hip implants? Clinical Orthopaedics & Related Research, 2003. 409: p. 138.
163. Barink, M., Kampen, A., Malefijt, M.W., and Verdonschot, N., A three-dimensional dynamic finite element model of the prosthetic knee joint: simulation of joint laxity and kinematics. Proceedings of the Institution of Mechanical Engineers, Part H: Journal of Engineering in Medicine, 2005. 219(6): p. 415-424.
164. Lichtenberger, R. and Schreier, H., Non-contacting measurement technology for component safety assessment. Limess Messlechnik u. Software GmbH, D-75180 Pforzheim.
165. Mguil-Touchal, S., Morestin, F., and Brunei, M., Various experimental applications of Digital Image Correlation method. International Conference on Computational Methods and Experimental Results, 1997: p. 45-48.

166. Moser, R. and Lightner, J.G., Using three-dimensional digital imaging correlation techniques to validate tire finite-element model. Experimental Techniques, 2007. 31(4): p. 29-36.
167. Dickinson, A.S., Taylor, A., Ozurk, H., and Browne, M., Experimental validation of a finite element model fo the proximal femur using digital image correlation and a composite bone model. Journal of Biomechanical Engineering, 2011. 133(1).
168. Tarigopula, V., Hopperstad, O., Langseth, M., Clausen, A., Hild, F., Lademo, O.G., and Eriksson, M., A Study of Large Plastic Deformations in Dual Phase Steel Using Digital Image Correlation and FE Analysis. Experimental Mechanics, 2008. 48(2): p. 181-196.
169. Avril, S., Ferrier, E., Vautrin, A., Hamelin, P., and Surrel, Y., A full-field optical method for the experimental analysis of reinforced concrete beams repaired with composites. Composites Part A: Applied Science and Manufacturing, 2004. 35(7-8): p. 873-884.
170. Sjodahl, M., Some recent advances in electronic speckle photography. Optics and Lasers in Engineering, 1998. 29(2-3): p. 125-144.
171. Peters, W.H. and Ranson, W.F., Digital imaging techniques in experimental stress analysis. Optical Engineering, 1982. 21: p. 427-431.
172. Sutton, M.A., Wolters, W.J., Peters, W.H., Ranson, W.F., and McNeill, S.R., Determination of displacements using an improved digital correlation method. Image Vision Computation, 1983. 1(3): p. 133–139.
173. Helm, J.D., McNeill, S.R., and Sutton, M.A., Improved three-dimensional image correlation for surface displacement measurement. Optical Engineering, 1996. 35: p. 1911.
174. Wattrisse, B., Chrysochoos, A., Muracciole, J.M., and Némoz-Gaillard, M., Kinematic manifestations of localisation phenomena in steels by digital image correlation. European Journal of Mechanics and Solids, 2001. 20(2): p. 189-211.
175. Zhang, D., Eggleton, C.D., and Arola, D.D., Evaluating the mechanical behavior of arterial tissue using digital image correlation. Experimental Mechanics, 2002. 42(4): p. 409-416.
176. Zhang, D., Nazari, A., Soappman, M., Bajaj, D., and Arola, D., Methods for examining the fatigue and fracture behavior of hard tissues. Experimental Mechanics, 2007. 47(3): p. 325-336.
177. Zhang, G., Latour, R.A., Jr., Kennedy, J.M., Del Schutte, H., Jr., and Friedman, R.J., Long-term compressive property durability of carbon fibre-reinforced polyetheretherketone composite in physiological saline. Biomaterials, 1996. 17(8): p. 781-9.
178. Guo, L.P., Sun, W., Carpinteri, A., Chen, B., and He, X.Y., Real-time Detection and Analysis of Damage in High-performance Concrete under Cyclic Bending. Experimental Mechanics, 2009.
179. Meng, L.B., Jin, G.C., Yao, X.F., and Yeh, H.Y., 3D full-field deformation monitoring of fiber composite pressure vessel using 3D digital speckle correlation method. Polymer Testing, 2006. 25(1): p. 42-48.
180. Cox, M.A.J., Driessen, N.J.B., Boerboom, R.A., Bouten, C.V.C., and Baaijens, F.P.T., Mechanical characterization of anisotropic planar biological soft tissues using finite indentation: Experimental feasibility. Journal of Biomechanics, 2008. 41(2): p. 422-429.

181. Moerman, K.M., Holt, C.A., Evans, S.L., and Simms, C.K., Digital image correlation and finite element modelling as a method to determine mechanical properties of human soft tissue in vivo. Journal of Biomechanics, 2009. 42(8): p. 1150-1153.
182. Evans, S.L., Holt, C.A., Ozturk, H., Saidi, K., and Shrive, N.G. Measuring soft tissue properties using digital image correlation and finite element modelling. 2007: Springer.
183. Lecompte, D., Smits, A., Bossuyt, S., Sol, H., Vantomme, J., Van Hemelrijck, D., and Habraken, A.M., Quality assessment of speckle patterns for digital image correlation. Optics and Lasers in Engineering, 2006. 44(11): p. 1132-1145.
184. Hung, P.C. and Voloshin, A.S., In-plane strain measurement by digital image correlation. Journal of the Brazilian Society of Mechanical Sciences and Engineering, 2003. 25(3): p. 215-221.
185. Haddadi, H. and Belhabib, S., Use of rigid-body motion for the investigation and estimation of the measurement errors related to digital image correlation technique. Optics and Lasers in Engineering, 2008. 46(2): p. 185-196.
186. Sun, Z., Lyons, J.S., and McNeill, S.R., Measuring microscopic deformations with digital image correlation. Optics and Lasers in Engineering, 1997. 27(4): p. 409-428.
187. Jeffers, J.R.T., Browne, M., Lennon, A.B., Prendergast, P.J., and Taylor, M., Cement mantle fatigue failure in total hip replacement: Experimental and computational testing. Journal of Biomechanics, 2007. 40(7): p. 1525-1533.
188. Linde, F. and Sørensen, H.C.F., The effect of different storage methods on the mechanical properties of trabecular bone. Journal of Biomechanics, 1993. 26(10): p. 1249-1252.
189. Udofia, I.J. and Jin, Z.M., Elastohydrodynamic lubrication analysis of metal-on-metal hip-resurfacing prostheses. Journal of Biomechanics, 2003. 36(4): p. 537-544.
190. Jalali-Vahid, D., Jagatia, M., Jin, Z.M., and Dowson, D., Prediction of lubricating film thickness in UHMWPE hip joint replacements. Journal of Biomechanics, 2001. 34(2): p. 261-266.
191. Scholes, S.C., Unsworth, A., Hall, R.M., and Scott, R., The effects of material combination and lubricant on the friction of total hip prostheses. Wear, 2000. 241(2): p. 209-213.
192. Kim, Y.S., Brown, T.D., Pedersen, D.R., and Callaghan, J.J., Reamed surface topography and component seating in press-fit cementless acetabular fixation. The Journal of Arthroplasty, 1995. 10: p. S14.
193. Mackenzie, J., Callaghan, J., Pedersen, D., and Brown, T.D., Areas of Contact and Extent of Gaps With Implantation of Oversized Acetabular Components in Total Hip Arthroplasty. Clinical Orthopaedics & Related Research, 1994. 298: p. 127-136.
194. Alexander, J.W., Kamaric, E., and Noble, P.C. The accuracy of acetabular reaming in total hip replacement. in 45th annual meeting of the orthopaedic research society. 1999. Anaheim, CA.
195. Baad-Hansen, T., Kold, S., Fledelius, W., and Nielsen, P., Comparison of performance of conventional and minimially invasive acetabular reamers. Clinical Orthopaedics & Related Research, 2006. 448: p. 173-179.

196. SawBones. Composite Bones http://www.sawbones.com/products/bio/composite.aspx. 2009 [page accessed on 21st May 2009].
197. Kosuge, D., Mak, S., and Khan, I., In-vitro assessment for deformation of uncemented acetabular cup.
198. Reeves, A., ABT shell deformation tests: R&D test report 400. 2006.
199. Reeves, A., Exceed ABT 54 mm shell deformation tests; R&D test report 408. 2006.
200. ISO, Draft Standard; Implants for Surgery - Deformation Test for Acetabular Cups. 2008.
201. Thompson, M.S., Flivik, G., Juliusson, R., Odgaard, A., and Ryd, L., A comparison of structural and mechanical properties in cancellous bone from the femoral head and acetabulum. Proceedings of the Institution of Mechanical Engineers, Part H: Journal of Engineering in Medicine, 2004. 218(6): p. 425-429.
202. Ding, M., Odgaard, A., Linde, F., and Hvid, I., Age-related variations in the microstructure of human tibial cancellous bone. Journal of Orthopaedic Research, 2002. 20(3): p. 615.
203. Majumder, S., Roychowdhury, A., and Pal, S., Simulation of hip fracture in sideways fall using a 3D finite element model of pelvis-femur-soft tissue complex with simplified representation of whole body. Medical Engineering & Physics, 2007. 29(10): p. 1167-1178.
204. Majumder, S. and Roychowdhury, A., Variations of stress in pelvic bone during normal walking considering all active muscles. Trends in Biometerials and Artificial Organs, 2004. 17(2): p. 48-53.
205. Scholes, S.C., Burgess, I.C., Marsden, H.R., Unsworth, A., Jones, E., and Smith, N., Compliant layer acetabular cups: friction testing of a range of materials and designs for a new generation of prosthesis that mimics the natural joint. Proceedings of the Institution of Mechanical Engineers, Part H: Journal of Engineering in Medicine, 2006. 220(5): p. 583-596.
206. Shirazi-Adl, A., Dammak, M., and Paiement, G., Experimental determination of friction characteristics at the trabecular bone/porous-coated metal interface in cementless implants. Journal of Biomedical Materials Research, 1993. 27(2): p. 167-75.
207. Alexander, J.W., Kamaric, E., and Noble, P.C., The accuracy of acetabular reaming in total hip replacement. 45th Annual Meeting of the Orthopaedic Research Society, 1999: p. 906.
208. Cha, C.W., Shanbhag, A.S., Hasselman, C.T., May, D., Kovach, C.J., Clineff, T.D., and Rubash, H.E., Bone ingrowth and wear debris distribution around press-fit acetabular components with and without supplemental screw fixation in a canine cementless total hip arthroplasty (THA) model. Orthopaedic Research Society, 1998: p. 373-373.
209. Taddei, F., Cristofolini, L., Martelli, S., Gill, H.S., and Viceconti, M., Subject-specific finite element models of long bones: An in vitro evaluation of the overall accuracy. Journal of Biomechanics, 2006. 39(13): p. 2457-2467.
210. Schmidig, G., Patel, A., Liepins, I., Thakore, M., and Markel, D.C., The effects of acetabular shell deformation and liner thickness on frictional torque in ultrahigh-molecular-weight polyethylene acetabular bearings. Journal of Arthroplasty, 2009.

211. Keyak, J.H., Lee, I.Y., and Skinner, H.B., Correlations between orthogonal mechanical properties and density of trabecular bone: Use of different densitometric measures. Journal of Biomedical Materials Research, 1994. 28(11): p. 1329-1336.
212. Zhang, Y., Ahn, P.B., Fitzpatrick, D.C., Heiner, A.D., Poggie, R.A., and Brown, T.D., Interfacial frictional behavior: cancellous bone, cortical bone, and a novel porous tantalum biomaterial. Journal of Musculoskeletal Research, 2000. 3(4): p. 245-252.
213. Kim, Y.S., Brown, T.D., Pedersen, D.R., and Callaghan, J.J., Reamed surface topography and component seating in press-fit cementless acetabular fixation. Journal of Arthroplasty, 1995. 10: p. S14.
214. Macdonald, W., Carlsson, L.V., Charnley, G.J., Jacobsson, C.M., and Johansson, C.B., Inaccuracy of acetabular reaming under surgical conditions. The Journal of Arthroplasty, 1999. 14(6): p. 730-737.
215. Zhang, Q., A subject-specific pelvic bone model and its applicationto cemented acetabular replacements. Journal of Biomechancs, 2010.
216. Fehily, A.M., Coles, R.J., Evans, W.D., and Elwood, P.C., Factors affecting bone density in young adults. Americal Society for Clinical Nutrition, 1992. 56: p. 579-86.
217. Wolff, J., The law of bone remodeling. Translated by Maquet P and Furlong R. 1986, Berlin: Springer.
218. Carter, D.R. and Hayes, W.C., Bone compressive strength: the influence of density and strain rate. Science, 1976. 194(4270): p. 1174.
219. Brockett, C., Harper, P., Williams, S., Isaac, G., Dwyer-Joyce, R., Jin, Z., and Fisher, J., The influence of clearance on friction, lubrication and squeaking in large diameter metal-on-metal hip replacements. Journal of Materials Science: Materials in Medicine, 2008. 19(4): p. 1575-1579.
220. Afshinjavid, S., Youseffi, M., Dössel, O., and Schlegel, W.C., The effect of clearance upon friction of large diameter hip resurfacing prostheses using blood, clotted blood and bovine serum as lubricants. World Congress on Medical Physics and Biomedical Engineering, September 7 - 12, 2009, Munich, Germany, 2009. 25/9: p. 418-420.
221. Aspenberg, P., Goodman, S., Toksvig-Larsen, S.Ã.R., Ryd, L., and Albrektsson, T., Intermittent micromotion inhibits bone ingrowth. Acta Orthopaedica, 1992. 63(2): p. 141-145.
222. Williams, J.A., Engineering Tribology. 1994: Oxford University Press.
223. Flanagan, S., Jones, E., and Birkinshaw, C., In vitro friction and lubrication of large bearing hip prostheses. Proceedings of the Institution of Mechanical Engineers, Part H: Journal of Engineering in Medicine, 2009.
224. Unsworth, A., The effects of lubrication in hip joint prostheses. Physics in Medicine and Biology, 1978. 23(2): p. 253–268.
225. Scholes, S.C. and Unsworth, A., The effects of proteins on the friction and lubrication of artificial joints. Proceedings of the Institution of Mechanical Engineers, Part H: Journal of Engineering in Medicine, 2006. 220(6): p. 687-693.
226. Scholes, S.C. and Unsworth, A., Comparison of friction and lubrication of different hip prostheses. Proceedings of the Institution of Mechanical Engineers, Part H: Journal of Engineering in Medicine, 2000. 214(1): p. 49-57.

227. Smith, S.L., Ash, H.E., and Unsworth, A., A tribological study of UHMWPE acetabular cups and polyurethane compliant layer acetabular cups. Journal of Biomedical Materials Research, 2000. 53(6).
228. Jones, E., Scholes, S.C., Burgess, I.C., Ash, H.E., and Unsworth, A., Compliant layer bearings in artificial joints. Part 2: simulator and fatigue testing to assess the durability of the interface between an elastomeric layer and a rigid substrate. Proceedings of the Institution of Mechanical Engineers, Part H: Journal of Engineering in Medicine, 2009. 223(1): p. 1-13.
229. Hamrock, B. and Dowson, D., Elastohydrodynamic lubrication of elliptical contacts for materials of low elastic modulus. 1: Fully flooded conjunction. Journal of Lubriction Technology, 1977. 100(2): p. 236-245.
230. English, T.A. and Kilvington, M., In vivo records of hip loads using a femoral implant with telemetric output (a preliminary report). Journal of Biomedical Engineering, 1979. 1(2): p. 111.
231. Cooke, A.F., Dowson, D., and Wright, V., The rheology of synovial fluid and some potential synthetic lubricants for degenerate synovial joints. Engineering in Medicine, 1978. 7: p. 66–72.
232. Cooke, A.F., Dowson, D., and Wright, V., The rheology of synovial fluid and some potential synthetic lubricants for degenerate synovial joints. Engineering Medicine, 1978. 7: p. 66–72.
233. Johnson, K.L., Greenwood, J.A., and Poon, S.Y., A simple theory of asperity contact in elastohydro-dynamic lubrication. Wear, 1972. 19(1): p. 91-108.
234. Brockett, C., Williams, S., Jin, Z., Isaac, G., and Fisher, J., Friction of total hip replacements with different bearings and loading conditions. Journal of Biomedical Materials Research Part B: Applied Biomaterials, 2007. 81B(2): p. 508-515.
235. Brockett, C., Williams, S., Jin, Z., Isaac, G., and Fisher, J., A comparison of friction in 28 mm conventional and 55 mm resurfacing metal-on-metal hip replacements. Proceedings of the Institution of Mechanical Engineers, Part J: Journal of Engineering Tribology, 2007. 221(3): p. 391-398.
236. Williams, S., Ingham, E., Stone, M., and Fisher, J., Friction of ceramic-on-ceramic and metal on metal total hip replacements tested under different lubrication regimes. Journal of Bone Joint Surgery British volume, 2008. 90-B(SUPP_I): p. 189-195.
237. Williams, S., Wu, J., Unsworth, A., and Khan, I., Wear, friction and surface analysis of 38mm ceramic-on-metal total hip replacements Journal of Bone and Joint Surgery British Volume, 2008. 92-B(SUPP_I): p. 101-c-102.

Table 19 Examples of standard (i.e. not resurfacing) press-fit acetabular cups currently available

Manufacturer	Type	Material	Design features
Biomet	Exceed ABT	Titanium alloy	Morse taper liner retention for ceramic inserts and CoCr, or locking mechanism for UHMWPE liners, porous titanium bone contacting surface
Stryker	Trident	Titanium alloy	Ceramic insert has pre-assembled titanium sleeve, porous titanium bone contacting surface
Depuy	Pinnacle	Titanium alloy	Intended for use with UHWMPE or CoCr inserts, porous titanium bone contacting surface
Smith and Nephew	Bicon plus	Titanium alloy	Indented for use with ceramic, CoCr or UHMWPE liners, self tapping screw shell
Smith and Nephew	EP Fit plus	Titanium alloy	Indented for use with UHMWPE liners, porous titanium bone contacting surface

Table 20 Examples of resurfacing acetabular cups

Manufacturer	Type	Material	Bone contacting surface
Biomet	ReCap	Cast, High Carbon, high Carbide	Porous Ti or Ti and HA
Smith & Nephew	Birmingham (BHR)	Cast, High carbon, high carbide	Porocast cast in porous surface
Zimmer Inc.	Durom	Forged High Carbon CoCr	Porous Ti
J &J DePuy	ASR	Cast CoCr	Porocoat and HA